UNIVERSITÀ DEGLI STUDI
DI GENOVA

UNIVERSITY OF GENOVA

DOCTORAL THESIS

Perturbing critical phenomena: from CPT to Holography

Author:
Marcello SCANAVINO

Supervisor:
Prof. Nicodemo MAGNOLI,
Dr. Andrea AMORETTI

A thesis submitted in fulfillment of the requirements
for the degree of Doctor of Philosophy

in the

Department of Physics

October 9, 2020

UNIVERSITY OF GENOVA

Abstract

Department of Physics

Doctor of Philosophy

**Perturbing critical phenomena:
from CPT to Holography**

by Marcello SCANAVINO

In this thesis we analyze different aspects of conformal field theories, one of the most powerful tools to study the physics of critical phenomena. Even though many progresses have been made in the knowledge and comprehension of conformal field theories, where the strong constraints imposed by conformal symmetry make the system easier to solve, still much needs to be done when a perturbation is introduced. We describe two different approaches which can be useful to tackle this problem. In particular in Chapter 2, we carefully describe the basic properties of Conformal Perturbation Theory (CPT), a mathematical tool to study conformal systems perturbed by relevant operators. We also provide two examples of how it can be applied and we match our finding with numerical Monte Carlo simulations. In Chapter 3, we study a conformal and relativistic hydrodynamic system,also making use of the AdS/CFT (or holographic) correspondence. This powerful technique, introduced in the context of string theory, becomes extremely relevant when one needs to study strongly correlated systems. In this case indeed, standard perturbative approaches usually fail: the holographic duality can be thought as a valid and complementary approach to investigate these important systems.

Acknowledgements

I would like to thank all the people who participated to the writing of this thesis: to them is devoted all my gratitude. Firstly, and most importantly, I wish to thank *Nico* and *Andrea*: they were to me more than just supervisors and collaborators, helping me during the last three years with their precious advices, not only in Physics, but for my life in general.

A special thank goes to all the other people who collaborated with me in the writing the three articles on which the thesis is based, rigorously in alphabetic order: Alessandro, Daniel, Gianluca, Marco and Michele.

Of course, I can not forget to mention all the people who supported and sustained me during the PhD: all my family, my parents and my sister Claudia. With their words they always encouraged me and gave me the strength to go on and reach the goal.

Last but not least, I would like to thank my girlfriend Deia: with her I shared the happiest and hardest moments in these years and she has always been an important presence in my life, being close to me when I needed her.

Contents

Abstract iii

Acknowledgements v

1 Introduction 1
- 1.1 Critical phenomena . . . 1
- 1.2 Renormalization Group . . . 2
- 1.3 Conformal field theories . . . 4

2 Conformal Perturbation Theory 7
- 2.1 Conformal Field Theories . . . 7
  - 2.1.1 The conformal group . . . 7
  - 2.1.2 Conformal invariance and Field Theory . . . 10
    - Representations of the Conformal Group at classical level . . . 10
    - The stress-energy tensor . . . 12
    - Representations of the Conformal Group at quantum level . . . 12
    - Conformal Ward Identities . . . 14
  - 2.1.3 Radial quantization and OPE . . . 15
    - Remarks on quantization . . . 15
    - States in radial quantization . . . 16
    - Example: two-point function in radial quantization . . . 18
    - Unitarity bounds . . . 18
    - Operator Product Expansion (OPE) . . . 19
- 2.2 Conformal Perturbation Theory . . . 21
  - 2.2.1 The underlying hypothesis . . . 21
  - 2.2.2 A basic example . . . 24
  - 2.2.3 Higher order expansion . . . 26
  - 2.2.4 Advantages of the approach . . . 27
- 2.3 $SU(2)$ gauge theory in $3+1$ dimensions . . . 28
  - 2.3.1 Model and analytic results . . . 30
  - 2.3.2 Numerical results for $SU(2)$ Yang-Mills theory . . . 33
    - Setup of the lattice calculation . . . 33
    - Comparison with CPT predictions . . . 36
    - Technical details . . . 41
    - Systematic uncertainties . . . 42
  - 2.3.3 Concluding remarks . . . 43

2.4 Energy-trapped Ising Model . . . 43
2.4.1 The model and the trap size scaling . . . 44
Two-point functions . . . 46
Wilson coefficients in the $d = 3$ case . . . 46
2.4.2 Conversion to the lattice and numerical results . . . 48
Lattice implementation . . . 48
One-point functions . . . 49
Two-point functions . . . 51
2.4.3 Discussion . . . 52

3 Magneto-thermal transport **55**
3.1 Introduction . . . 55
3.2 Magnetohydrodynamics . . . 57
3.2.1 The diffeomorphism and $U(1)$ gauge symmetry Ward identities 58
3.2.2 Equilibrium magnetohydrodynamics . . . 60
3.2.3 AC diffusivities in magnetohydrodynamics . . . 60
3.2.4 Constraining hydrodynamic correlators with the Ward identities 64
3.3 Revisiting the dyonic black hole . . . 66
3.3.1 An incoherent conductivity . . . 68
3.3.2 Matching the correlators . . . 70

4 Final discussion **73**

A Mellin transform technique **75**

B Additional details on magnetohydrodynamics **77**
B.1 Standard formulation of relativistic magnetohydrodynamics . . . 77
B.2 Miscellaneous additional results . . . 78

Bibliography **81**

Chapter 1

Introduction

1.1 Critical phenomena

One of the most interesting and studied topics in statistical physics is, with no many doubts, the physics of phase transitions. Phase transitions occur when the macroscopic physical properties of a given medium change as a consequence of a change of external condition (such as temperature, pressure, etc.). According to the modern classification, phase transitions can be distinguished in two broad categories: first- and second-order phase transition.

The first are characterized by the fact that they involve a latent heat and two phases coexist during the passage. In particular, during the transition a usually large amount of heat can be absorbed or released by the system: the solid-liquid and the liquid-vapor transition of the water are typical examples. On the other side, the latter, is a sharp transition with no coexistence of different phases nor the presence of any latent heat. A very famous example of this kind of transition is the ferromagnetic transition of a metal at the Curie point.

Nevertheless, the most important feature of this kind of transition is the divergence of the correlation length, which indeed becomes a key observation to define a phase transition to be of the second order. This fact brings the consequence that the system loses any characteristic length (or equivalently any characteristic mass): it means that we could not find differences observing the fluctuations in a limited part of the system or in a larger one. At this point the correlation functions start following a power-law behavior, instead of the usual exponential-decay.

This observation leads to conclude that in a critical phenomenon the details of the microscopic interactions are not relevant, rather the behavior is determined by the general symmetry properties of the system. This feature of critical phenomena is known as *Universality*: even very different systems (from a microscopical point of view) show the same macroscopic behavior if they belong to same universality class (i.e. they respect the same symmetries at microscopic level). For instance, the water at the critical point and a ferromagnet at the Curie point belong to the same universality class (the Ising class) even though they may seem very different systems at a first sight.

In order to distinguish between different universality classes, an important mark is given by the so called *critical exponents*. At the critical point, not only the correlation functions show a power-law behavior, but also other physical quantities have similar scaling laws. The values of these exponents is the same for any system belonging to a certain universality class, as reported in table 1.1. Besides the already cited liquid-vapor critical point and the ferromagnet at critical point, in table 1.1 are reported the critical exponents of binary mixtures (multicomponent fluid mixtures) and micellar systems (mixtures of surfactants in a liquid).

System	α	β	γ	ν
liquid-vapor critical point	0.111(2)	0.324(2)	1.14(5)	0.6297(4)
uniaxial ferromagnet	0.111(5)	0.325(2)	1.25(2)	0.6300(17)
binary mixture	0.111(2)	0.327(3)	1.236(9)	0.6297(7)
micellar systems		0.329(3)	1.26(5)	0.63(1)

TABLE 1.1: Experimental values of the critical exponents for different systems[1]. The critical exponent reported are α, β, γ and ν that describe the power law exponents at the critical point respectively for the specific heat, the system order parameter (as the magnetization for the ferromagnet), its second moment (as the susceptibility) and the correlation length.

1.2 Renormalization Group

One of the best and most used tools to understand critical phenomena is the Renormalization Group (RG). The first application of the theory comes from renormalization problems in particle physics (from where the name derives, even if misleading: the set of transformation is more properly a *semigroup*). Only starting from the '70s, with the work of Kenneth Wilson the ideas of RG found applications to statistical physics.

The modern theory can be formulated in a very precise and consistent mathematical way, but we will follow a more pragmatic approach (see for instance ref. [2]) based on scaling arguments, to give an idea of what RG is and how it can be useful for us. The common idea of all RG studies is to re-express the parameters defining a problem in terms of other parameters, while keeping unchanged the physical aspects of the problem. To fix the idea in mind, let us think to a regular lattice with interacting molecules placed at each site of the lattice. Now, if we regroup the microscopic sites into larger clusters and zoom out, we obtain a new coarse-grained system where the clusters are the new elementary units.

Iterating the procedure over and over, the parameters evolve according mathematical equations describing the *renormalization group flow* in the parameter space. This is due to the fact that, at critical point, we do not observe differences with the length scale: the partition functions of the two systems must be the same, but since

we changed the elementary variables, the parameters of the system will change accordingly.

The coarse-graining, that can be parametrized by a factor of scaling b, and the redefinition of the system parameters are a single step of the renormalization group transformations. The set of all the transformations defines a dynamical flow in the parameter space (i.e. the RG flow) and the study of this flow is a precious tool to explain the features of the critical phenomena.

We mentioned that critical points are fixed point in the renormalization group flow, this means that calling $\{K\}$ the set of all the parameters of the theory, fixed points are those for which is true that:

$$R(\{K^*\}) = \{K^*\} \tag{1.1}$$

where R is a step in the RG flow and in general will depend on the specific transformation chosen.

Let us suppose that R is at least differentiable at the critical point, so that the renormalization group equations, linearized about the fixed point, are:

$$K'_a - K^*_a = \sum_b T_{ab}(K_b - K^*_b) \tag{1.2}$$

where $T_{ab} = \frac{\partial K'_a}{\partial K_b}|_{K^*}$. We call ϕ^i_a its left eigenvectors (since we cannot assume T to be symmetric a priori), so that:

$$\sum_a \phi^i_a T_{ab} = \lambda^i \phi^i_b \tag{1.3}$$

Then let us define the scaling variables u_i the following linear combination:

$$u_i = \sum_a \phi^i_a (K_a - K^*_a) \tag{1.4}$$

which under the action of the RG transform multiplicatively as:

$$\begin{aligned} u'_i &= \sum_a \phi^i_a (K'_a - K^*_a) = \sum_{a,b} \phi^i_a T_{ab}(K_b - K^*_b) = \\ &= \sum_b \lambda^i \phi^i_b (K_b - K^*_b) = \lambda^i u_i \end{aligned} \tag{1.5}$$

Now it is very useful to write these eigenvalues in terms of the scaling parameter $\lambda^i = b^{y_i}$, so that we can distinguish three possibilities:

- $y_i > 0$: the field is called *relevant*,
- $y_i < 0$: the field is called *irrelevant*,
- $y_i = 0$: the field is called *marginal*.

As the name may suggest, relevant perturbations are crucial to determine the behavior of the system near the critical point. If we start from a point close to (but not exactly at) the critical point, iterated steps of the RG flow will drive the system away from the fixed point. On the contrary, if we start sufficiently close to the fixed point, irrelevant perturbations will drive the system towards the fixed point. For the marginal ones, we are not able to tell from the linearized equation whether u_i will move away or towards the fixed point.

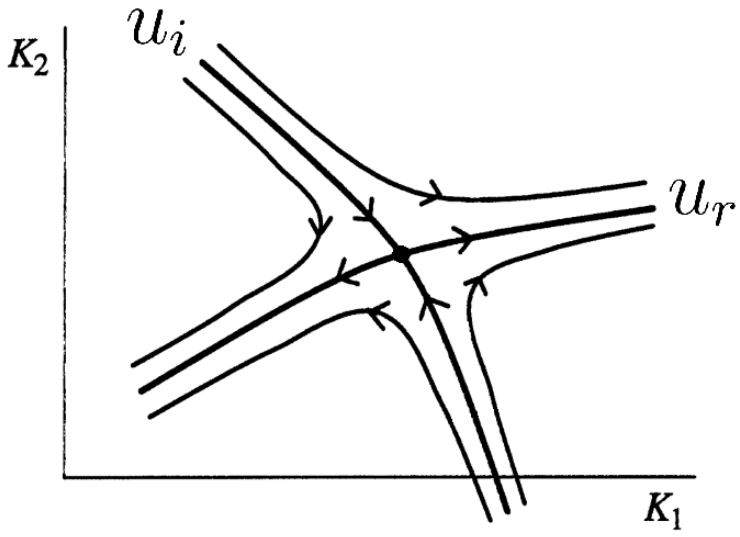

FIGURE 1.1: A two dimensional example of RG flow. Relevant fields drive the system away from the fixed point, meaning that relevant observables are needed to describe the macroscopic behavior of the system.

However, the dynamics of critical phenomena is ruled by the relevant fields. For example, in the uniaxial ferromagnet there are two relevant operators, associated to the temperature and the external magnetic field. The same is true for a simple fluid (where the critical point is determined by the values of pressure and temperature). The formalism introduced, even if so far it is very abstract, can explain the universality of the critical phenomena: if two very different systems have the same kind of relevant eigenvalues of the RG transformations, they will have the same critical behavior. In other words, systems belonging to the same universality class differ only for irrelevant perturbations, meaning that they will have the same scaling laws and critical exponents.

1.3 Conformal field theories

We already mentioned that at fixed points, the action of the Renormalization Group flow leaves the system unchanged, or said in other words the system becomes *scale invariant*. One may wonder what happens if we add scale invariance to a system which is already invariant under the action of the Poincaré group. The answer is that we can not simply add dilatation invariance to get a well defined mathematical

structure, but we need a stronger condition defined by the so called *special conformal transformation*. The set of these transformations realizes the famous *conformal group*, a very important set of transformations we will describe in details in the next sections.

Starting from its rigorous and coherent introduction in the paper by Belavin, Polyakov and Zamolodchikov [3] in 1984, Conformal Field Theory (CFT) rapidly became one of the most studied and used tools in theoretical physics. Possible applications of conformal field theory are truly wide: starting from string theory (where it has become one of the fundamental principles of the theory), it also finds an almost uncountable amount of applications to critical phenomena, and even in many areas of pure mathematics.

The strong constraints imposed by the dilatation invariance, in many cases make the theory simpler to solve because the arbitrary degrees of freedom are considerably reduced: this may be one of the reasons of the great success of conformal field theories in so many and so different areas. Nevertheless, despite the great success and widespread use of conformal field theories, there are many interesting systems (even real ones) which, even if close to a critical point, cannot be described by a CFT.

In the following chapters, we shall see some interesting examples of how one can deform a CFT by perturbing it with different operators. In particular, in chapter 2 we will give a more exhaustive and detailed discussion of conformal field theories and we will describe a mathematical tool to investigate the neighborhood of a critical point when it is perturbed by a relevant perturbation. In chapter 3 instead, we will show how the Gauge/Gravity duality can be applied to get precious insights about a conformal magnetohydrodynamic system.

At a first sight, the two approaches may seem very different: the first, starting from very general assumptions, provides a method to explore the neighborhood of a critical point, while the latter makes use of a conjecture developed in the string theory framework to study more easily a strongly coupled CFT. Actually, both the approaches can be adopted to study conformal field theories perturbed by different kinds of operators. For this reason they can be somehow considered complementary, since starting from very different assumptions they can eventually be used to study the same system from different perspectives.

Chapter 2

Conformal Perturbation Theory

2.1 Conformal Field Theories

Conformal field theories (CFTs) have been widely studied for more than a century and in many different fields. They describe critical behavior of systems at second order phase transition and more in general of those systems that show scale invariance. For this reason they find important application in condensed matter physics, statistical mechanics, quantum field theory and even string theory, where requiring scale invariance leads to important constraints as for instance the allowed space-time dimension.

Nevertheless, it is not possible adding simply scale invariance into a system with Poincaré invariance, so the result is that conformal symmetry is much more constraining (specially in 2 dimensions as we will see later) than ordinary scale invariance. The consequence is that the set of all these transformations forms a group, whose characteristics are going to be investigated in the next section.

2.1.1 The conformal group

By definition, a conformal transformation is a transformation of the coordinates that leave the metric invariant up to a scaling factor:

$$g'_{\mu\nu}(x') = \Omega(x) g_{\mu\nu}(x) \tag{2.1}$$

Obviously, the Poicaré group is a subgroup with the scaling factor $\Omega = 1$, but more in general, conformal transformations are those that preserve angles.

Applying an infinitesimal transformation on the coordinates $x^\mu \to x^\mu + \epsilon^\mu$, we get the infinitesimal generators of the conformal group

$$\partial_\mu \epsilon_\nu + \partial_\nu \epsilon_\mu = f(x)\eta_{\mu\nu} \tag{2.2}$$

by imposing the condition from Eq. 2.1, and taking trace both sides we get:

$$\partial_\mu \epsilon_\nu + \partial_\nu \epsilon_\mu = \frac{2}{d}(\partial \cdot \epsilon)\eta_{\mu\nu} \tag{2.3}$$

By applying an extra derivative, permuting the indices and taking a linear combination we find

$$2\partial_\mu\partial_\nu\epsilon_\rho = +\eta_{\mu\rho}\partial\nu f - \eta_{\nu\rho}\partial\mu f\eta_{\mu\nu}\partial\rho f \tag{2.4}$$

From here it is not difficult to show that holds:

$$(d-1)\partial^2 f(x) = 0 \tag{2.5}$$

That means that the previous equation is meaningless for $d = 1$: any transformation is conformal in 1 dimension, because even the notion of angle does not est. The case $d = 2$ deserves a more detailed discussion later, so let us consider the case $d = 3$ for the moment.

The second derivative of f vanishes, meaning that f can be at most linear in the coordinates:

$$f(x) = A + B_\mu x^\mu, \qquad A, B_\mu \text{ constant} \tag{2.6}$$

Plugging this result back in Eq. 2.4 we see that ϵ can be at most quadratic in the coordinates

$$\epsilon_\mu = a_\mu + b_{\mu\nu}x^\nu + c_{\mu\nu\rho}x^\nu x^\rho, \qquad a_\mu, b_{\mu\nu}, c_{\mu\nu\rho} \text{ constant} \tag{2.7}$$

Eq. 2.2 and 2.4 give constraints on these parameters that hold for all x, we may treat each power of the coordinates separately. It follows that:

- a^μ is free of constraints and it amounts to an infinitesimal transformation
- $b_{\mu\nu} = \alpha\eta_{\mu\nu} + m_{\mu\nu}$ is the sum of an antisymmetric part (corresponding to infinitesimal rigid rotation) and a pure trace part (corresponding to infinitesimal scale transformation)
- $c_{\mu\nu\rho} = \eta_{\mu\rho}b_\nu + \eta_{\mu\nu}b_\mu - \eta_{\nu\rho}b_\mu$, where $b_\mu = \frac{1}{d}c^\sigma{}_{\sigma\mu}$ corresponds to the so-called Special Conformal Transformation, whose corresponding infinitesimal transformation is
$$x'^\mu = x^\mu + 2(x\cdot b)x^\mu - b^\mu x^2 \tag{2.8}$$

The last transformation is the less familiar but it can be shown that corresponds to an inversion plus translation.

By exponentiating the infinitesimal transformations, the finite transformations become:

$$\begin{aligned}
\text{Translation} \qquad & x'^\mu = x^\mu + a^\mu \\
\text{Rigid Rotation} \qquad & x'^\mu = M^\mu_\nu x^\nu \\
\text{Dilatation} \qquad & x'^\mu = \alpha x^\mu \\
\text{SCT} \qquad & x'^\mu = \frac{x^\mu - b^\mu x^2}{1 - 2b\cdot x + b^2x^2}
\end{aligned} \tag{2.9}$$

The generators of Eq. 2.9 are:

$$\begin{aligned} \text{Translation} \quad & P_\mu = -i\partial_\mu \\ \text{Rigid Rotation} \quad & L_{\mu\nu} = i(x_\mu\partial_\nu - x_\nu\partial_\mu) \\ \text{Dilatation} \quad & D = -ix^\mu\partial_\mu \\ \text{SCT} \quad & K_\mu = -i(2x_\mu x^\nu\partial_\nu - x^2\partial_\mu) \end{aligned} \tag{2.10}$$

They satisfy the following algebra:

$$\begin{aligned} \big[D, P_\mu\big] &= iP_\mu \\ \big[D, K_\mu\big] &= -iK_\mu \\ \big[K_\mu, P_\nu\big] &= 2i(\eta_{\mu\nu}D - L_{\mu\nu}) \\ \big[K_\rho, L_{\mu\nu}\big] &= i(\eta_{\rho\mu}K_\nu - \eta_{\rho\nu}K_\mu) \\ \big[P_\rho, L_{\mu\nu}\big] &= i(\eta_{\rho\mu}P_\nu - \eta_{\rho\nu}P_\mu) \\ \big[L_{\mu\nu}, L_{\rho\sigma}\big] &= i(\eta_{\rho\nu}L_{\mu\sigma} + \eta_{\mu\sigma}L_{\nu\rho} - \eta_{\mu\rho}L_{\nu\sigma} - \eta_{\nu\sigma}L_{\mu\rho}) \end{aligned} \tag{2.11}$$

However the generators can be reorganized in the following form in order to get simpler commutation rules:

$$J_{MN} = \begin{pmatrix} L_{\mu\nu} & \frac{K_\mu - P_\mu}{2} & -\frac{K_\mu + P_\mu}{2} \\ -\frac{K_\mu - P_\mu}{2} & 0 & D \\ \frac{K_\mu + P_\mu}{2} & -D & 0 \end{pmatrix}, \quad \text{with } M, N = 1, ..., d+2 \tag{2.12}$$

The antisymmetric matrix J_{MN} is indeed a rotation in a $d+2$-dimensional space-time with signature $(2, d)$, whose commutators are:

$$\big[J_{MN}, J_{RS}\big] = i(\eta_{RN}J_{MS} + \eta_{MS}J_{RN} - \eta_{MR}J_{NS} - \eta_{NS}J_{MR}) \tag{2.13}$$

This shows the isomorphism between the conformal group in d dimensions and the group $SO(d+1, 1)$ with $\frac{1}{2}(d+1)(d+2)$ generators. More in general, it can be shown that the conformal group of a space-time with signature (p, q) is $SO(p+1, q+1)$.

Let us look in more detail the case $d = 2$ where the conformal group is much more powerful. In $d = 2$, Eq.2.3 becomes the Cauchy-Riemann equation:

$$\partial_1\epsilon_1 = \partial_2\epsilon_2, \qquad \partial_1\epsilon_2 = -\partial_2\epsilon_1 \tag{2.14}$$

It is then natural to introduce complex variables $\epsilon(z) = \epsilon_1 + i\epsilon_2$ and $\bar{\epsilon}(\bar{z}) = \epsilon_1 - i\epsilon_2$, with $z, \bar{z} = x_1 \pm ix_2$. For this reason the volume element becomes $ds^2 = dzd\bar{z}$ and under analytic transformation $z \to f(z)$, $\bar{z} \to f(\bar{z})$, the metric transform as $g'_{\mu\nu} = |f(z)|^2 g_{\mu\nu}$. This implies that any analytic transformation corresponds to a conformal transformation in two dimensions and that the $2 - d$ conformal group is infinite dimensional, because any transformation of the kind $\delta z \sim z^n, n > 2$ is allowed.

Then, how can be possible that the conformal group is infinite dimensional only in two dimensions, while it is finite for any $d > 2$? The answer is that we must be more careful in distinguishing between local and global transformations. If $d \geq 3$ any local transformation is automatically also global, while in $d = 2$ we only considered local ones. In order to be global indeed, the transformation must be invertible on the entire Riemann sphere. This additional request reduces the infinite dimensional conformal group to a finite dimensional one, called proper conformal group. The complete set of these transformations is given by:

$$f(z) = \frac{az + b}{cz + d}, \quad \text{with} \quad ad - bc = 1 \tag{2.15}$$

which forms the $SL(2, \mathbb{C})$ group. It is known that this group is isomorphic to $SO(3, 1)$, then if we just look at the global transformations, there are no differences between two and higher dimensions.

2.1.2 Conformal invariance and Field Theory

In the previous section we have shown what conformal invariance is, and at classical level a field theory is conformal if its action is invariant under conformal transformations. At quantum level instead, the situation is not so straightforward: a quantum field theory needs to be regularized in order to make sense, but this procedure introduces a scale in the theory. This scale, in general, breaks the conformal symmetry except at particular values of the parameters, which constitute the renormalization-group fixed points.

Representations of the Conformal Group at classical level

Let us start showing how classical fields transform under conformal transformations. Given an infinitesimal transformation parametrized by ω_g, let T_g be a matrix representation such that the multicomponent field $\phi(x)$ transforms as

$$\phi'(x') = (1 - \omega_g T_g)\phi(x) \tag{2.16}$$

The generator Tg must be added to the space-time part of the transformation 2.11 in order to obtain the full generator of the symmetry. Then, in order to find the complete form of these generators, we define the action of the generators at the point $x = 0$ and subsequently we translate the action of the generators at an arbitrary point by using the Baker-Campbell-Hausdorff (BCH) formula. As an example, let us consider the angular momentum: firstly we introduce the spin matrix representation $S_{\mu\nu}$ to define the action of the angular momentum on the field $\phi(0)$:

$$L_{\mu\nu}\phi(0) = S_{\mu\nu}\phi(0) \tag{2.17}$$

Then we can translate the generator $L_{\mu\nu}$ with the BCH formula, finding

$$e^{ix^\rho P_\rho} L_{\mu\nu} e^{-ix^\rho P_\rho} = S_{\mu\nu} - x_\mu P_\nu + x_\nu P_\mu \tag{2.18}$$

This allow us to write the action of the generators on the fields:

$$\begin{aligned} P_\mu \phi(x) &= -i\partial_\mu \phi(x) \\ L_{\mu\nu}\phi(x) &= i(x_\mu \partial_\nu - x_\nu \partial_\mu)\phi(x) + S_{\mu\nu}\phi(x) \end{aligned} \tag{2.19}$$

We can proceed in the same way for the full conformal group. The subgroup that leaves the origin invariant is generated by rotations, dilatations and special conformal transformations. What we have obtained by removing the translation from the complete algebra 2.11 is the Poincaré algebra augmented by dilatations. Calling $S_{\mu\nu}, \tilde{\Delta}$, and k_μ the respective values of the generators $L_{\mu\nu}, D$ and K_μ at $x = 0$, the reduced algebra takes the form:

$$\begin{aligned} \left[\tilde{\Delta}, S_{\mu\nu}\right] &= 0 \\ \left[\tilde{\Delta}, k_\mu\right] &= -ik_\mu \\ \left[k_\mu, k_\nu\right] &= 0 \\ \left[k_\rho, S_{\mu\nu}\right] &= i(\eta_{\rho\mu}k_\nu - \eta_{\rho\nu}k_\mu) \\ \left[S_{\mu\nu}, S_{\rho\sigma}\right] &= i(\eta_{\rho\nu}S_{\mu\sigma} + \eta_{\mu\sigma}S_{\nu\rho} - \eta_{\mu\rho}S_{\nu\sigma} - \eta_{\nu\sigma}S_{\mu\rho}) \end{aligned} \tag{2.20}$$

With these commutation rules we are able to apply the BCH formula as we have done before for the angular momentum also for the other generators:

$$\begin{aligned} D\phi(x) &= (-ix^\nu \partial_\nu + \tilde{\Delta})\phi(x) \\ K_\mu \phi(x) &= (k_\mu + 2x_\mu \tilde{\Delta} - x^\nu S_{\mu\nu} - 2ix_\mu x^\nu \partial_\nu + ix^2 \partial_\mu)\phi(x) \end{aligned} \tag{2.21}$$

From the Shur's lemma, we know that any matrix that commutes with all the generators $S_{\mu\nu}$ must be a multiple of the identity. So if we demand that the field $\phi(x)$ belong to an irreducible representation of the Lorentz group, then the matrix $\tilde{\Delta}$ is a multiple of the identity and the algebra 2.20 forces all the matrices k_μ to vanish. $\tilde{\Delta}$ is then a simple number, manifestly equal to $-i\Delta$, where Δ is the scaling dimension of the field ϕ.

We are now ready to find the finite conformal transformation for a general field $\phi(x)$. For a scalar field ($S_{\mu\nu} = 0$), we have:

$$\phi'(x') = \left|\frac{\partial x'}{\partial x}\right|^{-\frac{\Delta}{d}} \phi(x) = \Omega(x)^{\frac{\Delta}{2}} \phi(x) \tag{2.22}$$

where $\Omega(x)$ is the conformal scaling factor of Eq. 2.1. A field transforming such as in Eq. 2.22 is called a primary field. If the field $\phi(x)$ belongs to an irreducible representation R of the Lorentz group with non zero spin instead, the transformation

rule will depend also on the rotation matrix M^μ_ν defined in 2.9, so that the result becomes:

$$\phi'(x') = \Omega(x)^{\frac{\Delta}{2}} R[M^\mu_\nu]\phi(x) \tag{2.23}$$

where $R[M^\mu_\nu]$ is a representation matrix acting on the indices of $\phi(x)$.

The stress-energy tensor

Let us look now at the consequences on the stress-energy tensor brought by an arbitrary transformation of the coordinates $x^\mu \to x^\mu + \epsilon^\mu$. The action change as follows:

$$\begin{aligned} \delta S &= \int d^d x T^{\mu\nu} \partial_\mu \epsilon_\nu \\ &= \frac{1}{2} \int d^d x T^{\mu\nu} (\partial_\mu \epsilon_\nu + \partial_\nu \epsilon_\mu) \end{aligned} \tag{2.24}$$

We assumed the stress tensor $T^{\mu\nu}$ to be symmetric (indeed the stress tensor can always be made symmetric if the theory is invariant under rotation). Then by recalling Eq. 2.2 the previous expression becomes:

$$\delta S = \frac{1}{d} \int d^d x T^\mu_\mu \partial_\rho \epsilon^\rho \tag{2.25}$$

Note that the tracelessness of the stress-energy tensor implies the invariance of the action under conformal transformations. The converse is not true, because $\partial_\rho \epsilon^\rho$ is not an arbitrary function.

However, even if it is not true in general, under very general conditions it can be proven that also the converse is true (see [4] for details). Then, in the large majority of field theory at the classical level, conformal invariance is a consequence of scale invariance and Poincaré invariance.

Representations of the Conformal Group at quantum level

In this sections we analyze the consequences of conformal invariance on a field theory at quantum level, in particular let us start looking at the constraints given by conformal invariance on two- and three-point correlation function of primary scalar fields.

The two point function is defined as follows:

$$\langle \phi_1(x_1)\phi_2(x_2) \rangle = \frac{1}{Z} \int [D\Phi] \phi_1(x_1)\phi_2(x_2) e^{-iS[\phi]} \tag{2.26}$$

where ϕ_1 and ϕ_2 are two primary scalar fields (not necessarily distinct), ϕ is the set of all functionally independent field of the theory and $S[\phi]$ is the conformally invariant action.

Since the integration measure and the action are assumed to be conformally invariant, Eq. 2.22 leads to the following transformation rule for the correlation function:

$$\langle \phi_1(x_1)\phi_2(x_2)\rangle = \left|\frac{\partial x'}{\partial x}\right|^{\frac{\Delta_1}{d}}_{x=x_1} \left|\frac{\partial x'}{\partial x}\right|^{\frac{\Delta_2}{d}}_{x=x_2} \langle \phi_1(x'_1)\phi_2(x'_2)\rangle \tag{2.27}$$

The result can be straightforwardly generalized to higher-point function and to fields with non-zero spin.

Firstly, ordinary translation invariance implies that a correlation function does not depend on two independent coordinates, but rather only on their differences $x_1 - x_2$ while rotation invariance tells us that it should depend in particular on the distance $|x_1 - x_2|$. Putting together this means:

$$\langle \phi_1(x_1)\phi_2(x_2)\rangle = f(|x_1 - x_2|) \tag{2.28}$$

If we consider now a scale transformation $x \to \lambda x$, Eq. 2.27 becomes:

$$\langle \phi_1(x_1)\phi_2(x_2)\rangle = \lambda^{\Delta_1+\Delta_2}\langle \phi_1(\lambda x_1)\phi_2(\lambda x_2)\rangle \tag{2.29}$$

From the two previous equations we understand that:

$$\langle \phi_1(x_1)\phi_2(x_2)\rangle = \frac{C_{12}}{|x_1 - x_2|^{\Delta_1+\Delta_2}} \tag{2.30}$$

where C_{12} is a constant coefficient.

Finally we must impose the invariance under SCT ($\Omega(x) = (1 - 2b\cdot x + b^2x^2)^{-d}$) we get the following constraint:

$$\frac{C_{12}}{|x_1 - x_2|^{\Delta_1+\Delta_2}} = \frac{C_{12}}{\gamma_1^{\Delta_1}\gamma_2^{\Delta_2}} \frac{(\gamma_1\gamma_2)^{\frac{\Delta_1\Delta}{2}}}{|x_1 - x_2|^{\Delta_1+\Delta_2}} \tag{2.31}$$

with $\gamma_i = (1 - 2b\cdot x_i + b^2x_i^2)$. This constraint is identically satisfied only if $\Delta_1 = \Delta_2$: this means that two primary fields are correlated only if they have the same scaling dimension:

$$\langle \phi_1(x_1)\phi_2(x_2)\rangle = \begin{cases} \frac{C_{12}}{|x_1-x_2|^{2\Delta_1}} & \text{if} \quad \Delta_1 = \Delta_2 \\ 0 & \text{if} \quad \Delta_1 \neq \Delta_2 \end{cases} \tag{2.32}$$

Actually, the constant C_{12} can be absorbed in the definition of the fields, so that the two-points function is completely fixed, with no undetermined constant: $\langle \phi_i(x_i)\phi_j(x_j)\rangle = \delta_{ij}|x_i - x_j|^{-2\Delta_i}$.

Following the same steps, also the three-points function can be constrained by conformal invariance and for three scalar primary fields we get:

$$\langle \phi_1(x_1)\phi_2(x_2)\phi_3(x_3)\rangle = \frac{C_{123}}{x_{12}^{\Delta_1+\Delta_2-\Delta_3}x_{13}^{\Delta_1+\Delta_3-\Delta_2}x_{23}^{\Delta_2+\Delta_3-\Delta_1}} \tag{2.33}$$

where $x_{12} = |x_1 - x_2|$ and C_{123} is an undetermined constant.

After the successful results for 2- and 3-points function, one may expect that similar procedures can be adopted also for generic n-points functions. Unfortunately this impressive performance stops at $n = 3$. Indeed, when $n \geq 4$ it is possible to construct conformal invariant ratios and the n-point function may have an arbitrary dependence on these ratios. For instance, the 4-points function becomes:

$$G^{(4)}(x_1, x_2, x_3, x_4) = F\Big(\frac{x_{12}x_{34}}{x_{13}x_{24}}, \frac{x_{12}x_{34}}{x_{23}x_{14}}\Big) \prod_{i<j}^{4} x_{ij}^{\Delta/3-\Delta_i-\Delta_j} \tag{2.34}$$

with $\Delta = \sum_{i=1}^{4} \Delta_i$

Conformal Ward Identities

Ward identities are identities between correlation functions that reflect symmetries possessed by the theory: they are the quantum version of classical current conservation associated to a continuous symmetry.

An infinitesimal symmetry transformation on the field $\phi(x)$ can be written in terms of generator as:

$$\delta\phi'(x) = -i\omega_a T_a \phi(x) \tag{2.35}$$

being T_a the generators of the transformation and ω_a the infinitesimal parameters associated to the symmetry. Then, calling j_a^μ the conserved current associated to the symmetry 2.35, the corresponding Ward identity can be derived in the functional integral formulation of correlation functions. The results reads:

$$\partial_\mu \langle j_a^\mu(x)\phi(x_1)...\phi(x_n)\rangle = -i\sum_{i=1}^{n} \delta(x - x_i)\langle\phi(x_1)...T_a\phi(x_i)...\phi(x_n)\rangle \tag{2.36}$$

Let us see now what happens for conformal transformations. The generator associated to translational invariance is $P_\mu = -i\partial_\mu$, consequently the associated Ward identity is:

$$\partial_\mu \langle T_\nu^\mu X\rangle = -i\sum_i \delta(x - x_i)\partial_\nu^i \langle X\rangle \tag{2.37}$$

where X denotes a general collection of fields $\phi_1...\phi_n$.

The conserved current associated to Lorentz invariance (once the stress-energy tensor has been made symmetric) is

$$j^{\mu\nu\rho} = T^{\mu\nu}x^\rho - T^{\mu\rho}x^\nu \tag{2.38}$$

Recalling the corresponding generator $T_a = -i(x_\nu\partial_\rho - x_\rho\partial_\nu) + S_{\nu\rho}$, and substituting these expressions in 2.36, we obtain:

$$\partial_\mu \langle (T^{\mu\nu}x^\rho - T^{\mu\rho}x^\nu)X\rangle = \sum_i \delta(x - x_i)\big[(x_i^\nu\partial_i^\rho - x_i^\nu\partial_i^\rho) - iS_i^{\nu\rho}\big]\langle X\rangle \tag{2.39}$$

Acting with the derivatives on the stress-energy tensor or on the coordinates, the previous expression can be further simplified using 2.37, leading to:

$$\langle (T^{\nu\rho} - T^{\nu\rho})X\rangle = -i\sum_i \delta(x-x_i)S_i^{\nu\rho}\langle X\rangle \tag{2.40}$$

The previous expression states that the stress-energy tensor is symmetric within correlation function, except at the contact points (i.e. the positions of the other fields of the correlator). The last identity we are going to analyze concerns the dilatation invariance: the associate current can be written as

$$j_D^\mu = T^{\mu\nu}x_\nu \tag{2.41}$$

The infinitesimal generator is $D = -ix^\nu\partial_\nu - i\Delta$, then the Ward identity is:

$$\partial_\mu\langle T^\mu_\nu x^\nu X\rangle = -\sum_i \delta(x-x_i)\big[x_i^\nu\partial_\nu^i + \Delta\big]\langle X\rangle \tag{2.42}$$

Again, acting with the derivative and using Eq. 2.36 we find:

$$\langle T^\mu_\mu X\rangle = -\sum_i \delta(x-x_i)\Delta_i\langle X\rangle \tag{2.43}$$

Last equation tells us that the stress energy tensor of a conformal quantum field theory is traceless up to contact terms.

Equations 2.37, 2.40 and 2.43 are the Ward Identities associated with conformal invariance.

2.1.3 Radial quantization and OPE

In the previous section we have talked about correlation function of local operators and we have seen how they are constrained by conformal symmetry via the Ward identities. However, we have never made use of operator formalism or Hilbert space and indeed correlation functions could be in principle obtained in the path integral formalism.

In the next section, we shall see a parallel approach based on Hilbert space and operator formalism, which will be very useful for understanding many questions that would be hard to tackle such as Unitary Bounds and Operator Product Expansion (OPE).

Remarks on quantization

When we construct an Hilbert space in a quantum field theory, we need to choose a foliation of space-time. Each leaf of the foliation is endowed with its own Hilbert space. We can define in states $|\psi_{in}\rangle$ and out states $\langle\psi_{out}|$ by inserting operators respectively in the past or in the future of a given surface. The overlap of the two states

gives the correlation function $\langle\psi_{out}|\psi_{in}\rangle$ if they belong to the same foliation. On the other side, if they live on different foliations, there exists an unitary operator U that connects the two states, such that the correlation function is:

$$\langle\psi_{out}|U|\psi_{in}\rangle \tag{2.44}$$

Usually, one should choose a proper foliation according to the symmetry of the system, for instance in the case of Poincaré invariance it is convenient to foliate the space by surfaces of constant time. With this choice, the evolution operator is simply given by the exponentiation of the generator P^0, i.e. $U = \exp(iP^0\Delta t)$.

Nevertheless, this foliation is not the best choice in the case of CFTs, where the best choice is given by S^{D-1} spheres of constant radius. This is called radial quantization. We will assume that the spheres have the center at $x = 0$, but of course we could quantize with respect to any other point and get the same correlators.

In radial quantization, the evolution operator is obtained by exponentiating the dilatations generator D, that will play the role of the Hamiltonian:

$$U = e^{iD\Delta\tau} \tag{2.45}$$

where $\tau = \log r$. The states living on the sphere are then classified according to their scaling dimension:

$$D|\Delta\rangle = i\Delta|\Delta\rangle \tag{2.46}$$

and by their $SO(D)$ splin l:

$$M_{\mu\nu}|\Delta, l\rangle_a = S^b_{\mu\nu,a}|\Delta, l\rangle_b \tag{2.47}$$

since the angular momentum is the only generator that commutes with D. Note also that the matrices $S_{\mu\nu}$ acting on the spin indices are non-zero only for non-zero spin.

States in radial quantization

Now we will see how to generate states in radial quantization and what is their relation with operators. We already know that states are generated by inserting operators inside the spheres. This means that the vacuum state $|0\rangle$ corresponds to inserting nothing and its dilatation eigenvalue (i.e. the energy of the state) is simply zero.

If we insert an operator with scaling dimension Δ at the origin $\mathcal{O}_\Delta(x = 0)$, the corresponding state $|\Delta\rangle$ has energy equal to Δ, indeed:

$$D|\Delta\rangle = D\mathcal{O}_\Delta(x = 0)|0\rangle = [D, \mathcal{O}_\Delta(x = 0)]|0\rangle = i\Delta|\Delta\rangle \tag{2.48}$$

where we used the commutation relations

Finally, if the operator is inserted at certain $x \neq 0$, the corresponding state is not an eigenstate of D, as dilatations move the insertion point. In detail, this state is a

superposition of states with different energies:

$$|\Psi\rangle = \mathcal{O}_\Delta(x)|0\rangle = e^{iPx}\mathcal{O}_\Delta(0)e^{-iPx}|0\rangle = e^{iPx}|\Delta\rangle = \sum_n \frac{1}{n!}(iPx)^n|\Delta\rangle \tag{2.49}$$

In fact, the operator P_μ acts as the creation operator in radial quantization, and when it acts on a state $|\Delta$, it raises its energy by one unit. In the same way the operator K_μ is the annihilation operator and it lowers the energy by one unit. This becomes evident recalling the commutation relations of these operators, which are:

$$\begin{aligned}[D, P_\mu] &= iP_\mu \\ [D, K_\mu] &= -iK_\mu\end{aligned} \tag{2.50}$$

With this algebraic construction of the states, becomes clearer the notion of primary fields, namely the fields which are annihilated by K_μ. In order for a theory to be unitary, the energy spectrum must be bounded by below, so if we keep hitting with K_μ on a general state, at a certain point we must find a state that is annihilated (namely a primary field).

Note that the correspondence between states and operators is a one-to-one correspondence. This means that inserting a local operator at the origin, we construct a state with scaling dimension Δ that is annihilated by K_μ, but also the converse is true. Given a state with scaling dimension Δ which is annihilated by K_μ, we can construct a local primary operator. In order to construct an operator, we must define its correlation function with other operators. It is easy to see that

$$\langle\phi_1\phi_2...\mathcal{O}_\Delta(0)\rangle = \langle 0|\phi_1\phi_2...|\Delta\rangle \tag{2.51}$$

is a good definition which satisfies all the usual transformation properties dictated by conformal invariance.

Finally, it is interesting looking at the definition of conjugate operators in radial quantization. Let us start with the operators K_μ and P_μ: the first can be obtained by applying the inversion operator $\mathcal{R}$ twice on the second:

$$K_\mu = \mathcal{R}P_\mu\mathcal{R} \tag{2.52}$$

since a special conformal transformation is obtained by inversion followed by translation followed by inversion. Moreover, we previously identified these two operators as the creation and annihilation operators, so it is quite natural to try to define the conjugation operator as the inversion, so that

$$K_\mu = P_\mu^\dagger \tag{2.53}$$

Then, given a state $\Psi\rangle = \phi(x)|0\rangle$, its conjugate is given by

$$\langle\Psi| = \langle 0|[\phi(x)]^\dagger, \quad \text{with} \quad [\phi(x)]^\dagger = r^{-2\Delta_\phi}\phi(\mathcal{R}x) = \mathcal{R}[\phi(x)] \tag{2.54}$$

where r is the radial distance of x expressed in radial coordinates $x = (r, \vec{n})$.

From last equation, it also follows that in a unitary theory, correlation functions are $\mathcal{R}$-reflection positive

$$\langle 0|[\phi(y)]^\dagger[\phi(x)]^\dagger ...\phi(x)\phi(y)|0\rangle > 0. \tag{2.55}$$

Example: two-point function in radial quantization

For a better understanding, it is useful considering a brief example: the two-point function of scalar fields. We know that $\phi(x_1)|0\rangle = e^{iPx_1}|\Delta_\phi\rangle$ and from Eq. 2.54 we can build its conjugate, so that we get:

$$\langle 0|\phi(x_1)\phi(x_2)|0\rangle = r_2^{-2\Delta_\phi}\langle\Delta_\phi|e^{-iK\mathcal{R}x_2}e^{iPx_1}|\Delta_\phi\rangle \tag{2.56}$$

Expanding in series inside the mean value we get

$$\langle 0|\phi(x_1)\phi(x_2)|0\rangle = \frac{1}{r_1^{\Delta_\phi}r_2^{\Delta_\phi}}\sum_N \langle N, \vec{n}_2|N, \vec{n}_1\rangle \left(\frac{r_1}{r_2}\right)^{\Delta+n} \tag{2.57}$$

where the state $|N, \vec{n}\rangle = \frac{1}{N!}(P_\mu \vec{n}^\mu)^N|\Delta\rangle$ and we used the fact that the expectation value of product of operator involving different power of P_μ and K_μ is zero since two states with different energies are orthogonal.
This means that the coefficients of the expansion take the form $\langle\Delta|KKK...PPP|\Delta\rangle$, namely they are certain matrix elements which can be evaluated just using conformal algebra. The computation is quite simple for the 2-point function:

$$\begin{aligned}\langle\Delta|K_\mu P_\nu|\Delta\rangle &= \langle\Delta|[K_\mu, P_\nu]|\Delta\rangle = \\ &= \langle\Delta|2i(D\delta_{\mu\nu} - M_{\mu\nu})|\Delta\rangle = \Delta\delta_{\mu\nu}\end{aligned} \tag{2.58}$$

but it can be generalized to the case of multi-point function. In practice it is much simpler using the constraints fixed by conformal invariance, but in any case it is important to show that radial quantization works and it can be adopted as an alternative approach in more complex cases where the only kinematics is not sufficient.

Unitarity bounds

The first example of how radial quantization may help in deriving some interesting result is the case of unitarity bounds. This famous result tells us that the dimension of a traceless primary filed in a unitary theory must be above a minimal allowed value $\Delta \geq \Delta_{min}(l)$, depending on the spin l, such as

$$\begin{aligned}\Delta_{min}(l) &= l + d - 2, \quad \text{it} \quad l = 1, 2, 3... \\ \Delta_{min}(0) &= \frac{d}{2} - 1\end{aligned} \tag{2.59}$$

Similar bound can be derived for antisymmetric tensor and fermionic representations of the Lorentz group. In what follows we will show a sketch of the proof. Let us consider the matrix element

$$A_{\nu\mu} = \langle \Delta, l | K_\nu P_\mu | \Delta, l \rangle \tag{2.60}$$

The corresponding eigenvalues will be necessarily positive in a unitary theory. Let us suppose that there exist a negative eigenvalue $\lambda < 0$ with χ_μ the corresponding eigenvector.Then the state $|\psi\rangle = \chi_\mu P_\mu |l\rangle$ will have negative norm:

$$\langle \psi | \psi \rangle = \chi^\dagger A \chi = \lambda \chi^\dagger \chi < 0 \tag{2.61}$$

that clearly violates the unitarity of the theory.

Now, using $[K_\nu, P_\mu] \sim i(D\delta_{\mu\nu} - M_{\mu\nu})$ we see that the eigenvalues of A receive two contributions, the first proportional to Δ, while the second will be the eigenstates of an Hermitian matrix depending on the spin:

$$B_{\nu\{t\}\mu\{s\}} = \langle \{t\} | i M_{\mu\nu} | \{s\} \rangle \tag{2.62}$$

($\{s\}, \{t\}$ are the spin indices). The condition $\lambda_A \geq 0$ is equivalent to $\Delta \geq \lambda_{max}(B)$ (i.e. the maximum eigenvalue of B). The computation of these eigenvalues can be done in analogy with the treatment of spin-orbit interaction in quantum mechanics. Performing all the computation one finds (for details see [5]):

$$\lambda_{max}(B) = d - 2 + l, \quad \text{for} \quad l \geq 1 \tag{2.63}$$

which proves the first of the unitarity bounds.

What happens if we consider matrix elements with more K and P? Actually, when $l \geq 1$, the constraint 2.63 is a necessary and sufficient condition to have unitarity at all levels. When $l = 0$ instead, a stronger bound comes from the second level, namely from:

$$A_{\mu\nu\,\rho\sigma} = \langle \Delta | K_\mu K_\nu P_\rho P_\sigma | \Delta \rangle \tag{2.64}$$

we obtain

$$\Delta(l = 0) \geq \frac{d}{2} - 1 \tag{2.65}$$

Which is the second of the previous unitarity bounds.

Operator Product Expansion (OPE)

The notion of OPE comes from usual Quantum Field Theory and it is introduced to define the product of two local operators (in the limit when they are very close to each other) as a series of operators inserted at the midpoint. This kind of approach offers a non-perturbative approach to QFT, and not only it still holds in Conformal

Field Theory, but it acquires additional and very powerful properties thanks to a connection with radial quantization.

Let us now derive OPE using radial quantization. Consider two operators inserted inside a sphere as shown in figure 2.1:

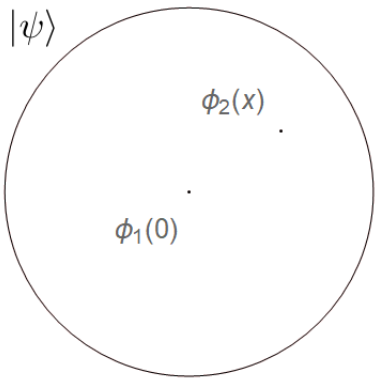

FIGURE 2.1: The state $|\psi\rangle$ is generated by the insertion of the two operators inside the sphere.

They generate the state $|\psi\rangle = \phi_2(x)\phi_1(0)|0\rangle$ on the surface of the sphere. Moreover, this state can be always written as an expansion into the basis of energy (i.e. dilatation) eigenstates:

$$|\psi\rangle = \sum_n c_n |E_n\rangle, \quad c_n = c_n(x) \tag{2.66}$$

But from state-operator correspondence, we know that each state $|E_n\rangle$ is in a one-to-one correspondence with operators (primary or descendants, i.e. derivatives of primaries). Thus, we can write:

$$\phi_2(x)\phi_1(0)|0\rangle = \sum_{\mathcal{O} \text{ primaries}} C_{\mathcal{O}}(x, \partial_y)\mathcal{O}(y)|_{y=0}|0\rangle \tag{2.67}$$

where $C_{\mathcal{O}}(x, \partial_y)$ is intended as a power series in ∂_y. This simple argument proves the existence of an OPE.

However, there is an important difference with the usual definition of OPE given in QFT, where it is usually used only in the asymptotic short-distance limit. In particular, since in a CFT the OPE can be understood as an expansion in a Hilbert space, the OPE is not just an asymptotic expansion, but is actually a convergent series expansion at finite point separation.

We just proved the existence of OPE, so now we may ask if it is possible to determine the structure of the coefficients. The coefficients can be constrained by asking they are consistent with conformal algebra. For example, let us focus on a certain

term of the expansion:

$$\phi_2(x)\phi_1(0)|0\rangle = \frac{\text{const.}}{|x|^k}[\mathcal{O}(0)+...]|0\rangle \; + \; \text{contributions of other primaries} \tag{2.68}$$

where the "..." stand for terms containing the descendants of $\mathcal{O}$. The power of k can be determined by acting with D on both sides. It is straightforward to conclude that $k = \Delta_1 + \Delta_2 - \Delta_{\mathcal{O}}$. Also the subsequent descendant terms can be fixed (by acting with K_μ instead of D) with the result that conformal invariance fixes completely the function of $C_{\mathcal{O}}(x, \partial_y)$, up to a numerical constant:

$$\sum_{\mathcal{O}} \lambda_O C_{\mathcal{O}}(x, \partial_y)\mathcal{O}(y)|_{y=0}|0\rangle, \quad \text{with} \quad \lambda_O \text{ free parameter} \tag{2.69}$$

The above procedure is useful from a conceptual point of view, but it is not the smartest way to compute the function $C_{\mathcal{O}}(x, \partial_y)$. In practice it is much easier to use OPE to reduce an n-point function to an $(n-1)$-point function and fixing the function from the knowledge of the multi-point functions.

2.2 Conformal Perturbation Theory

In the previous section we discussed some properties of the conformal field theories, which describe physical system at the critical point (i.e. at second order phase transition point). Nevertheless, most of the interesting physical systems are not exactly at the transition point, but away from criticality. In particular, when the critical system is perturbed by a relevant operator some problems may occur because the corrections to the conformal correlation function are typically afflicted by infrared divergences.

In the next sections we will present a general method to deal with conformal field theories perturbed by relevant operators, since the standard approach based on the Gell-Mann and Low theorem is not useful in this situation. The general idea presented in [6] is to express the short distance behavior using the OPE so that the perturbative and non-perturbative contributions split up. The non-perturbative behavior is encoded in the vacuum expectation values (VEV) of the local operators, while the Wilson coefficients include the part that can be calculated perturbatively.

2.2.1 The underlying hypothesis

In order to show the general approach to extract the short distance behavior of correlator functions, we have to introduce first a list of underlying hypothesis. Let us now introduce the action of the model we are going to analyze.

$$S = S_{\text{CFT}} - \int dx \sum_i m_B^i \mathcal{O}_{iB}(x) \tag{2.70}$$

The model represents a D-dimensional euclidean conformal field theory, perturbed by one or more relevant operators $\mathcal{O}_i$ (of canonical dimensions $0 < x_D i$) with dimensionful couplings m^i ("generalized masses" of dimensions $y_i = D - x_i$). In what follows we may refer also to the unperturbed model as "massless theory" while the complete theory will be the "deformed theory".

We assume the massless theory to be at least perturbatively UV renormalizable with respect to some coupling λ and that only logarithmic corrections can arise to tree level scale invariance. Nevertheless in the following we will forget about the λ dependence and all the results must be intended as results holding order by order in the renormalized perturbative expansion in λ.

As we said, a crucial point of our discussion is the introduction of an OPE to rewrite to short-distance behavior of a correlator function. In general we can write:

$$\langle \Phi_{a_1}(r_1)...\Phi_{a_n}(r_n)X(R)\rangle_m \sim C^c_{a_1...a_n}(r_1-r_n,...,r_{n-1}-r_n;m)\langle \Phi_c(r_n)X(R)\rangle_m \quad (2.71)$$

where $\Phi_{a_i}(r_i)$ is a complete set of composite operators of dimension x_i, $X(R)$ is a multi-local operator defined on $|R| > \max|r_1|,...,|r_n|$ (or eventually the identity operator ($X(R) = \mathbb{1}$) and the index m indicates that correlators are evaluated at fixed sources m_i.

In order to be able to evaluate the derivatives of the coefficients $C^c_{a_1...a_n}$, we must first introduce three hypothesis.

Hypothesis 1: Regularity.

An UV renormalization scheme for correlators of the deformed theory is assumed such that counterterms are polynomial in renormalized generalized masses (Minimal Mass Dependence, MMD) and the Wilson coefficients are regular (i.e. C^∞) in generalized masses at $m_i = 0$.

The request of Minimal Mass Dependence is crucial because it guarantees the smoothness in the $m_i \to 0$ from the point of view of UV renormalization. In fact the presence of a renormalization scheme which introduce a scale mass would break conformal invariance of the unperturbed theory. On the contrary, any subtraction scheme that only subtracts the infinite part (i.e. Minimal Subtraction), satisfies MMD because it does not introduce any additional mass dependence in the counterterms.

Let us stress that Minimal Mass Dependence and the regularity of Wilson coefficients are equivalent in the framework of perturbative renormalization. Indeed, Minimal Subtraction (MS) in dimensional renormalization satisfies MMD and regularity. Moreover, any other renormalization scheme that satisfies MMD will differ from MS only by finite counterterms (i.e. polynomial in the masses). In particular, a renormalized operator will change under change of scheme accordingly as:

$$[\Phi_a]' = N^b_a[\Phi_b] \quad (2.72)$$

where $N^b_a = \delta^b_a + Y^b_a$ and Y is a $O(\hbar)$ matrix polynomial in the masses. Consequently the Wilson coefficients transform as:

$$C'^{c}_{a_1 \dots a_n} = N^{b_1}_{a_1} \dots N^{b_n}_{a_n} N^{-1}{}^{c}_{d} C^{d}_{b_1 \dots b_n} \tag{2.73}$$

The matrices of change of scheme are chosen to be regular, thus since the Wilson coefficient of the original scheme are regular, also the new ones will be regular. Moreover the stronger assumption of analyticity of Wilson coefficient guarantees the convergence of the Taylor series we are building up, while in the general case only the asymptotic convergence is ensured.

The second assumption is necessary to evaluate the derivatives of Wilson coefficients with respect to generalized masses.

Hypothesis 2: Action Principle.
It is assumed that for each renormalized generalized mass m^i a conjugate operator $\mathcal{O}_i$ exists such that the derivative with respect to m^i is:

$$\partial_{m^i} \langle X \rangle_m = \int dx \langle : \mathcal{O}_i : \ X \rangle_m, \quad : \mathcal{O}_i : \equiv \mathcal{O}_i - \langle \mathcal{O}_i \rangle_m \tag{2.74}$$

for each multilocal operator X.

The above hypothesis is known to hold in perturbative renormalization in schemes satisfying Hypothesis 1 such as Dimensional Renormalization and Analytic Renormalization. Moreover it is rather simple with respect to other approaches in literature and this aspect will be important later because it will allow us to deal with expressions for derivatives of generic order and to give the inductive IR finiteness proof.

Last hypothesis we need to introduce concerns the convergence of the OPE. While the convergence of the OPE in the unperturbed theory (i.e a conformal field theory) is well understood, the convergence in a general theory (i.e. $m^i \neq 0$) is far from being proved. From our purposes, we don't need a complete proof of the convergence, but it is sufficient a weaker assumption.

Hypothesis 3: OPE asymptotic weak convergence.
It is assumed that the remainder of OPE

$$\Delta^{(N)}(X_R, m) \equiv \langle (\Phi_{a_1}(r_1) \dots \Phi_{a_n}(r_n) - \sum_{c}^{x_c \leq N} C^{c}_{a_1 \dots a_n} \Phi_c) X_R \rangle_m \tag{2.75}$$

(X_R being the unity or a multilocal operator with support outside $R > |r_1|, \dots, |r_n|$) satisfies

$$\lim_{N \to \infty} \lim_{m \to 0} \lim_{R \to \infty} \partial_{i_1} \dots \partial_{i_k} \Delta^{(N)}(X_R, m) = 0 \tag{2.76}$$

for any k. Equivalently we can write

$$\lim_{N\to\infty}\lim_{R\to\infty}\langle(\Phi_{a_1}(r_1)...\Phi_{a_n}(r_n)-\sum_c^{x_c\leq N}C^c_{a_1...a_n}\Phi_c)X_R\rangle\sim 0 \tag{2.77}$$

in the sense of asymptotic series in m^i.

Let us make some comments about this statement. First of all Eq. 2.77 for $k=0$ is equivalent to asking for the convergence of the OPE in the unperturbed theory when inserted in correlators with "far" operators, a well known property of conformal field theories. Then, in general quantum field theory, it is known from perturbative as well as axiomatic considerations that the OPE is an asymptotic expansion in power of r. In our case, the limit $R\to\infty$ is reached and the contribution of X_R factorizes: this means that the only physical scale in the OPE comes from the generalized mass. The remainder will be order $O((m^{\frac{1}{y}}r)^\nu)$ by dimensional analysis, and thus the OPE series with respect to powers of the generalized masses reasonably becomes asymptotic.

2.2.2 A basic example

In order to understand better what we said in the previous section, it may be helpful to consider a basic but very instructive example. Suppose we want to compute the first derivative with respect to m^i (in $m^i=0$) of the two point Wilson coefficient C^1_{ab} (where the indices label the renormalized operators Φ_a, Φ_b and $\mathbb{1}$). Let us consider the remainder of the OPE:

$$\Delta^{(N)}(X_R,m)\equiv\langle(\Phi_a(r)\Phi_b(0)-\sum_c^{x_c\leq N}C^c_{ab}\Phi_c(0))X_R\rangle_m \tag{2.78}$$

As usual X_R is the identity or a multilocal operator with support in $E_R\equiv\{x/|x|>R\}$ (we call I_R the complement set of E_R, i.e. $I_R=\mathbb{R}^D-E_R$).

Then, taking derivatives both sides with respect to m^i, we can write by using the Action Principle 2.74:

$$\begin{aligned}\partial_i\Delta^{(N)}(X_R,m)=\int dx\langle:\mathcal{O}_i(x):(\Phi_a\Phi_b-\sum_c^{x_c\leq N}C^c_{ab}\Phi_c)X_R\rangle_m+\\-\sum_c^{x_c\leq N}\partial_iC^c_{ab}\langle\Phi_cX_R\rangle_m\end{aligned} \tag{2.79}$$

In the limit of zero generalized masses, the integral on the right hand side must be IR divergent. In order to deal with this problem, we must proceed as follow and split

the integral in two pieces:

$$\begin{aligned}\partial_i \Delta^{(N)}(X_R, m) = &\int_{I_{R_1}} dx \langle : \mathcal{O}_i : (\Phi_a \Phi_b - \sum_c^{x_c \leq N} C_{ab}^c \Phi_c) X_R \rangle_m + \\ &+ \int_{E_{R_1}} dx \langle : \mathcal{O}_i : (\Phi_a \Phi_b - \sum_c^{x_c \leq N} C_{ab}^c \Phi_c) X_R \rangle_m + \\ &- \sum_c^{x_c \leq N} \partial_i C_{ab}^c \langle \Phi_c X_R \rangle_m\end{aligned} \tag{2.80}$$

where $R1 > R$. The second integral may be rewritten as a remainder:

$$\int_{E_{R_1}} dx \langle : \mathcal{O}_i : (\Phi_a \Phi_b - \sum_c^{x_c \leq N} C_{ab}^c \Phi_c) X_R \rangle_m = \Delta^{(N)}(X'_R, m) \tag{2.81}$$

with support on $X'_R \equiv \int_{E_{R_1}} : \mathcal{O}_i : X_R$, satisfying the same hypothesis on the support of X_R.

Thanks to the the hypothesis of asymptotic weak convergence of the OPE (inserted in correlator functions) 2.77, we can state that in the limit $N \to \infty$, the remainder of Eq. 2.81 is zero for any $R_1 > R > |r|$ and the subsequent $m \to 0$ limit is safe and can be exchanged with the first (IR cut off) integral. This leads to the desired result:

$$\begin{aligned}0 = \lim_{N \to \infty} \Big\{ &\int_{I_{R_1}} dx \langle : \mathcal{O}_i : (\Phi_a \Phi_b - \sum_c^{x_c \leq N} C_{ab}^c \Phi_c) X_R \rangle_{m=0} + \\ &- \sum_c^{x_c \leq N} \partial_i C_{ab}^c \langle \Phi_c X_R \rangle_{m=0} \Big\}\end{aligned} \tag{2.82}$$

From now on, the symbol $\langle ... \rangle$ (with no suffix) is meant to be at $m = 0$, namely evaluated at the critical point.

We are now ready to take also the limit $R_1 \to \infty$ and to set $X_R = \mathbb{1}$, finding:

$$0 = \lim_{N, R_1 \to \infty} \Big\{ \int_{I_{R_1}} dx \langle : \mathcal{O}_i : (\Phi_a \Phi_b - \sum_c^{x_c \leq N} C_{ab}^c|_0 \Phi_c) \rangle - \sum_c^{x_c \leq N} \partial_i C_{ab}^c|_0 \langle \Phi_c \rangle \Big\} \tag{2.83}$$

We exchanged the limit over m and R preventing any possible issue coming from eventual IR divergences. Taking the $m \to 0$ limit, also the Wilson coefficients are evaluated at $m = 0$ as indicated by "$|_0$" (we will omit this specification in the future for simplicity of notation).

To have a useful formula we must observe that by dimensional considerations is true in general that

$$\lim_{R_i \to \infty} \int_{I_{R_1}} dx_1 ... \int_{I_{R_k}} dx_k \langle : \mathcal{O}_{i_1} : ... : \mathcal{O}_{i_k} : \Phi_c(0) \rangle = 0 \tag{2.84}$$

if $x_c - \sum_{j=1}^k y_j > 0$ (where y_j are the mass dimensions of m^i). This is due to the fact

that the unperturbed theory has not physical scales since the renormalization point μ does not give powerlike corrections.

Then, the series in the c index in Eq. 2.83 is truncated and we finally get:

$$\partial_i C^1_{ab}(0) = \lim_{R\to\infty} \int_{I_R} dx \langle : \mathcal{O}_i : (\Phi_a \Phi_b - \sum_c^{x_c \leq y_i} C^c_{ab} \Phi_c) \rangle \tag{2.85}$$

In this way we were able to express the first derivative of a Wilson coefficient in term of well defined quantities of the unperturbed theory. It is interesting to observe that the formulae above as well as the formulae we are going to derive in the next sections do not depend on the choice of the UV renormalization scheme, provided that the Hypothesis 1-3 are satisfied.

2.2.3 Higher order expansion

We are now ready to generalize the illustrated procedure to a more general case involving the n^{th} derivative of the Wilson coefficient $C^c_{a_1 \dots a_l}$. We will prove by induction the formula for the general case, by assuming that at order n is true that:

$$\begin{aligned}
&\lim_{N,R\to\infty} \partial_{i_1} \dots \partial_{i_n} \Delta^{(N)}(X_R, m) \sim \\
&\lim_{N,R\to\infty} \Big\{ \int_{I_1} dx_1 \dots \int_{I_n} dx_n \langle : \mathcal{O}_{i_n} : \dots : \mathcal{O}_{i_1} : (\Phi_{a_1} \dots \Phi_{a_l} - \sum_c^{x_c \leq N} C^c_{a_1 \dots a_l} \Phi_c) X_R \rangle_m + \\
&\quad - \sum_c^{x_c \leq N} \partial_{i_1} C^c_{a_1 \dots a_l} \int_{I_2} dx_2 \dots \int_{I_n} dx_n \langle : \mathcal{O}_{i_n} : \dots : \mathcal{O}_{i_2} : \Phi_c X_R \rangle_m + P. + \\
&\quad - \dots + \\
&\quad - \sum_c^{x_c \leq N} \partial_{i_1} \dots \partial_{i_n} C^c_{a_1 \dots a_l} \langle \Phi_c X_R \rangle_m \Big\}
\end{aligned} \tag{2.86}$$

where we have defined $I_1 \equiv I_{R_1}$ for shortness and the series are to be intended asymptotic as explained before. With $P.$ we mean all the terms obtained by the possible permutations of the suffix (1,...,$k-1$) of the Wilson coefficients' derivatives with (k,...,n) inside the integrals without distinguishing the ordering.

Hypothesis 3 ensures that Eq. 2.86 holds for the $n = 0$ case. Then, if we are able to prove that the order n relation holds also at order $n+1$ we will demonstrate the desired result. Thus, let us take derivative with respect to m^{i+1} both sides of Eq. 2.86 and call $\{n\}$ the terms coming from the order n formula.

The derivative $\partial_{i_{n+1}}$ may acts on the correlators or on the Wilson coefficients. In the first case, it gives terms of the form:

$$\lim_{N,R\to\infty} \int dx_{n+1} \langle : \mathcal{O}_{i_{n+1}}(x_{n+1}) \{n\} \rangle_m \tag{2.87}$$

namely, the same terms as before, but with the addition of $:\mathcal{O}_{i_{n+1}}:$. In the second case the derivative acts on the Wilson coefficients present at order n. In the limit of $R_n, R_{n-1}, ..., R_1 \geq R \to \infty$, is true that:

$$\lim_{N,R\to\infty} \int dx_{n+1} \langle :\mathcal{O}_{i_{n+1}}\{n\}\rangle_m = \lim_{N,R\to\infty} \int_{I_{R_{n+1}}} dx_{n+1} \langle :\mathcal{O}_{i_{n+1}}\{n\}\rangle_m \tag{2.88}$$

Finally, by summing the two contributions, we reproduce the $n+1$ expression according to 2.86, showing that induction works.

For generic X_R, Eq. 2.86 provides a set of constraints which relate the derivatives of the Wilson coefficients with respect to the coupling to correlators of the unperturbed theory. This system can be consistently solved in terms of the derivatives of the Wilson coefficients if one knows the properties of the model at the critical point.

In order to make contact with a practical example, let us consider once again a simpler case and let us set $X_R = \mathbb{1}$. Then, taking the limit $m \to 0$ and reminding the dimensional selection rule 2.84 we get:

$$\begin{aligned}
&\partial_{i_1}...\partial_{i_n} C^{\mathbb{1}}_{a_1...a_l} = \\
&\qquad \lim_{R\to\infty} \Big\{ \int_{I_1} dx_1 ... \int_{I_n} dx_n \langle :\mathcal{O}_{i_n}: ... :\mathcal{O}_{i_1}: (\Phi_{a_1}...\Phi_{a_l} - \sum_c^{x_c \leq \bar{x}} C^c_{a_1...a_l}\Phi_c)\rangle + \\
&\qquad\quad - \sum_c^{x_c\leq\bar{x}} \partial_{i_1} C^c_{a_1...a_l} \int_{I_2} dx_2 ... \int_{I_n} dx_n \langle :\mathcal{O}_{i_n}: ... :\mathcal{O}_{i_2}:\Phi_c\rangle + P. + \\
&\qquad\quad - ... + \\
&\qquad\quad - \sum_c^{x_c\leq\bar{x}} \partial_{i_1}...\partial_{i_{n-1}} C^c_{a_1...a_l} \int_{I_n} dx_n \langle\, \mathcal{O}_{i_n} : \Phi_c\rangle + P. \Big\}
\end{aligned} \tag{2.89}$$

The sum over c is restricted (in virtue of 2.84) to Φ_c such that $x_c \leq \bar{x} = y_{i_k} + ... + y_{i_n}$.

As a final comment, let us outline that even though we restricted ourselves to a particular choice of IR spatial cutoff to derive our results by induction, the same results hold for a wide class of IR regularizations. In [7], it has been shown that an analogous result of Eq. 2.86 holds considering a generic IR cutoff $\theta_{R'}(x)$ such that $\lim_{R'\to\infty} \theta_{R'}(x) = 1$ and repeating the usual procedure. Of course, the choice of a clever IR cutoff may help to simplify considerably the computation. For instance, if the cutoff $\theta_{R'}(x)$ is rotation invariant, then only scalar operators are involved in the expressions.

2.2.4 Advantages of the approach

As we have seen in the previous section, Conformal Perturbation Theory is a mathematical tool to realize an expansion for the short-distance behavior of correlation functions of quantum field theories, in the vicinity of a conformally invariant critical point. In particular, CPT can be seen as a way to derive the coefficients of the Wilson

operator-product expansion that is induced, when a conformally invariant theory is perturbed by a relevant operator. The method deals with short-distance divergences in a standard fashion, and is self-consistent in the long-distance limit, where it yields finite results: this is a clear advantage over more conventional expansions, say, in powers of the mass perturbing the conformal theory, which are often plagued by infrared divergences.

A clear advantage of this kind of approach is that, by construction, CPT expansions separate the non-perturbative features of the theory (i.e. the vacuum expectation values of different operators) from those that can be computed perturbatively (i.e. the Wilson coefficients). Another important feature of CPT is that it only requires the knowledge of limited information characterizing the theory: this includes universal (like the critical indices) as well as non-universal data, (like critical amplitudes of one-point functions, which can be obtained using off-critical methods, such as strong or weak-coupling expansions, or numerical simulations).

In the next sections we are going to see some examples of how Conformal Perturbation Theory may be applied in rather different fields to extract informations on the behavior of the systems in the proximity of a critical point.

2.3 $SU(2)$ gauge theory in $3+1$ dimensions

In the first example we are going to analyze, we propose to use CPT to study the behavior of quantum chromodynamics (QCD) and other strongly coupled non-Abelian gauge theories near the critical points associated with a continuous phase transition in their phase diagram. The long-term goal of this approach is to derive theoretical predictions for the dynamics of strong interactions under the extreme conditions of temperature and density that are realized in heavy-ion collisions, for the values of center-of-mass energy and nuclear masses allowing one to probe the neighborhood of the critical end-point appearing at finite temperature T and quark chemical potential μ in the QCD phase diagram. It is well known that such a line does not extend to the $\mu = 0$ axis (i.e. the baryon density axis), where the deconfining and chiral-symmetry restoring transition is actually a crossover. Hence, the first-order transition line is believed to terminate at an end-point corresponding to a continuous phase transition, where the infrared behavior of the theory should be described by the critical exponents characteristic of an effective field theory compatible with the expected symmetry and dimension requirements, which is just the Ising model in three dimensions.

The experimental search for the QCD critical end-point, proposed more than 20 years ago, remains a very active line of research. Meanwhile, despite a great effort, a derivation of the existence and location of this critical end-point is still missing: this is mainly due to the fact that the tool of choice for theoretical studies of strong interactions in the regime probed in heavy-ion collisions, namely numerical calculations in the lattice regularization is obstructed by a computational sign problem when

the quark chemical potential is finite. As a consequence, complementary theoretical approaches could provide valuable information on the region of the phase diagram in the neighborhood of the critical end-point. We argue that conformal perturbation theory could allow one to study the physics of strongly coupled QCD matter at values of temperature and net baryonic density lying along the "trajectories" (in the phase diagram) scanned in experiments, as long as such trajectories pass sufficiently close to the critical point.

For this reason, it is important to understand how well conformal perturbation theory works at a quantitative level, i.e. how large is the range of parameters of the underlying microscopic theory (in this case, QCD), for which the resulting low-energy physics can be approximated well by the associated conformal model (in this case, the Ising model in three dimensions) at or near criticality.

To this purpose, we present a detailed comparison of theoretical predictions from conformal perturbation theory, with those derived numerically using lattice simulations. We do this for $SU(2)$ Yang-Mills theory, a strongly coupled non-Abelian gauge theory in four space-time dimensions exhibiting a continuous phase transition at a finite deconfinement temperature T_c, which is in the same universality class as the one associated with the critical end-point of QCD, namely the one of the Ising model in three dimensions. In contrast to the critical end-point of QCD, however, the critical behavior at the deconfinement transition in finite-temperature $SU(2)$ Yang-Mills theory can be studied numerically to very high precision, making this theory a useful proxy with which to test the quantitative accuracy of conformal-perturbation-theory predictions.

In particular, we focus our comparison on the two-point correlation function of Wilson lines winding around in the Euclidean-time direction, also known as Polyakov loops. They are important observables in lattice gauge theory, which, at $T = 0$, can be directly linked to the potential $V(r)$ of a pair of static color sources a distance r apart from each other, and, as a consequence, to the spectrum of heavy-quark bound states.

Presently, much analytical information is known about the behavior of the potential derived from this correlator in non-supersymmetric non-Abelian gauge theories: at short distances, asymptotic freedom implies that its dominant contribution is a Coulomb term, arising from one-gluon exchange, and the separation between the momentum and mass scales allows one to organize the different terms appearing in perturbative calculations in a systematic way. Conversely, the long-distance physics is dominated by non-perturbative features, resulting in a linearly rising potential $V(r)$ at asymptotically large r: assuming the formation of a confining flux tube, with energy per unit length σ (the "string tension"), it is then possible to show that its dominant excitations in the infrared limit are described by massless bosonic oscillations in the transverse direction, that yield a characteristic $1/r$ correction to $V(r)$.

This picture can be described by a low-energy effective theory, associated with the spontaneous breaking of translational and rotational symmetries in the presence

of a confining string: the requirement of a non-linear realization of Lorentz-Poincaré invariance poses very tight constraints on the terms of this effective theory, making it highly predictive.

The situation in finite-temperature QCD is more subtle, because the finite temperature T introduces an additional energy scale and the infrared divergences play a non-trivial rôle with screening and dumping effects. The modern, proper definition of the potential between heavy color sources has a real and an imaginary part, which can be reconstructed from a spectral-function analysis of thermal Wilson loops. Nevertheless, the Euclidean correlator of Polyakov lines (and $-T$ times its logarithm, which, for simplicity, we still denote as V) still encodes interesting information about the thermal behavior of the theory. In the confining phase, the long-distance properties of this correlator can be accurately modeled assuming that the flux tube joining the color sources oscillates with a Euclidean action proportional to the area it spans, i.e. that in the infrared limit the dynamics of the theory is described by a low-energy effective action equal to the Nambu-Gotō action. At intermediate quark-antiquark distances r, however, deviations from the ideal picture of a Nambu-Gotō string do show up, as well as corrections induced by the finite temperature. In fact, it has been known for a long time that the Polyakov-loop operator captures much of the dynamics of Yang-Mills theory close to the deconfinement temperature.

In what follows, we are going to derive analytically the expressions for the two-point correlation function of Polyakov lines in the pure $SU(2)$ Yang-Miills theory, at temperatures in the vicinity of its second-order deconfinement transition, and to compare this results with numerical results obtained from Monte Carlo simulations on the lattice. As will be discussed below, our main findings are:

- The results obtained from conformal perturbation theory are in very good agreement with those from lattice simulations in a rather wide temperature interval; i.e. conformal perturbation theory provides reliable predictions in a rather large neighborhood of the conformal point.

- Conformal perturbation theory predicts the Polyakov-loop correlator to be described by an operator-product expansion (OPE) with different coefficients above and below the critical temperature T_c; the ratio of these coefficients is fixed by the universality class of the conformal model, and can be predicted in conformal field theory. The numerical values of the coefficients extracted from our lattice simulations of the $SU(2)$ Yang-Mills theory above and below T_c are such, that their ratio agrees with the value predicted by conformal theory for the Ising universality class.

2.3.1 Model and analytic results

The first aspect we must point out is the universality class of the corresponding field theory at the critical point. We are dealing with a purely gluonic Yang-Mills theory with an $SU(2)$ gauge group and in this situation the correspondence between the

degrees of freedom of the gauge theory and those of the spin model is clear. As conjectured by Svetitsky and Yaffe [8], n-point correlation functions of thermal Wilson lines (or Polyakov loops) are mapped to n-point correlators of spin degrees of freedom. In particular, here we are interested in the behavior of the two-point correlator of Polyakov loops in the gauge theory, which, denoting the spin degrees of freedom by σ, is mapped to the $\langle\sigma(r)\sigma(0)\rangle$ correlator in the Ising model.

The CPT analysis for the three-dimensional Ising model is straightforward. This model is characterized by two relevant operators, namely the energy density ϵ and the magnetization (the one-point correlation function of the spin σ); the dimensions of these operators have been recently computed [9] and are $\Delta_\epsilon = 1.412625(10)$ and $\Delta_\sigma = 0.5181489(10)$. The action of the perturbed model is defined as

$$S = S_{\text{CFT}} + t \int d^3x\, \epsilon(x) \tag{2.90}$$

where S_{CFT} denotes the action at the critical point, and the parameter t is related to the deviation from the critical temperature of the model. For the non-critical theory at finite t, the behavior of the two-point correlation function of operators $\mathcal{O}_i$ and $\mathcal{O}_j$ at short separation r can be expressed in terms of the Wilson coefficients C_{ijk} appearing in the expansion:

$$\langle\mathcal{O}_i(r)\mathcal{O}_j(0)\rangle_t = \sum_k C_{ij}^k(r,t)\langle\mathcal{O}_k\rangle_t \tag{2.91}$$

The Wilson coefficients can be expanded in Taylor series in t,

$$C_{ij}^k(r,t) = \sum_{n=0}^{\infty} \frac{t^n}{n!}\frac{\partial^n C_{ij}^k}{\partial t^n} \tag{2.92}$$

As proved before, the partial derivatives appearing on the right-hand side of this equation are not divergent at large r. Defining $\Delta_t = 3 - \Delta_\epsilon$ and writing the one-point correlation functions for the energy density and magnetization at finite t as

$$\langle\epsilon\rangle_t = A^{\pm}|t|^{\frac{\Delta_\epsilon}{\Delta_t}}, \qquad \langle\sigma\rangle_t = B_\sigma|t|^{\frac{\Delta_\sigma}{\Delta_t}} \tag{2.93}$$

the leading terms in the conformal perturbative expansion of the $\langle\sigma(r)\sigma(0)\rangle_t$ correlator are

$$\langle\sigma(r)\sigma(0)\rangle_t = C_{\sigma\sigma}^{\mathbb{1}}(0,r) + C_{\sigma\sigma}^{\epsilon}(0,r)A^{\pm}|t|^{\frac{\Delta_\epsilon}{\Delta_t}} + t\partial_t C_{\sigma\sigma}^{\mathbb{1}}(0,r) + \dots \tag{2.94}$$

where the Wilson coefficients evaluated at $(0,r)$ are the usual structure constants with the r dependence factorized:

$$C_{\sigma\sigma}^{\mathbb{1}}(0,r) = \frac{1}{r^{2\Delta_\sigma}}, \qquad C_{\sigma\sigma}^{\epsilon}(0,r) = C_{\sigma\sigma}^{\epsilon}\frac{1}{r^{2\Delta_\sigma-\Delta_\epsilon}} \tag{2.95}$$

We have also chosen the standard normalization for the fields, so that $C_{\sigma\sigma}^{\mathbb{1}} = 1$ and we know that $C_{\sigma\sigma}^{\epsilon} = 1.0518537(41)$ from [9].

The derivative of the Wilson coefficient can be computed following Eq. 2.85, leading to

$$\partial_t C^{\mathbb{1}}_{\sigma\sigma}(0,r) = -\int dr_1 \big(\langle\sigma(r)\sigma(0)\epsilon(r_1)\rangle_0 - C^{\epsilon}_{\sigma\sigma}\langle\epsilon(r_1)\epsilon(0)\rangle_0\big) \tag{2.96}$$

Where the three-point function at critical point is known:

$$\langle\sigma(r)\sigma(0)\epsilon(r_1)\rangle_0 = \frac{C_{\sigma\sigma\epsilon}}{r^{2\Delta_\sigma-\Delta_\epsilon} r_1^{\Delta_\epsilon}(r^2+r_1^2-2rr_1\cos\theta)^{\frac{\Delta_\epsilon}{2}}} \tag{2.97}$$

while $C^{\epsilon}_{\sigma\sigma} r^{-2\Delta_\epsilon}$ since we choose again a normalization of the fields such that $C^{\mathbb{1}}_{\epsilon\epsilon} = 1$.

Integral 2.96 can be evaluated using a Mellin transform technique (for details, see Appendix A) or numerically. In the first case, the second term of the integrand acts just as an infrared counterterm and only the first term contributes, giving:

$$\partial_t C^{\mathbb{1}}_{\sigma\sigma}(0,r) = -r^{\Delta_t-2\Delta_\sigma} C^{\epsilon}_{\sigma\sigma}\int dy \frac{y^{-\Delta_\epsilon}}{(1+y^2-2y\cos\theta)^{\Delta_\epsilon/2}} \tag{2.98}$$

where $y = r_1/r$. It is convenient to define

$$\partial_t C^{\mathbb{1}}_{\sigma\sigma}(0,r) = -r^{\Delta_t-2\Delta_\sigma} C^{\epsilon}_{\sigma\sigma} I \tag{2.99}$$

Thus, after performing the angular integrals we get

$$I = 2\pi\int dy \frac{|1+y|^{2-\Delta_\epsilon} - |1-y|^{2-\Delta_\epsilon}}{2-\Delta_\epsilon} y^{1-\Delta_\epsilon} \tag{2.100}$$

The previous integral can be written in terms of Gamma functions giving as a final result $I \simeq -62.5336$. It is also important to notice that Eq. 2.94 defines the non-connected correlation function.

Sometimes it may be useful to introduce the scaling variable

$$s = t r^{\Delta_t} \tag{2.101}$$

in this case, the two-point correlator becomes:

$$r^{2\Delta_\sigma}\langle\sigma(r)\sigma(0)\rangle_t = 1 + C^{\epsilon}_{\sigma\sigma} A^{\pm}|s|^{\frac{\Delta_\epsilon}{\Delta_t}} + I C^{\epsilon}_{\sigma\sigma} s + \dots \tag{2.102}$$

In order to compare this analytical prediction from CPT with the numerical results from Monte Carlo simulations of $SU(2)$ Yang-Mills theory, we have to fix some non-universal quantities. These include the following:

- The normalization of the Polyakov loop, i.e. a proportionality factor relating the σ spin expectation value in the Ising model, and the Polyakov loop P of $SU(2)$ Yang-Mills theory, evaluated on the lattice. It should be noted that the latter quantity is a *bare* one, which would tend to zero in the continuum limit. As a consequence, the proportionality factor relating σ and P is a function of the

lattice spacing of the Yang-Mills theory a, or, equivalently, of the Wilson parameter $\beta = 4/g^2$, where g denotes the bare lattice coupling. We decided to fix this normalization by matching the two-point correlation function of Polyakov loops at the critical point to the corresponding spin-spin correlator in the critical Ising model.

- Identifying r with the spatial separation R between the Polyakov lines, we reabsorb all non-universal factors into the definition of the perturbation coefficient t in the spin model. This quantity is related to the perturbing parameter of the $SU(2)$ lattice gauge theory, which is $\beta - \beta_c(N_t)$, where $\beta_c(N_t)$ is the value of the Wilson parameter (or of the bare gauge coupling) corresponding to a lattice spacing a such that aN_t is the inverse of the critical deconfinement temperature in natural units. Note that the $\beta - \beta_c(N_t)$ difference controls the deviation of the temperature from its critical value. To fix the non-universal relation between t and $\beta - \beta_c(N_t)$, we take advantage of the universality of the last term on the right-hand side of eq. (2.102), by fitting our results for the correlator as a function of r, and using the result to fix the relation between t and $\beta - \beta_c(N_t)$.

- The amplitudes $A^{\pm}$ can be determined using the second term in the expansion above. The numerical value of these amplitudes is one of the non-trivial results of our analysis; the A^+/A^- ratio is universal, and this expectation provides a useful check of the self-consistency and robustness of the whole analysis.

2.3.2 Numerical results for $SU(2)$ Yang-Mills theory

In order to test the predictions discussed in the previous section, we studied the behavior of the Polyakov loop correlators in the vicinity of the deconfinement transition of the $3+1$-dimensional $SU(2)$ Yang-Mills theory. In the following subsection 2.3.2, we define the setup of our lattice regularization of this theory; then, we present our numerical results, comparing them with CPT predictions in subsection 2.3.2, and discussing their uncertainties in subsection 2.3.2.

Setup of the lattice calculation

We regularize the theory on a finite hypercubic lattice of spacing a and sizes aN_t in the $\hat{0}$ ("Euclidean-time") direction and $L = aN_s$ in the three other ("spatial") directions, labeled as $\hat{1}$, $\hat{2}$, and $\hat{3}$. We always take $aN_s \gg aN_t$. The fundamental degrees of freedom of the lattice theory are matrices $U_\mu(x)$, taking values in the defining representation of the $SU(2)$ group, and associated with parallel transporters between neighboring sites x and $x + a\hat{\mu}$. Periodic boundary conditions are assumed in all directions. The dynamics of the theory is defined by the Wilson action [10]

$$S_W = -\frac{2}{g^2} \sum_x \sum_{0 \le \mu < \nu \le 3} \mathrm{Tr} U_{\mu\nu}(x) \tag{2.103}$$

where $U_{\mu\nu}(x) = U_\mu(x)U_\nu\left(x+a\hat{\mu}\right)U_\mu^\dagger\left(x+a\hat{\nu}\right)U_\nu^\dagger(x)$ is a plaquette having the site x as a corner and lying in the oriented (μ,ν) plane, and g^2 is the squared bare coupling; we also introduce the parameter $\beta = 4/g^2$.

The temperature T is related to the extent of the shortest compact size of the lattice as $aN_t = 1/T$: as a consequence, T can be varied by changing N_t, a, or both. The physical value of the lattice spacing a is set non-perturbatively, as discussed in ref. [11], and is controlled by the parameter β. We express our results in terms of the deconfinement temperature T_c, using the value for the ratio of T_c over the square root of the zero-temperature string tension $T_c/\sqrt{\sigma} = 0.7091(36)$, which was reported in ref. [12].

The Polyakov loop at a spatial coordinate $\vec{x}$ is defined as the trace of the closed Wilson line in the $\hat{0}$ direction:

$$P\left(\vec{x}\right) = \frac{1}{2}\mathrm{Tr}\prod_{t=0}^{N_t} U_0\left(ta,\vec{x}\right). \tag{2.104}$$

The two-point correlation function of Polyakov loops is then defined as

$$G(R) = \left\langle \frac{1}{N_s^3}\sum_{\vec{x}} P\left(\vec{x}\right)P\left(\vec{x}+R\hat{k}\right)\right\rangle, \tag{2.105}$$

where $\hat{k}$ denotes one of the three "spatial" directions, the sum is over all spatial coordinates $\vec{x}$, while the $\langle\ldots\rangle$ average is taken over all values of all of the $U_\mu(x)$ variables, with a measure that is proportional to the product of the Haar measures of all $U_\mu(x)$ matrices and to $\exp(-S_W)$, and normalized in such a way that the expectation value of the identity operator is 1.

We remark that, like eq. (2.94), eq. (2.105) defines the *non-connected* (i.e. full) correlator, in which the square of the average value of the Polyakov loop (which, in the thermodynamic limit, is non-zero in the deconfined phase) is *not* subtracted. The reason for this choice is that we are going to compare the lattice results for this correlator with the analogous correlator in conformal perturbation theory, where the correlation function of interest is the non-connected one. The fact that the CPT formalism deals with the non-connected correlators (i.e. does not encode any information on long-wavelength physics, including a possibly non-vanishing vacuum expectation value of the field) is unsurprising, given that it is ultimately formulated in terms of a particular type of operator-product expansion, which is expected to capture the behavior of physical correlators at short distances only. Accordingly, as will be discussed below (see also the values reported in table 2.3), we will restrict our fit ranges to distances shorter than the characteristic correlation length of the theory at that temperature.

One may wonder whether it might be possible to carry out a meaningful fit to CPT using the connected correlator, too. The answer is no: the reason is that, as discussed in section 2.2, the non-trivial information from CPT is expressed in terms of a function

of a non-trivial combination of the variables that describe the temperature and the distance, see eqs. (2.101) and (2.102), whereas the quantity that is subtracted from the full correlator to obtain the connected one, i.e. the square of the average value of the Polyakov loop, is, by definition, R independent, but *temperature dependent*.

Finally, it is also worth noting that, by contrast, the fact that the lattice correlator defined in eq. (2.105) is a *bare* one does not hinder the possibility of a comparison with CPT predictions, thanks to the fact that the Polyakov loop undergoes a purely multiplicative renormalization.

As we already said, CPT gives reliable predictions in the range of short distances, or in other words, the numerical results from lattice simulations of the $SU(2)$ Yang-Mills theory can be compared with the analytical predictions from conformal perturbation theory only when the distances involved are much smaller than the typical correlation length of the system. For this reason we decided to estimate the correlation length in the confining phase (i.e. for $T < T_c$) by fitting our numerical results for $G(R)$ to the functional form

$$G(R) = A \left\{ \frac{\exp\left(-R/\xi\right)}{R} + \frac{\exp\left[-(L-R)/\xi\right]}{L-R} \right\}, \tag{2.106}$$

with ξ (which is the largest correlation length of the theory) and A (which is an overall amplitude, with no direct physical meaning) as fitting parameters. Note that the second summand on the right-hand side of eq. (2.106) accounts for the effect of the closest periodic copy of the Polyakov line on the hypertorus; we neglect the effect of other periodic copies (at distances L, $\sqrt{L^2+R^2}$, $\sqrt{R^2+2L(L-R)}$, $\ldots$) as well as corrections due to higher-energy states.

As expected in the presence of a continuous phase transition, $\xi \to \infty$ for $T \to T_c$. More precisely, in the proximity of the critical point, ξ diverges like $[(T-T_c)/T_c]^{-\nu}$ (which defines the hyperscaling exponent ν), with two different *amplitudes*, respectively denoted as ξ_{0^+} and as ξ_{0^-}, for $T > T_c$ and $T < T_c$. While these amplitudes are not universal, their ratio is, and for the universality class of the Ising model that ratio was evaluated to be $\xi_{0^+}/\xi_{0^-} = 1.95(2)$ in ref. [13]. This allows one to obtain an estimate of the typical correlation length also in the deconfined phase (at least for temperatures not very far from T_c). Anyway, in all of the fits that we carried out, we always restricted our comparison of the $G(R)$ correlator with CPT predictions to distances not larger than a maximum Polyakov-loop separation R_{max}, with $R_{\text{max}} \ll \xi$. At the same time, the shortest R distances probed in the fits are always larger than a few units of the lattice spacing a. The double constraint $a \ll R \ll \xi$ enforces the hierarchy of scales making a sensible comparison between lattice results and CPT predictions possible.

Table 2.1 summarizes the parameters of the Monte Carlo simulations that we carried out.

$N_t \times N_s^3$	β	T/T_c	n_{conf}	ξ/a
8×80^3	2.48479	0.90	8×10^4	9.24(3)
	2.50311	0.96	8×10^4	23.3(2)
	2.50598	0.97	8×10^4	43.3(4)
	2.51165	1	8×10^4	
	2.52295	1.02	8×10^4	~ 85
	2.52567	1.05	8×10^4	~ 45
	2.54189	1.10	8×10^4	~ 18
10×80^3	2.55	0.90	10^5	11.72(8)
	2.569	0.96	10^5	29.4(3)
	2.572	0.97	10^5	42.9(4)
	2.58101	1	8×10^4	
	2.58984	1.02	1.6×10^5	~ 85
	2.59271	1.05	1.6×10^5	~ 55
	2.61	1.10	1.6×10^5	~ 23
12×96^3	2.60573	0.90	8×10^4	12.89(15)
	2.626	0.96	8×10^4	34.8(4)
	2.62923	0.97	8×10^4	41.3(3)
	2.63896	1	8×10^4	
	2.64558	1.02	1.6×10^5	~ 81
	2.65541	1.05	1.6×10^5	~ 65
	2.67085	1.10	1.6×10^5	~ 25

TABLE 2.1: Information about the parameters of our lattice calculations for $SU(2)$ Yang-Mills theory. The first two columns show the lattice sizes in units of the lattice spacing a and the parameter $\beta = 4/g^2$, while in the third we display the temperature in units of T_c and in the fourth the statistics for the Polyakov-loop correlators. Finally, in the last column we present our estimates for the correlation length ξ, in units of a.

Comparison with CPT predictions

We analyzed our lattice results for the Polyakov-loop correlators in $SU(2)$ Yang-Mills theory as follows.

1. First, we fixed the normalization constant for the Polyakov loops by matching the value of $G(R)$ at the critical temperature $T = T_c$ to the corresponding quantity in the Ising model at criticality, i.e. the spin-spin correlator.

2. Then, we fitted the numerical value of the correlator to eq. (2.102), as a function of R, keeping the coefficients of the second and third term on the right-hand side of that equation as the parameters to be fitted.

3. Finally, we used our best estimates for these coefficients to fix the remaining quantities, and studied how they depend on the temperature T.

For the first of these steps, fig. 2.2 shows an example of our results for the $G(R)$ correlator at the critical temperature: the lattice data confirm the expected power-law behavior (revealing itself as a straight line in the plot with logarithmic axes), and the presence of significant finite-size effects for the points at the largest values of R.

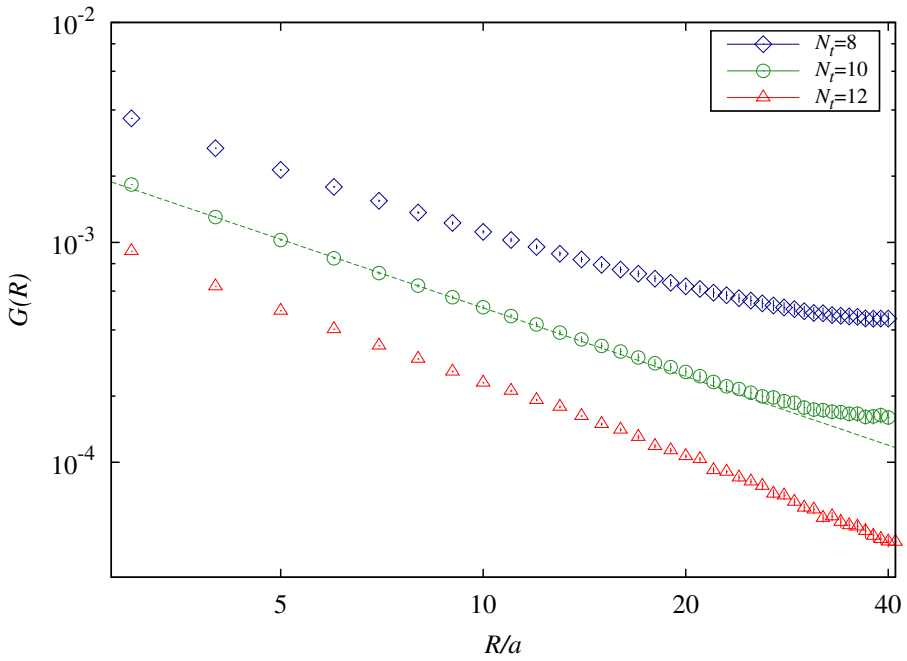

FIGURE 2.2: Logarithmic plot of our results for the two-point correlation function of Polyakov loops $G(R)$ in the $SU(2)$ gauge theory at the deconfinement temperature, as a function of the distance R.

R_{min}/a	R_{max}/a	C_P^2	χ^2_{red}
4	12	0.005463(12)	0.25
4	20	0.005477(15)	0.40
4	30	0.005492(19)	0.66
4	40	0.005513(31)	1.96

TABLE 2.2: Results of our fits of the Polyakov-loop correlator $G(R)$ at $N_t = 10$, $N_s = 80$ and $\beta = 2.58101$, corresponding to $T = T_c$, to eq. (2.107). The results for C_P^2, shown in the third column, are obtained from fits for $R_{\text{min}} \leq R \leq R_{\text{max}}$ (first two columns); the values of the reduced χ^2 are listed in the last column.

Thus, we fit the correlator at criticality to the form

$$G(R) = \frac{C_P^2}{R^{2\Delta_\sigma}} \tag{2.107}$$

for different ranges of values of the Polyakov-loop separation $R_{\text{min}} \leq R \leq R_{\text{max}}$. In order to avoid excessive contamination from lattice discretization artifacts (on the gauge-theory side) and/or from other charge-conjugation-odd operators (in the comparison with the conformal field theory), we set $R_{\text{min}} = 4a$, and fitted the data for different values of R_{max}. An example of the results of this analysis (from a lattice with $N_t = 10$ at $T = T_c$) is shown in tab. 2.2. As expected, the data at the largest values of R (close to $L/2$) are affected by non-negligible contamination due to the periodic copies of the lattice. Combining the results from the fits with $R_{\text{max}} = 12a$ and $R_{\text{max}} = 20a$, we take $C_P^2 = 0.00547(2)$ as our final estimate for the critical-correlator fit at this value of N_t.

For the analysis of the Polyakov loop correlators $G(R)$ at $T \neq T_c$ we fitted the results of the correlator to the functional form

$$G(R) = \frac{C_P^2}{R^{2\Delta_\sigma}} \left(1 + c_1 R^{\Delta_\epsilon} + c_2 R^{\Delta_t}\right), \tag{2.108}$$

where the exponents Δ_σ, Δ_ϵ and Δ_t are those discussed in section 2.2, while c_1 and c_2 are the free parameters. The results of this analysis are reported in table 2.3 and shown in fig. 2.3, where the inset shows a zoom onto the smaller range of distances, where the results at $T > T_c$ are fitted.

Next, we investigated the relation between the perturbing parameter t and the difference $\beta - \beta_c(N_t)$ using the following relation:

$$c_2 = I \cdot C_{\sigma\sigma}^{\epsilon} \cdot t. \tag{2.109}$$

Using the values for $I \simeq -62.5336$ and for $C_{\sigma\sigma}^{\epsilon} = 1.0518537(41)$, the analysis of the data set corresponding to $N_t = 10$ yields the values for t reported in tab. 2.4.

The table also reports the values of $\Delta\beta = [\beta - \beta_c(N_t)]/2$, which for the $SU(2)$

β	T/T_c	$R_{\rm max}/a$	ξ/a	c_1	c_2
2.55	0.90	$[7-8]$	11.72(8)	$-0.169(1)$	0.099(1)
2.569	0.96	$[11-14]$	29.4(3)	$-0.067(2)$	0.037(1)
2.572	0.97	$[12-21]$	42.9(4)	$-0.048(3)$	0.026(2)
2.58984	1.02	$[18-25]$	~ 85	0.067(2)	$-0.019(1)$
2.59271	1.05	$[13-19]$	~ 55	0.091(2)	$-0.0256(15)$
2.61	1.10	$[8-9]$	~ 23	0.221(3)	$-0.081(3)$

TABLE 2.3: Example of results of the fits of the correlator $G(R)$ to eq. (2.108), obtained from simulations on lattices with $N_t = 10$ at different values of $\beta = 4/g^2$ (first column), corresponding to the temperatures reported in the second column, in the range $4a \leq R \leq R_{\rm max}$, and for the values of $R_{\rm max}$ shown in the third column. In the fourth column, we display our estimates for the correlation lengths in units of the lattice spacing, while the fitted parameters c_1 and c_2 are listed in the fifth and in the sixth column, respectively. Note that, as discussed in the text, at each temperature, the largest distances at which the correlators are fitted (shown in the third column) are always chosen to be shorter, or much shorter, than the corresponding correlation lengths reported in the fourth column.

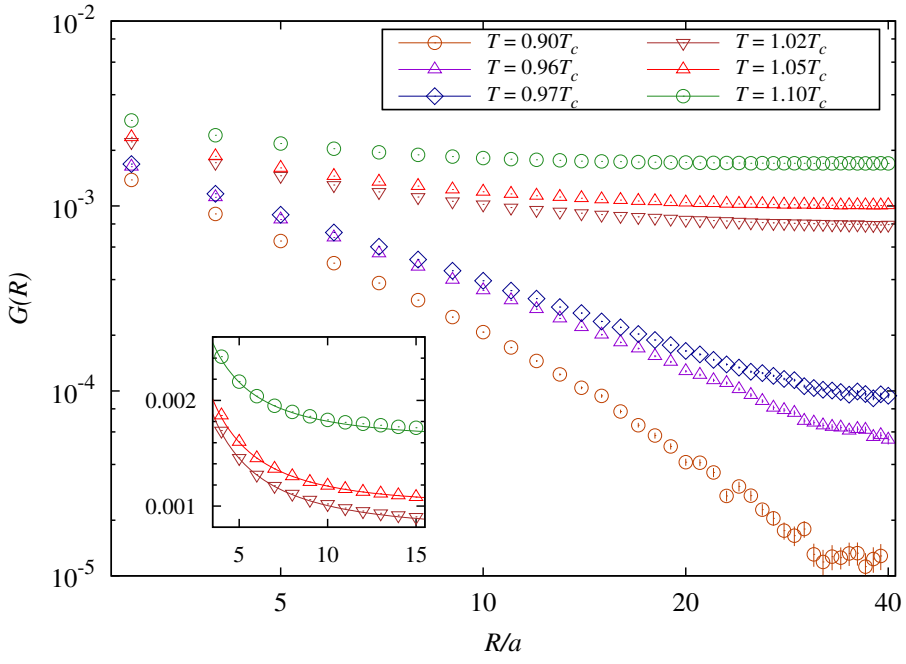

FIGURE 2.3: Example of results for the Polyakov-loop two-point correlation function (in logarithmic scale), plotted against the spatial separation R (in linear scale), for different temperatures T off T_c. These results were obtained from simulations on lattices with $N_t = 10$ lattice spacings in the Euclidean-time direction. The inset (in which both axes are in a linear scale) shows an enlargement of the region where the correlators at $T > T_c$ were fitted to the CPT prediction, eq. (2.108), as discussed in the text.

β	T/T_c	t	$\Delta\beta$
2.55	0.90	0.001505(15)	−0.01550
2.569	0.96	0.000563(15)	−0.00600
2.572	0.97	0.000395(30)	−0.00450
2.58984	1.02	−0.000284(18)	0.00440
2.59271	1.05	−0.000389(23)	0.00585
2.61	1.10	−0.001231(45)	0.01450

TABLE 2.4: Results for the perturbing parameter t and for $\Delta\beta$, obtained from eq. (2.109), at different values of the temperature in the proximity of the deconfining transition. The analysis is based on a set of data obtained from simulations on a lattice with $N_t = 10$ lattice spacings in the Euclidean-time direction.

lattice gauge theory is the perturbing parameter with respect to the plaquette operator $\sum_x \sum_{0\leq\mu<\nu\leq 3} \mathrm{Tr} U_{\mu\nu}(x)$. As expected, t has a negative sign in the deconfined phase, where the center symmetry is broken, and a positive sign in the confining, $\mathbb{Z}_2$-symmetric phase. The magnitude of these values of t is similar to those studied in ref. [14], for which conformal perturbation theory was found to give reliable predictions, which leads us to expect that this should also be the case here.

We note that, interestingly, t is almost exactly proportional to $\Delta\beta$: this means that, in the neighborhood of the critical temperature, the energy operator of the three-dimensional Ising model encodes the dynamics of the Euclidean-action density operator of the four-dimensional $SU(2)$ gauge theory in a quantitatively accurate way.

By fixing t, it is possible to derive the values of the amplitudes A^+ (in the confining phase, i.e. for $T < T_c$) and A^- (at $T > T_c$) from the relation

$$A^{\pm} = \mp \frac{c_1}{C^{\epsilon}_{\sigma\sigma}} |t|^{-\frac{\Delta_\epsilon}{\Delta_t}}. \tag{2.110}$$

The determination of these amplitudes allows for a non-trivial test of the validity of this CPT analysis: in particular, A^+ should be constant and negative in the confining phase, while in the deconfined phase the amplitude A^- should be constant and positive. Furthermore, the A^+/A^- ratio should be universal and is predicted to be $A^+/A^- = -0.536(2)$ [15].

Our results for $A^{\pm}$ are reported in table 2.5: in the confining phase, the values for A^+ are indeed compatible with a constant (that we estimate as $A^+ = -50(2)$), while in the deconfined phase the values are slightly less stable, with a quantitatively significant deviation at the largest temperature. This may indicate that the largest temperature that we investigated is close to the limit where our leading-order conformal-perturbation-theory analysis breaks down. We remark that, as our fits to CPT were limited to spatial separations shorter (or much shorter) than the correlation length at that temperature, this slight instability of the fits in the deconfined phase is not simply interpretable as an effect caused by the fact that our fits do not include an

β	T/T_c	A^+	A^-
2.55	0.90	$-52.6(6)$	
2.569	0.96	$-50(2)$	
2.572	0.97	$-49(5)$	
2.58984	1.02		91(6)
2.59271	1.05		94(5)
2.61	1.10		82(3)

TABLE 2.5: Results for the amplitude A^+ in the confining phase (first three rows) and for A^- in the deconfining phase (last three rows), for the values of inverse coupling β and of the temperature T reported in the first two columns, as discussed in the text.

R-independent term. Rather, it may be a numerical artifact induced by the fact that, in the deconfined phase, as the temperature is increased to values larger and larger than T_c, the correlation length decreases, and, as a consequence, the fitting range in R (whose upper limit is bound to be shorter than the correlation length) reduces to only a few points.

We estimate the amplitude in the deconfined phase to be $A^- = 89(6)$. Accordingly, we obtain the numerical value $A^+/A^- = -0.56(4)$, which is compatible with the one computed in ref. [15].

Technical details

Lattice setup and choice of parameters have been already declared in Tab. 2.1, so let us now specify some details of the algorithm and the data analysis.

The algorithm we adopted is based on a combination of *Heath bath* and *Overrelaxation*, common algorithms applied to gauge fields. In contrast to standard Metropolis algorithm they have the advantage to optimize the local acceptance rate and improve the step size in the Markov chain. They must be applied together because the only Overrelaxation, exploiting the symmetry properties of the action, is not sufficient to guarantee the ergodicity of the Markov chain.

In the heat bath method one combines two steps of the single link Metropolis update into a single step and chooses the new value $U_\mu(x)'$ according to the local probability distribution defined by the surrounding link variables:

$$dP(U) = dU \exp\Big(\frac{\beta}{2}\text{Re Tr}[UA]\Big) \tag{2.111}$$

where $U = U_\mu(n)'$ is the updated link, dU is the Haar integration measure and A is the sum of the *staples* P_i:

$$\begin{aligned} A = \sum_{i=1}^{6} P_i = \sum_{\nu\neq\mu} & U_\nu(x+a\hat{\mu})U_{-\mu}(x+a\hat{\mu}+a\hat{\nu})U_{-\nu}(x+a\hat{\nu}) + \\ & + U_{-\nu}(x+a\hat{\mu})U_{-\mu}(x+a\hat{\mu}-a\hat{\nu})U_\nu(x-a\hat{\nu}) \end{aligned} \tag{2.112}$$

The overrelaxation algorithm utilizes the property that in the Metropolis algorithm new configurations are always accepted if they do not change the action. The idea of the overrelaxation method is to find a new value U' which has the same probability weight as U and thus is automatically accepted. For the non-abelian groups (like $SU(2)$), one suggests a change according to the ansatz:

$$U \to U' = V^\dagger U^\dagger V^\dagger, \tag{2.113}$$

with a gauge group element V chosen such that the action is invariant.

Nevertheless, the overrelaxation algorithm alone is not ergodic, because it samples the configuration space on the subspace of constant action. This is called the microcanonical ensemble. Since one wants to determine configurations according to the canonical ensemble, i.e., distributed according to the Boltzmann weight, one has to combine the overrelaxation steps with other updating algorithms, such as heat bath steps.

Systematic uncertainties

We conclude this section with a few comments on the uncertainties involved in our analysis.

In order to test the impact of finite-volume effects, we repeated a subset of our calculations also on lattices at a larger value of N_s (the extent of the system in each of the spatial directions), namely $N_s = 96$. In all cases, we found that the results obtained from simulations with $N_s = 96$ were compatible with those at $N_s = 80$ within their uncertainties.[1]

While in this work we have not carried out a systematic study of the continuum limit, we remark that, in addition to the results discussed here (from the analysis of data obtained at $N_t = 10$), we also repeated the analysis for those at $N_t = 8$ and at $N_t = 12$, finding the same qualitative picture.

One may wonder, why conformal perturbation theory describes the dynamics of this gauge theory so well. The main reason is that, for the underlying conformal theory that is involved in this case (i.e. the one describing the Ising model in three dimensions at criticality), the conformal weights of the terms included in the expansion in eq. (2.102) and the subleading terms, that are neglected, are separated by a finite (and sufficiently large) gap. More precisely, the terms appearing in the parentheses on the right-hand side of eq. (2.102), besides the constant, have exponents (for t) which are approximately equal to 0.6 and 1.2, while the first subleading correction, that is neglected in eq. (2.102), scales at least quadratically in t, see ref. [16, eq. (5)]. In turn, this feature of the conformal spectrum for the three-dimensional Ising universality class is due to the intrinsic simplicity of the operator content of the model.

[1] We also observed that, on smaller lattices with $N_s = 64$, some deviations start to be visible, at least for temperatures sufficiently close to T_c.

Our results show that conformal perturbation theory works well in a wide neighborhood of the critical point, and at least for temperatures down to $T/T_c = 0.90$. While in principle it would be possible to test the CPT predictions at even lower temperatures, this would require significantly finer lattices (and, as a consequence, computationally much more demanding simulations), in order to keep the physical correlation length well separated from the lattice spacing.

2.3.3 Concluding remarks

We have presented a numerical test of conformal perturbation theory as a tool to predict the behavior of strongly interacting gauge theories in the proximity of a critical point.

Specifically, we focused on $SU(2)$ Yang-Mills theory at finite temperature T: this theory, which can be studied to high precision by numerical calculations on the lattice, has a second-order deconfinement phase transition at a finite temperature T_c, which is in the universality class of the three-dimensional Ising model. Accordingly, correlation functions in the gauge theory at criticality are mapped to those in the spin model, and universality arguments imply a set of interesting predictions for the behavior of the gauge theory at $T = T_c$. Conformal perturbation theory extends these predictions from the critical *point* to a whole *finite neighborhood*: as we discussed in detail in section 2.3.2, the physical correlation functions of the strongly coupled gauge theory near the critical point can be successfully described by means of the corresponding truncated conformal perturbation theory expansions, such as eq. (2.102). The approximation involved in the truncation is robust, as long as the terms that are neglected are sufficiently suppressed. For the universality class of the Ising model in three dimensions, this is indeed the case, and conformal perturbation theory successfully predicts the behavior of the gauge theory in a large interval of temperatures.

2.4 Energy-trapped Ising Model

The second example we propose concerns a quite different model: a classical spin model in three dimensions. It is known (and we also gave an example before), that combining this numerical high-precision technique to analytical methods developed in the framework of Conformal Perturbation Theory, it is possible to determine the behavior of the off-critical correlators of many different systems. This approach has been applied successfully to the well known $3D$ Ising model, by adding perturbations proportional to the spin and the energy operator [11, 16].

Starting from a slightly different perspective, CPT can be also combined to Monte Carlo simulations to get insight both on the behavior of the correlators outside the critical point and on the CFTs data at the critical point. In [17], the author followed this approach to study the Ising model perturbed by a confining potential coupled to the spin operator. This model is particularly interesting because the behavior of

the 1-point expectation values can be argued just by applying simple renormalization group arguments [18–20], and depends only on the trap potential parameters (trap size scaling (TSS) behavior). Moreover, many experiments involving Bose-Einstein condensates and cold atoms show a critical behavior even in the presence of a trapping potential [21, 22].

In what follows we pursue further this program, studying the Ising model perturbed by a trapping potential coupled to the energy operator in 3 dimensions. There are many reasons to investigate this system. From a purely theoretical point of view, one can wonder if the TSS argument still holds if the trapping potential is coupled to the energy operator instead of the spin operator. Moreover, studying the effects of the energy-trapping potential on the 2-point functions out of criticality provides an alternative method to estimate the CFT data at the critical point.

Finally, the study of the correlation functions out of the critical point is relevant also from the experimental point of view. Indeed, a trapping potential coupled to the energy operator can be effectively seen as a perturbation of the system by a non-uniform thermal gradient, a *thermal trap*. This setup might be implemented in real system experiments and the knowledge of the correlators is fundamental in order to understand the behavior of the observables of this system out of the critical point.

2.4.1 The model and the trap size scaling

We consider the Ising model perturbed by a confining potential coupled to the energy operator:

$$S = S_{CFT} + \int d^d z U(z)\epsilon(z) \,, \tag{2.114}$$

where S_{CFT} is the d-dimensional Ising model action, z is the radial coordinate and $U(z) = \rho|z|^p$ is the trap potential. In this following we will consider $p \geq 2$, focusing mostly on the harmonic potential case $p = 2$. The parameter ρ is the trap parameter, which is related to the characteristic trap length $l^{-p} \equiv \rho$ defined in [18], and determines the shape of the trap. Here we will study the large-trap case, namely the small ρ regime, where the CPT approach can be safely applied.

Before writing the expressions for the correlators down, it might be helpful recall the trap size scaling ansatz and the one-point functions we will use in the following.

From standard renormalization group argument, we can write the scaling behavior of the singular part of the free energy density near the critical point. The scaling variables are u_t, u_h associated to the energy and spin operators respectively, to which we must add a further variable u_ρ given by the trap. All the other irrelevant fields are neglected, because the do not affect the asymptotic behavior. The scaling law then becomes:

$$F_s(u_t, u_h, u_\rho; x) = b^{-d} F_s(u_t b^{y_t}, u_h b^{y_h}, u_\rho b^{y_\rho}; x b^{-1}) \tag{2.115}$$

Notice that we inserted also the space position x to stress that now the translational

symmetry is broken (by the presence of the trap) and the observables are point dependent. As usual for this kind of approach we can iterate the renormalization group n times, finding:

$$F_s(u_t, u_h, u_\rho; x) = b^{-nd} F_s(u_t b^{n y_t}, u_h b^{n y_h}, u_\rho b^{n y_\rho}; x b^{-n}) \tag{2.116}$$

At some point, there will be a fixed $u_{\rho_0} = u_\rho |b^{n y_\rho}|$: this point is arbitrary fixed, but it allows us to write explicitly the dependence on the trap variable:

$$F_s(u_t, u_h, u_\rho; x) = \left|\frac{u_\rho}{u_{\rho_0}}\right|^{d/y_\rho} F_s\left(u_t \left|\frac{u_\rho}{u_{\rho_0}}\right|^{-\frac{y_t}{y_\rho}}, u_h \left|\frac{u_\rho}{u_{\rho_0}}\right|^{-\frac{y_h}{y_\rho}}, u_{\rho_0}; x \left|\frac{u_\rho}{u_{\rho_0}}\right|^{\frac{1}{y_\rho}}\right) \tag{2.117}$$

Moreover, the u_i are defined as linear combinations of the parameter deviations from the fixed point, then near the critical point we can reliably substitute them with their corresponding physical parameters:

$$u_t \sim t, \quad u_h \sim h, \quad u_\rho \sim \rho = l^{-p} \tag{2.118}$$

Reabsorbing u_{v_0} in the definition of the free energy we finally arrive at

$$F_s = l^{-p\theta d} f(t l^{p\theta y_t}, h l^{p\theta y_h}; x l^{-p\theta}) \tag{2.119}$$

where we also defined $\theta = y_\rho^{-1}$, that is the characteristic trap exponent and can be deduced by means of scaling arguments if one notices that the perturbation has to be scale invariant. Indeed, rescaling the radial coordinate z by a factor b, $z \to \frac{z}{b}$, the perturbation transforms as

$$\int d^d z' U'(z') \epsilon'(z') = b^{-d+y_\rho-p+\Delta_\epsilon} \int d^d z U(z) \epsilon(z) \ , \tag{2.120}$$

Eventually the scale invariance condition yields

$$\theta = \frac{1}{p + d - \Delta_\epsilon} \ . \tag{2.121}$$

This expression depends only on the dimensionality and universality class of the system and the geometry of the confining trap, confirming that the trap size scaling ansatz shows universal features. It is also interesting noting that if p is sent to infinity, the trap becomes a wall with infinite boundary potential, namely a free system with fixed boundary conditions; in this limit $\theta = 1$, correctly recovering the finite size scaling ansatz.

From the free energy density 2.119 it is straightforward to derive the one-point functions of the spin and energy operators:

$$\langle \sigma(0) \rangle_\rho = A_\sigma \rho^{\theta \Delta_\sigma} \ , \qquad \langle \epsilon(0) \rangle_\rho = A_\epsilon \rho^{\theta \Delta_\epsilon} \ , \tag{2.122}$$

where Δ_σ, Δ_ϵ are the scaling dimensions of the operators σ and ϵ respectively, while A_σ and A_ϵ are non universal constants.

Two-point functions

Just like we did in section 2.3, the two-point functions can be expressed as a series involving one-point expectation values, making use of the Operator Product Expansion:

$$\langle O_i(z)O_j(0)\rangle_\rho = \sum_k C_{ij}^k(\rho,z)\langle O_k(0)\rangle_\rho \ . \tag{2.123}$$

Each of the Wilson coefficient $C_{ij}^k(\rho,z)$, evaluated outside the critical point, can be expanded in series of the trap characteristic parameter ρ, namely:

$$\langle O_i(z)O_j(0)\rangle_\rho = \sum_k [C_{ij}^k(0,z) + \rho\partial_\rho C_{ij}^k(0,z) + ...]\langle O_k(0)\rangle_\rho \tag{2.124}$$

We stress again that the series expansion asymptotically converges,all the coefficients are infrared finite and the derivatives of the coefficients can be evaluated systematically in terms of quantities of the unperturbed theory. But before doing that, it is useful to write the fusion rules, in order to understand which of the Wilson coefficients identically vanish. Among the primary operators of the 3D Ising model, we are interested in the identity I together with only two relevant ones, namely σ and ϵ. The corresponding fusion rules are:

$$[\sigma][\sigma] = [\mathbb{1}] + [\epsilon] + ... \ , \quad [\epsilon][\epsilon] = [\mathbb{1}] + [\epsilon] + ... \ , \quad [\sigma][\epsilon] = [\sigma] + ... \ . \tag{2.125}$$

These relations imply that any correlation functions containing an odd number of σs identically vanishes. Contrary to the $d = 2$ case, where Kramers-Wannier duality ($\langle[\epsilon]^n[\mathbb{1}]^l\rangle = (-1)^n\langle[\epsilon]^n[\mathbb{1}]^l\rangle$) implies that $C_{\epsilon\epsilon}^\epsilon = 0$, in $d = 3$ this Wilson coefficient is in general non-trivial and must be taken into account in the series expansions.

Wilson coefficients in the $d = 3$ case

In three spatial dimensions, the knowledge of correlators at the critical point is limited to two and three-point functions, and the scaling dimensions and structure constants have been evaluated numerically in [9]: $(\Delta_\sigma, \Delta_\epsilon) = (0.5181489(10), 1.412625(10))$ and $(C_{\sigma\sigma}^\epsilon, C_{\epsilon\epsilon}^\epsilon) = (1.0518537(41), 1.532435(19))$. Out of the critical point, the correlators can be expanded as a series of the parameter ρ in the following way:

$$\langle\sigma(z_1)\sigma(0)\rangle_\rho = C_{\sigma\sigma}^{\mathbb{1}}(z_1) + C_{\sigma\sigma}^\epsilon(z_1)A_\epsilon\rho^{\theta\Delta_\epsilon} + \rho\partial_\rho C_{\sigma\sigma}^{\mathbb{1}}(z_1) + ... \ , \tag{2.126}$$

$$\langle\epsilon(z_1)\epsilon(0)\rangle_\rho = C_{\epsilon\epsilon}^{\mathbb{1}}(z_1) + C_{\epsilon\epsilon}^\epsilon(z_1)A_\epsilon\rho^{\theta\Delta_\epsilon} + \rho\partial_\rho C_{\epsilon\epsilon}^{\mathbb{1}}(z_1) + ... \ , \tag{2.127}$$

$$\langle\sigma(z_1)\epsilon(0)\rangle_\rho = A_\sigma\rho^{\theta\Delta_\sigma}(C_{\sigma\epsilon}^\sigma(z_1) + \rho\partial_\rho C_{\sigma\epsilon}^\sigma(z_1) + ...) \ . \tag{2.128}$$

As said before, the derivatives of Wilson coefficient can be written in terms of known quantities. For instance, $\partial_\rho C^I_{\sigma\sigma}(z_1)$ reads:

$$-\partial_\rho C^I_{\sigma\sigma}(z_1) = \int d^3 z_2 \, |z_2|^p \Big[\langle\sigma(z_1)\sigma(0)\epsilon(z_2)\rangle - C^\epsilon_{\sigma\sigma}(z_1)\langle\epsilon(z_2)\epsilon(0)\rangle\Big] \, . \tag{2.129}$$

This integral can be evaluated using a Mellin transform technique (see appendix A for details). In particular, the second term is just a regulator needed to cancel the IR-divergent part, meaning that only the first term contributes to the final result. Expanding the first term in (2.129) in terms of the known correlation function at the critical point we find:

$$\partial_\rho C^I_{\sigma\sigma}(z_1) = -z_1^{\Delta_t - 2\Delta_\sigma + p} C^\epsilon_{\sigma\sigma} \int d^3 y \frac{y^p}{y^{\Delta_\epsilon}(1 + y^2 - 2y\cos\theta)^{\frac{\Delta_\epsilon}{2}}} \, , \tag{2.130}$$

where $\Delta_t = 3 - \Delta_\epsilon$ and $y = z_2/z_1$. We refer to Appendix A for the details of the computation. The final result is:

$$\partial_\rho C^I_{\sigma\sigma}(z_1) = -z_1^{\Delta_t - 2\Delta_\sigma + p} C^\epsilon_{\sigma\sigma} I(p) \, , \tag{2.131}$$

where $I(p)$ is numerical factor that can be expressed in terms of Gamma functions and the relevant parameters of the model, as shown in (A.8). In what follow we are going to consider mostly the harmonic potential case, $p = 2$, for which $I(2) \simeq -8.4448$.

Following the same procedure we can also evaluate the derivative of $C^I_{\epsilon\epsilon}$:

$$\partial_\rho C^I_{\epsilon\epsilon}(z_1) = -z_1^{\Delta_t - 2\Delta_\epsilon + p} C^\epsilon_{\epsilon\epsilon} I(p) \, . \tag{2.132}$$

Putting all together, the expressions (2.126)-(2.128) can be expressed as:

$$z_1^{2\Delta_\sigma}\langle\sigma(z_1)\sigma(0)\rangle_\rho = 1 + C^\epsilon_{\sigma\sigma} A_\epsilon (\rho^\theta z_1)^{\Delta_\epsilon} - C^\epsilon_{\sigma\sigma}\rho z_1^{\Delta_t+2} I(2) + \dots \, , \tag{2.133}$$

$$z_1^{2\Delta_\epsilon}\langle\epsilon(z_1)\epsilon(0)\rangle_\rho = 1 + C^\epsilon_{\epsilon\epsilon} A_\epsilon (\rho^\theta z_1)^{\Delta_\epsilon} - C^\epsilon_{\epsilon\epsilon}\rho z_1^{\Delta_t+2} I(2) + \dots \, , \tag{2.134}$$

$$z_1^{\Delta_\epsilon}\langle\sigma(z_1)\epsilon(0)\rangle_\rho = A_\sigma \rho^{\theta\Delta_\sigma}\left(C^\sigma_{\sigma\epsilon} + \#\rho z_1^{\Delta_t+2} + \dots\right) . \tag{2.135}$$

As usual in this approach, the asymptotic convergence of the series expansion is guaranteed for distances (measured from the center of the trap) less than about one correlation length. In the last equation the symbol $\#$ stands for the numerical value of the coefficient $\partial_\rho C^\sigma_{\sigma\epsilon}(z_1)$. The computation of this coefficient within the CPT framework involves the use of a 4-point correlation function at the critical point:

$$\begin{aligned} &-\partial_\rho C^\sigma_{\sigma\epsilon}(z_1) \lim_{|z_3|\to\infty}\langle\sigma(z_3)\sigma(0)\rangle = \\ &\lim_{|z_3|\to\infty}\int_{|z_2|<|z_3|} d^3 z_2 \, |z_2|^p \Big[\langle\sigma(z_1)\sigma(z_3)\epsilon(z_2)\epsilon(0)\rangle - C^\sigma_{\sigma\epsilon}(z_1)\langle\sigma(z_3)\sigma(0)\epsilon(z_2)\rangle\Big] \, . \end{aligned} \tag{2.136}$$

Since $\langle\sigma(z_1)\sigma(z_3)\epsilon(z_2)\epsilon(0)\rangle$ is not known analytically at the critical point, (2.136)

can not be evaluated exactly. However, as we will show later, this term can not be neglected and it will be determined a posteriori using Monte Carlo simulations.

2.4.2 Conversion to the lattice and numerical results

The model previously described can be solved on a lattice in order to verify the validity of the CPT expansion and to get some insights in the numerical factors which we have not been able to determine analytically. The Hamiltonian of the system on a cubic lattice can be expressed in the following form:

$$\mathcal{H} = -J \sum_{\langle ij \rangle} \sigma_i \sigma_j (1 + U(r_i)) + h \sum_i \sigma_i \tag{2.137}$$

where σ_i is the spin field, r_i is its distance from the center of the confining potential and h is a possible magnetic field perturbation whose importance will be shortly explained. The conformal point is recovered for $h = 0$. To get a more precise physical intuition about the trapping effect, it is convenient to perform the transformation $\sigma_i = 1 - 2\rho_i$. Then, the new variable ρ_i can only assume two values (0 and 1) and it can be thought as a density of particles in a d-dimensional gas. Eventually, the Hamiltonian reads:

$$\mathcal{H} = -4J \sum_{\langle ij \rangle} \rho_i \rho_j - \mu \sum_i \rho_i + 4J \sum_{\langle ij \rangle} U(r_i) \rho_i (1 - \rho_j) \tag{2.138}$$

where $\mu = 2h - 4qJ$ is the chemical potential and q is the coordination number ($q = 6$ in three dimensions). The main advantage of this transformation is that, since the potential $U(r_i)$ diverges at large r_i, it makes it apparent that the only way to prevent the last term in (2.138) to diverge is to set either $\langle \rho_i \rangle = 1$ or $\langle \rho_i \rangle = 0$ for all i far from the center of the trap. The first condition is not physically acceptable (all the particles running away to infinity) and it can be avoided by inserting a small and positive magnetic field h in eq. 2.137, namely:

$$\lim_{h \to 0^+} \lim_{|r| \to \infty} \langle \sigma_r \rangle = 1 \, . \tag{2.139}$$

This leaves us only with the second possibility, which is equivalent to require a null density of particles ($\langle \rho_i \rangle = 0$) far from the center of the lattice, which means that the system is trapped.

Lattice implementation

The Monte Carlo simulation is performed with the Metropolis algorithm on a cube with side L and fixed boundary. The trap is centered in the middle point of the cube. The spin i located on the lattice at distance r from the center is denoted with $\sigma_{r_i}^{lat}$. We calculate the following observables: the spin one-point function on the central site $\langle \sigma_0^{lat} \rangle$, and the energy one-point function in the middle of the lattice, defined as

$\langle \epsilon_0^{lat} \rangle \equiv \langle \sigma_0^{lat} \sigma_1^{lat} \rangle - E_{cr}$, where E_{cr} is the energy bulk contribution at the critical point and $\langle ... \rangle$ is the statistical average.

The correlation functions are calculated from the central site of the lattice up to the distance r on the central axis, averaging between the six orthogonal directions. Thus, they are defined as:

$$G_{\sigma\sigma}(r) \equiv \frac{1}{6}\langle \sum_{i=1}^{3} \sigma_0^{lat} \, (\sigma_{r_i}^{lat} + \sigma_{-r_i}^{lat}) \rangle \, , \tag{2.140}$$

$$G_{\epsilon\epsilon}(r) \equiv \frac{1}{6}\langle \sum_{i=1}^{3} \epsilon_0^{lat} \, (\epsilon_{r_i}^{lat} + \epsilon_{-r_i}^{lat}) \rangle \, , \tag{2.141}$$

$$G_{\sigma\epsilon}(r) \equiv \frac{1}{6}\langle \sum_{i=1}^{3} \epsilon_0^{lat} \, (\sigma_{r_i}^{lat} + \sigma_{-r_i}^{lat}) \rangle \, , \tag{2.142}$$

As the system breaks translational invariance, we may wonder $G_{\sigma\epsilon}$ to be different from $G_{\epsilon\sigma}$. However, we have verified that the differences between the two correlators are negligible within the parameter range used in the simulations and we will eventually focus on $G_{\sigma\epsilon}$ in the rest of our analysis.

We have performed our simulations focusing on the harmonic trap case, namely setting $p = 2$. Moreover we have fixed the following constants to their known Ising model values: the energy bulk value $E_{cr} = 0.3302022(5)$ and the critical temperature $\beta_c = 0.22165462(2)$ [23], the scaling dimensions $\Delta_\sigma = 0.51815(2)$ and $\Delta_\epsilon = 1.41267(13)$ [24]. Thus, $p\theta = 2/(5 - \Delta_\epsilon) \simeq 0.55752$. The uncertainty on these constants is negligible with respect to our numerical precision.

The simulations have been performed with a lattice side $L = 480$ that is large enough to avoid finite size effects within our current precision. Since our observables are closely sampled around the center of the trap, we adopt a hierarchical upgrading scheme [25]: instead of performing the Monte Carlo sweep on the whole lattice at each step, sweeps are performed in nested cycles over smaller cubic boxes of increasing size centered in the middle of the lattice. With this procedure computational times are reduced without affecting local central observables. In a single Monte Carlo simulation, starting from a configuration with all spins aligned, $5 \cdot 10^6$ sweeps have been performed, with about 10^4 sweeps for thermalization. Observable uncertainties have been calculated by using the batched mean method. Moreover, final results of all observables have been obtained by averaging about 100 repeated and independent Monte Carlo simulations.

One-point functions

Since the potential is coupled to the temperature, which in the lattice is non-zero at the critical point, the effective scaling parameter on the lattice to be compared with

analytical prediction is $\rho_{lat} \equiv \beta_c \rho$. Thus, the one-point functions on the lattice are:

$$\langle \sigma_0^{lat} \rangle = A_\sigma^{lat} \, \rho_{lat}^{\theta \Delta_\sigma} \, , \tag{2.143}$$

$$\langle \epsilon_0^{lat} \rangle = A_\epsilon^{lat} \, \rho_{lat}^{\theta \Delta_\epsilon} \, . \tag{2.144}$$

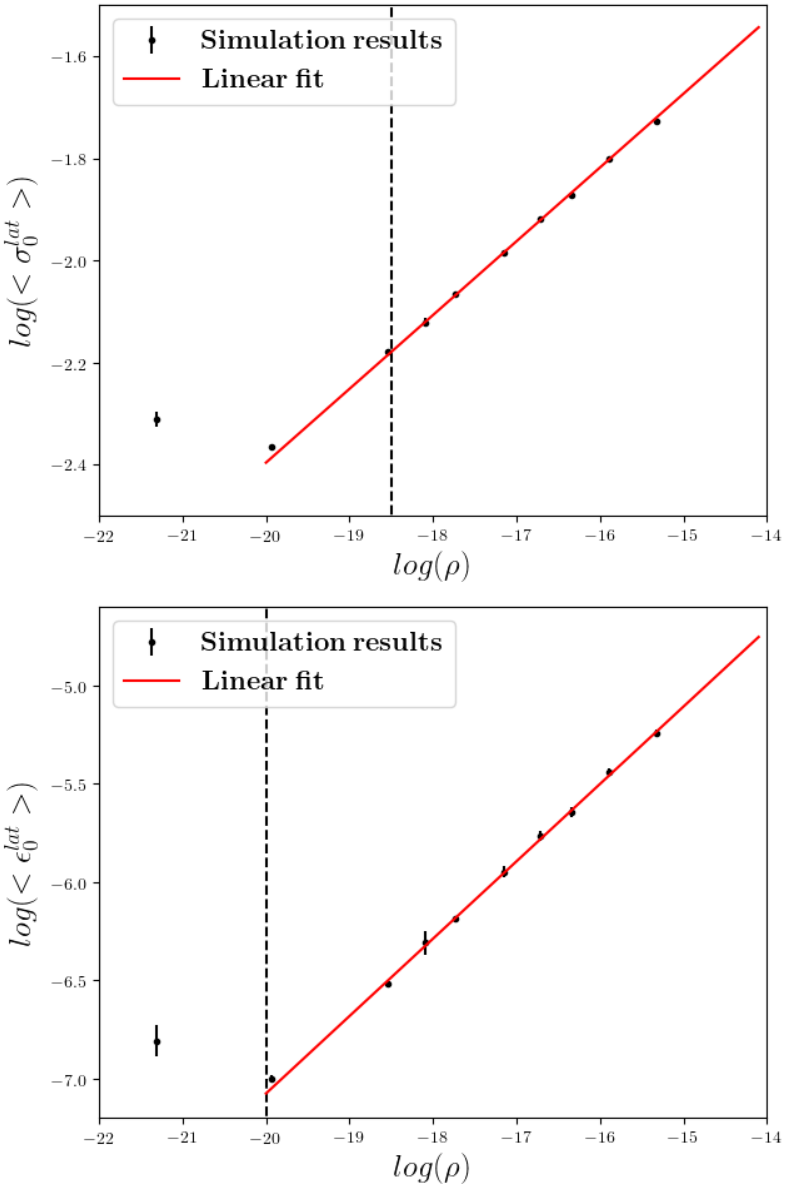

FIGURE 2.4: Bi-log plots of the the spin (Upper panel) and energy (Lower panel) one-point functions against power law fits (red line). Due to numerical accuracy, the fits have been performed for values of ρ greater than the ones indicated by the dashed vertical lines.

The results for the spin and energy one-point functions are shown in figure 2.4. The fit has been performed in the range $10^{-8} \leq \rho \leq 5.625 \times 10^{-7}$. Within this range, the scaling exponents are in good agreement with the theoretical result predicted by the TSS argument 2.143-2.144, as shown in table 2.6. This confirms the validity of

exponent	theory	simulation	$\chi^2/d.o.f.$
$\theta\Delta_\sigma$	0.144439(5)	0.144(1)	0.6
$\theta\Delta_\epsilon$	0.39379(5)	0.392(4)	1.4

TABLE 2.6: Exponents extracted from the fits shown in figure 2.4.

the TSS ansatz [18] also in the present case. Eventually, we fix the exponents to the value 2.143-2.144 and we repeat the fit with only two free parameters to find the remaining constants, obtaining $A_\sigma^{lat} = 1.6390(13)$ and $A_\epsilon^{lat} = 2.226(11)$.

Two-point functions

With the definitions 2.140-2.142 at hand, and taking into account the bulk contribution to the energy operator on the lattice E_{cr}, the two-point functions on the lattice (denoted with with the average $\langle ... \rangle_{lat}$) assume the following form:

$$\langle \sigma(r)\sigma(0)\rangle_{lat} = G_{\sigma\sigma}(r) \,, \tag{2.145}$$

$$\langle \epsilon(r)\epsilon(0)\rangle_{lat} = G_{\epsilon\epsilon}(r) + E_{cr}^2 - E_{cr}(\langle \epsilon_r^{lat}\rangle + \langle \epsilon_0^{lat}\rangle) \,, \tag{2.146}$$

$$\langle \sigma(r)\epsilon(0)\rangle_{lat} = G_{\sigma\epsilon}(r) - E_{cr}\langle \sigma_r^{lat}\rangle \,. \tag{2.147}$$

In order to make contact with the CPT theoretical results (2.126)-(2.128), we must consider the lattice conversion factors R_σ and R_ϵ. Regarding the first, $R_\sigma = 0.55245(13)$ according to [26]. Estimates of R_ϵ vary from 0.2306(38) [26] to 0.2377(9) [17]. This is the largest source of systematic uncertainty in our simulations. For this reason we will adopt the average $R_\epsilon = 0.2341$ with a variation ± 0.0030 to evaluate the final systematic error. Finally, the structure constant on the lattice $(C_{\sigma\sigma}^\epsilon)^{lat}$ must be converted taking into account the conversion rules for ϵ and ρ, namely $\langle \epsilon^{lat}\rangle = R_\epsilon\langle\epsilon\rangle$ and $\rho_{lat} = R_\epsilon^{-1}\rho$. Eventually, combining (2.126)-(2.128) with (2.145)-(2.147) we obtain:

$$\langle \sigma(r)\sigma(0)\rangle_{lat} = \frac{R_\sigma^2}{r^{2\Delta_\sigma}}\left(1 + C_{\sigma\sigma}^\epsilon\, R_\epsilon^{-1} A_\epsilon^{lat} \rho_{lat}^{\theta\Delta_\epsilon} r^{\Delta_\epsilon} - C_{\sigma\sigma}^\epsilon I(2) R_\epsilon \rho_{lat} r^{2+\Delta_t}\right) \tag{2.148}$$

$$\langle \epsilon(r)\epsilon(0)\rangle_{lat} = \frac{R_\epsilon^2}{r^{2\Delta_\epsilon}}\left(1 + C_{\epsilon\epsilon}^\epsilon\, R_\epsilon^{-1} A_\epsilon^{lat} \rho_{lat}^{\theta\Delta_\epsilon} r^{\Delta_\epsilon} - C_{\epsilon\epsilon}^\epsilon I(2) R_\epsilon \rho_{lat} r^{2+\Delta_t}\right) \tag{2.149}$$

$$\langle \sigma(r)\epsilon(0)\rangle_{lat} = \frac{R_\epsilon R_\sigma \rho_{lat}^{\theta\Delta_\sigma}}{r^{\Delta_\epsilon}}\left(C_{\sigma\epsilon}^\sigma\, R_\sigma^{-1} A_\sigma^{lat} + b\rho_{lat} r^{2+\Delta_t}\right) \,. \tag{2.150}$$

The parameter b in the second term of (2.150) is related to the coefficient (2.136), which, as already mentioned, we have not been able to compute analytical using CPT. This parameter will be evaluated a posteriori by fitting the numerical results.

We can now insert the lattice quantities A_ϵ^{lat} and A_σ^{lat} calculated in section 2.4.2, and directly fit the continuum structure constants $C_{\sigma\sigma}^\epsilon$ and $C_{\epsilon\epsilon}^\epsilon$. Fit results, reported in the table 2.7, are in good agreement with the known values: $C_{\sigma\sigma}^\epsilon = 1.0518537$, $C_{\epsilon\epsilon}^\epsilon = 1.532435$ [24]. Figure 2.5 shows the behavior of the correlators. More specifically,

ρ	range r	$C^{\epsilon}_{\sigma\sigma}$	$\chi^2/d.o.f.$
1×10^{-8}	7-13	1.059(20)[40]	3.5
4×10^{-8}	7-13	1.049(5)[15]	0.9
9×10^{-8}	7-13	1.043(3)[14]	0.2

ρ	range r	$C^{\epsilon}_{\epsilon\epsilon}$	$\chi^2/d.o.f.$
1×10^{-8}	6-13	1.46(15)[30]	0.9
4×10^{-8}	6-13	1.58(7)[24]	0.6
9×10^{-8}	6-13	1.50(8)[20]	1.1

TABLE 2.7: Results of the structure constant found by fitting the data with the function 2.148 for various trap sizes ρ. The number in round brackets denotes the statistical uncertainty of the fit, while the number in square brackets denotes the systematic error due to the uncertainty of the constants. Regarding the correlator related to the table on the right side, we have sampled all the distances in the same simulation, so that statistical errors have been estimated by means of the jack-knife technique.

data and fits are outlined for $\rho = 9 \times 10^{-8}$, and Monte Carlo data reproduce well the expected behavior. We obtained very similar results for the other trap-sizes reported in the tables 2.7.

Table 2.8 shows the fit results for the mixed correlator $\langle \sigma\epsilon \rangle$ without including the second term in (2.150) ($b = 0$), while table 2.9 shows the fits including b as a free parameter. As one can see from the tables, once $C^{\sigma}_{\sigma\epsilon}$ is left as a free parameter its value agrees better with the known result if we take into account the parameter b. This is confirmed in Figure 2.6, where it is evident that the presence of b significantly improves the agreement between the theoretical prediction and the numerics. This proves that the second term in (2.150) is definitely important and must be taken into account.

ρ	range r	b ($C^{\sigma}_{\sigma\epsilon} = 1.0518537$)	$\chi^2/d.o.f.$	$C^{\sigma}_{\sigma\epsilon}$ (b=0)	$\chi^2/d.o.f.$
1×10^{-8}	7-13	1.1(2)[3]$\cdot 10^4$	2.2	1.098(3)[10]	0.3
4×10^{-8}	6-13	2.8(4)[5]$\cdot 10^3$	0.98	1.082(6)[12]	1.6
9×10^{-8}	6-13	1.9(2)[4]$\cdot 10^3$	5.5	1.094(10)[14]	4.3

TABLE 2.8: Fit performed including the second term of Eq. 2.150 and fixing $C^{\sigma}_{\sigma\epsilon}$ to the known value (third column), and fit of the structure constant $C^{\sigma}_{\sigma\epsilon}$ setting $b = 0$ (fifth column). It is evident from the data that b contributes non-trivially to the correlator, as our numerical results do not match the known value for $C^{\sigma}_{\sigma\epsilon}$ if we set $b = 0$.

2.4.3 Discussion

With this simple model we have further developed the program of studying systems in their off-critical scaling regime, using the consolidated approach based on the OPE and the possibility of expanding the Wilson coefficients in terms of the perturbing

ρ	range r	$C^{\sigma}_{\sigma\epsilon}$	b	$\chi^2/d.o.f.$
1×10^{-8}	7-13	1.098(4)[10]	~ 0	0.3
4×10^{-8}	6-13	1.067(7)[12]	1.8(5)[1]·10^3	0.3
9×10^{-8}	6-13	1.080(9)[12]	1.0(2)[1]·10^3	0.8

TABLE 2.9: Performing the fit with two free parameters the situation improves and the numerical values of $C^{\sigma}_{\sigma\epsilon}$ are in agreement with the expected one within the numerical error. The results for $\rho = 1 \times 10^{-8}$ are probably affected by some finite-size effect, as it can been seen in the $\langle\sigma\sigma\rangle$ correlator as well.

parameter by means of conformal perturbation theory [7, 27, 28]. This has been done for the 3D Ising model perturbed by a trapping potential coupled to the energy operator. Nevertheless, the procedure can be applied in principle to other systems in a different universality class since the method only requires scale invariance at the critical point.

We have evaluated the first leading terms in the expansions of the correlators comparing the analytic predictions against numerical Monte Carlo simulations. The results for the 1-point functions outlined in Fig. 2.4 confirm once again the validity of the TSS ansatz [18] as a powerful tool to determine the behavior of the expectation values of the model outside the critical point.

Despite the necessity of using large size traps and consequently large lattices, the estimates of the structure constants shown in tables 2.7 are in good agreement with the known results found in literature. This fact shows the reliability of the approach and confirms that this method is a promising tool for studying different systems out of criticality. Additionally, we have proven that the behavior of the $\langle\sigma\epsilon\rangle$ correlator is influenced by the presence of a term which depends, according to the CPT approach, on an integral involving a 4-point function (2.136). Due to the lack of knowledge on the 4-point function at the critical point in the 3D Ising model, this integral can not be evaluated analytically. However, using the high quality CFT data in [29] one could compute the 4-point function needed in (2.136) analogously to what has been done for the σ 4-point function in [30]. The integral (2.136) may be eventually evaluated applying the procedure used to compute similar integrals involving the ϵ 4-point function in [31] and the σ 4-point function in [32]. This will allow us to validate our numerical estimation (Table 2.8 and 2.9) and constitutes a worthwhile future direction.

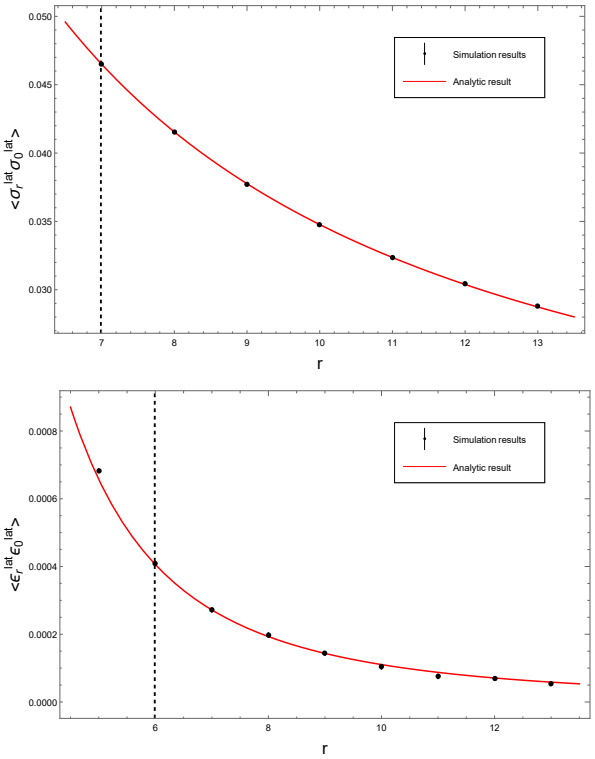

FIGURE 2.5: Results for the spin-spin (up) and energy-energy (down) two-point functions and their fits with the expected behavior (eq. 2.148 and 2.149) red line. Due to numerical accuracy, fits are performed for values of r greater than the ones indicated by the black dashed vertical lines. Error bars are small and usually hidden within the points size.

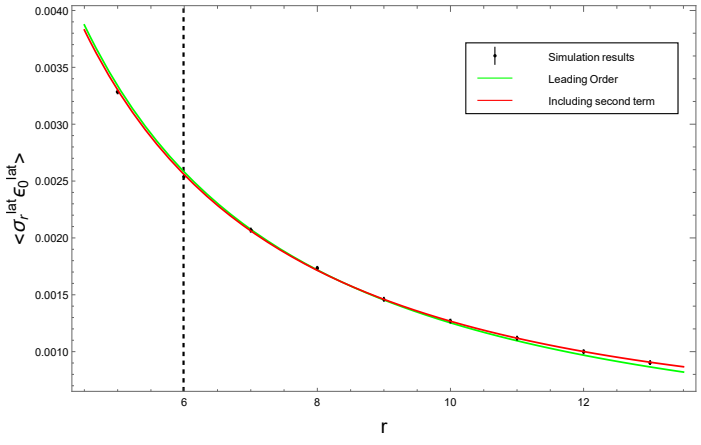

FIGURE 2.6: Fit for the spin-energy two-point function against the theoretically expected behavior performed not including (green line) and including (red line) the second term in Eq. 2.150. As it is evident, the red line agrees consistently better with the numerical result.

Chapter 3

Magneto-thermal transport

3.1 Introduction

The method described in the previous chapter is only one of the possible ways to study conformal field theories and systems near a critical point. For example, the very well known paper by Juan Maldacena [33] more than twenty years ago gave rise to the idea of the famous AdS-CFT correspondence. In a nutshell, the concept behind the duality is that it is possible to get informations about a (strongly coupled) conformal field theory by studying a classical theory of gravity in a one dimension more.

The applications of this approach are very disparate and almost countless, and in this chapter we are going to see how the AdS-CFT duality can be adopted to help us in a specific problem of magnetohydrodynamics.

Magnetohydrodynamics is a collective theory of hydrodynamic modes coupled to electromagnetic degrees of freedom. It is an effective field theory which describes the long-range correlations of near-equilibrium systems, when the microscopic theory is coupled to a $U(1)$ gauge field. The electromagnetic field can be dynamical, where the evolution of the gauge field is governed by the Maxwell equations from a given initial configuration, or external where the profile is arbitrary up to satisfying the Bianchi identity. We are interested in the latter.

In recent times magnetohydrodynamics has been intensively studied. New breakthroughs in the theoretical study of magnetohydrodynamics include, among others things, understanding the deeper underlying symmetries and structures that constrain the transport coefficients and subsequently formulating classification schemes [34, 35]. There have also been applications to the generalized global symmetry reformulation of hydrodynamics [36–39]. At a more practical level the formalism has been used to analyze the physics of relativistic plasmas [40], as well as to understand the behavior of strongly coupled condensed matter systems [41–46].

In the earliest formulations of $(2+1)$-dimensional relativistic magnetohydrodynamics [41–43, 47–51] the entire suite of physically relevant conductivities, electric, thermo-electric and thermal, were given in terms of a single incoherent longitudinal conductivity σ_0 for "not too strong magnetic fields". The latter requirement is a consequence of matching holographic and hydrodynamic results. In particular, it was

discovered that if one assumes the constitutive relation of [41, 48] for the charge current, which depends on only a single transport coefficient σ_0, then one matches precisely the DC electric and thermo-electric conductivities. However, the holographic DC thermal conductivities match the hydrodynamic prediction only in the extreme region where charge density completely suppresses the effect of the magnetic field.

We claim that a more appropriate hydrodynamic theory contains two non-trivial charge transport coefficients - the usual σ_0 and an incoherent Hall conductivity $\tilde{\sigma}_{\rm H}$. To fix these quantities we just use the fact that the diffeomorphism and $U(1)$ gauge Ward identities constrain the small frequency expansion of the charge conductivity [48, 52]. In particular, we note that the $\mathcal{O}(\omega^2)$ piece of the charge correlator relies on the values of the DC thermal conductivities. Thusly, by matching our hydrodynamic correlators at small frequency up to and including $\mathcal{O}(\omega^2)$, we find that σ_0 and $\tilde{\sigma}_{\rm H}$ can be expressed entirely in terms of two system dependent quantities - the longitudinal ($\kappa_{\rm L}$) and Hall ($\kappa_{\rm H}$) thermal DC conductivities - and the thermodynamics. Consequently our hydrodynamic correlators, being dependent only on σ_0, $\tilde{\sigma}_{\rm H}$ and the thermodynamics at order one in hydrodynamic derivatives, are also expressed entirely in terms of the same variables. It is important to note that the resultant relations are valid at any order in the magnetic field, provided that one knows $\kappa_{\rm L}$ and $\kappa_{\rm H}$ exactly.

In [53], where $(2+1)$-dimensional parity violating hydrodynamics is considered up to an including order one in derivatives, an incoherent Hall conductivity is included in the constitutive relation of the $U(1)$ charge current. However, because the authors of that paper consider $B \sim \mathcal{O}(\partial)$ this Hall conductivity is only non-zero to the order worked at if the theory violates spatial parity in the absence of the magnetic field. The incoherent Hall conductivity we will consider is proportional to the magnetic field - which we take to be order zero in derivatives - and exists in a theory that does not violate spatial parity microscopically. It could potentially appear in the formalism of [53] at $\mathcal{O}(\partial^2)$, as a new transport coefficient. In principle, our type of Hall conductivity was allowed for in the appendix of [45], but to our knowledge it has never been shown to be non-zero. Here we provide for the first time an expression for $\tilde{\sigma}_{\rm H}$ (and also σ_0) in terms of $\kappa_{\rm L}$, $\kappa_{\rm H}$ and the thermodynamics. We eventually verify the validity of our results using gauge/gravity duality, analyzing the simple holographic model of the dyonic black hole. In these kinds of holographic models, analytical formulae for the DC thermo-electric transport coefficients in terms of the thermodynamic data are very well known [42, 47–50, 52, 54–61]. Consequently we have been able, using the known result for $\kappa_{\rm L}$ and $\kappa_{\rm H}$, to completely determine the incoherent conductivities σ_0 and $\tilde{\sigma}_{\rm H}$, and eventually to compare the complete hydrodynamic correlators to the holographic ones.

In the next sections we will present in general the theory of a relativistic charged fluid in $(2+1)$-dimensions in the presence of an external magnetic field. After reviewing the Ward identities, we show that the incoherent conductivities σ_0 and $\tilde{\sigma}_{\rm H}$, and

eventually the hydrodynamic AC charge correlator for general frequencies, are completely determined by thermodynamic quantities and the DC longitudinal and Hall thermal conductivities $\kappa_{\rm L}$ and $\kappa_{\rm H}$. Subsequently, we return to the tried and tested example of the $(3+1)$-dimensional dyonic black hole and apply our formalism, finding that the system is very well described by the hydrodynamics derived in section 3.2.

3.2 Magnetohydrodynamics

Consider a $(2+1)$-dimensional system with a conserved, global $U(1)$ current. The (non-) conservation equations of the stress-energy-momentum (SEM) tensor and charge current are

$$\nabla_\mu \langle T^{\mu\nu} \rangle = F^\nu{}_\mu \langle J^\mu \rangle \,, \tag{3.1}$$

$$\nabla_\mu \langle J^\mu \rangle = 0 \,. \tag{3.2}$$

Here $\langle T^{\mu\nu} \rangle$ and $\langle J^\mu \rangle$ refer to the "total currents" given by variation of the source terms in the action describing our system. In the presence of an electromagnetic field which is $\mathcal{O}(\partial^0)$ in derivatives the right hand side of (3.1) has an explicit source term.

We assume the existence of a preferred time-like Killing vector field u^μ and $SO(2)$ rotational invariance. We define the following tensor structures

$$\Pi_{\mu\nu} = g_{\mu\nu} + u_\mu u_\nu \,, \qquad \Sigma_{\mu\nu} = \sqrt{-g}\epsilon_{\mu\nu\rho}u^\rho \,, \tag{3.3}$$

$$\Pi_{\mu\nu}\Pi^{\nu\rho} = \Pi_\mu{}^\rho \,, \qquad \Pi_{\mu\nu}\Sigma^{\nu\rho} = \Sigma_\mu{}^\rho \,, \qquad \Sigma_{\mu\nu}\Sigma^{\nu\rho} = -\Pi_\mu{}^\rho \,, \tag{3.4}$$

where $\epsilon_{\mu\nu\rho}$ is the Levi-Civita symbol with $\epsilon_{012} = 1$. With respect to these structures we can define a gauge and Lorentz invariant electric E^μ and magnetic field B by decomposing the field strength tensor into

$$F_{\mu\nu} = u_\mu E_\nu - u_\nu E_\mu + B\Sigma_{\mu\nu} \,. \tag{3.5}$$

Similarly we can decompose the stress tensor and the electric current in the following manner

$$\langle T^{\mu\nu} \rangle = \mathcal{E}u^\mu u^\nu + (\mathcal{P}^\mu u^\nu + \mathcal{P}^\nu u^\mu) + \mathcal{P}\Pi^{\mu\nu} + \mathcal{T}^{\mu\nu} \,, \tag{3.6}$$

$$\langle J^\mu \rangle = \mathcal{N}u^\mu + \mathcal{J}^\mu \,, \tag{3.7}$$

where all indices not present on u^μ are transverse and we have defined

$$\mathcal{E} = u_\mu u_\nu \langle T^{\mu\nu} \rangle \,, \qquad \mathcal{P} = \frac{1}{2}\Pi_{\mu\nu}\langle T^{\mu\nu} \rangle \,, \qquad \mathcal{N} = -u_\mu \langle J^\mu \rangle \,, \tag{3.8}$$

$$\mathcal{P}^\mu = -\Pi^\mu{}_\rho \langle T^{\rho\nu} \rangle u_\nu \,, \qquad \mathcal{J}^\mu = \Pi_{\mu\nu}\langle J^\nu \rangle \,, \tag{3.9}$$

$$\mathcal{T}^{\mu\nu} = \left(\Pi^\mu{}_\sigma \Pi^\nu{}_\rho - \frac{1}{2}\Pi^{\mu\nu}\Pi_{\rho\sigma} \right) \langle T^{\rho\sigma} \rangle \,. \tag{3.10}$$

The two index structure $\mathcal{T}^{\mu\nu}$ is symmetric and traceless.

3.2.1 The diffeomorphism and $U(1)$ gauge symmetry Ward identities

A key role in our derivation will be played by the Ward identities. Essentially, the presence of an order zero in derivative $O(\partial^0)$ source in the momentum conservation equation will mean that the thermo-electric and thermal conductivities are completely determined by the electric conductivity.

The Ward identities for the two point functions of the SEM tensor and charge current, on a flat spacetime with a non-zero electromagnetic field [52], are

$$\begin{aligned} 0 &= -k_\mu \langle J^\alpha T^{\mu\nu}\rangle + iF_\mu{}^\nu \langle J^\alpha J^\mu\rangle + k^\nu \langle J^\alpha\rangle - k_\mu \eta^{\alpha\nu}\langle J^\mu\rangle \,, && (3.11)\\ 0 &= k_\mu \left(\langle T^{\alpha\beta}T^{\mu\nu}\rangle + \eta^{\alpha\nu}\langle T^{\beta\mu}\rangle + \eta^{\beta\nu}\langle T^{\alpha\mu}\rangle - \eta^{\mu\nu}\langle T^{\alpha\beta}\rangle\right) \\ &\quad + i\eta^{\beta\nu}F_\mu{}^\alpha\langle J^\mu\rangle + i\eta^{\alpha\nu}F_\mu{}^\beta\langle J^\mu\rangle - iF_\mu{}^\nu\langle T^{\alpha\beta}J^\mu\rangle \,, && (3.12)\end{aligned}$$

where $k^\mu = (\omega, \vec{k})$ is the momentum. Contracting with the fluid velocity or spatial projector while specializing to zero wavevector we find that these identities can be written as

$$\begin{aligned} \omega\langle \mathcal{J}^\mu \mathcal{P}^\nu\rangle &= -\omega\mathcal{N}\Pi^{\mu\nu} - iE^\nu\langle \mathcal{J}^\mu\mathcal{N}\rangle + iB\Sigma_\rho{}^\nu\langle \mathcal{J}^\mu\mathcal{J}^\rho\rangle \,, && (3.13)\\ \omega\langle \mathcal{P}^\rho \mathcal{P}^\sigma\rangle &= -\left(\omega\mathcal{E} - iE_\mu\langle \mathcal{J}^\mu\rangle\right)\Pi^{\rho\sigma} - iE^\sigma\langle \mathcal{P}^\rho\mathcal{N}\rangle + iB\Sigma_\mu{}^\sigma\langle \mathcal{P}^\rho\mathcal{J}^\mu\rangle \,. && (3.14)\end{aligned}$$

In the case of the dyonic black hole that we investigate later, we will take $E^\mu \equiv 0$ and B to be constant. Evaluating the Ward identities with these restrictions causes terms proportional to E^μ to drop out. Further, replacing $\mathcal{P}^\mu$ by the spatially projected canonical heat current $\mathcal{Q}^\mu = \mathcal{P}^\mu - \mu\mathcal{J}^\mu$ we arrive at the following relations

$$\begin{aligned} \langle \mathcal{J}^\mu\mathcal{Q}^\nu\rangle &= -\mathcal{N}\Pi^{\mu\nu} - \left(\mu\Pi_\rho{}^\nu - \frac{iB}{\omega}\Sigma_\rho{}^\nu\right)\langle \mathcal{J}^\mu\mathcal{J}^\rho\rangle \,, && (3.15)\\ \langle \mathcal{Q}^\mu\mathcal{Q}^\nu\rangle &= -\left(\mathcal{E}+\mathcal{P}-\mathcal{N}\mu\right)\Pi^{\mu\nu} - \left(\mu\Pi_\rho{}^\nu - \frac{iB}{\omega}\Sigma_\rho{}^\nu\right)\langle \mathcal{Q}^\mu\mathcal{J}^\rho\rangle \,. && (3.16)\end{aligned}$$

The importance of the terms which depend on B/ω cannot be overstated. They are essential to the structure of the correlation functions as they mix different orders in frequency between the correlators. Consequently, knowing the complete AC behavior of the charge conductivity is sufficient to determine the thermo-electric and thermal conductivities.

More explicitly, we define the AC electric, thermo-electric and thermal conductivities to be

$$\begin{aligned} \langle \mathcal{J}^\mu\mathcal{J}^\nu\rangle &= i\omega\sigma^{\mu\nu}(\omega) \,, && (3.17)\\ \langle \mathcal{J}^\mu\mathcal{Q}^\nu\rangle &= i\omega\alpha^{\mu\nu}(\omega) \,, && (3.18)\\ \langle \mathcal{Q}^\mu\mathcal{Q}^\nu\rangle &= i\omega\kappa^{\mu\nu}(\omega) \,, && (3.19)\end{aligned}$$

respectively. In terms of these totally transverse tensor structures, the Ward identities become

$$\alpha^{\mu\nu} = i\frac{\mathcal{N}}{\omega}\Pi^{\mu\nu} - \left(\mu\Pi_{\rho}{}^{\nu} - \frac{iB}{\omega}\Sigma_{\rho}{}^{\nu}\right)\sigma^{\mu\rho} , \tag{3.20}$$

$$\kappa^{\mu\nu} = \frac{i}{\omega}\left(\mathcal{E}+\mathcal{P}-\mathcal{N}\mu\right)\Pi^{\mu\nu} - \left(\mu\Pi_{\rho}{}^{\nu} - \frac{iB}{\omega}\Sigma_{\rho}{}^{\nu}\right)\alpha^{\mu\rho} . \tag{3.21}$$

As the thermo-electric and thermal conductivities are given entirely in terms of the charge conductivity, and the Ward identities hold for all frequencies, it follows that complete specification of the charge conductivity at all frequencies is sufficient to determine the other two conductivities.

The microscopic theory has $SO(2)$ rotational invariance with B breaking spatial parity. Consequently we can decompose the conductivity tensor structures into

$$(\sigma(\omega),\alpha(\omega),\kappa(\omega))^{\mu\nu} = (\sigma_{\rm L},\alpha_{\rm L},\kappa_{\rm L})\Pi^{\mu\nu} + \frac{1}{B}(\sigma_{\rm H},\alpha_{\rm H},\kappa_{\rm H})\Sigma^{\mu\nu} , \tag{3.22}$$

where the tensors $\Pi^{\mu\nu}$ and $\Sigma^{\mu\nu}$ are treated as order zero in fluctuations, namely substituting $u^{\mu} = (1,\vec{0})$. In terms of this decomposition, and at low frequencies, we discover that

$$\sigma_{\rm L}(\omega) = -i\left(\frac{\mathcal{E}+\mathcal{P}}{B^2}\right)\omega + \frac{\kappa_{\rm L}(0)}{B^2}\omega^2 + \mathcal{O}(\omega^3) , \tag{3.23}$$

$$\sigma_{\rm H}(\omega) = \mathcal{N} + \frac{1}{B^2}\left(\kappa_{\rm H}(0) + \mu\left(2(\mathcal{E}+\mathcal{P}) - \mu\mathcal{N}\right)\right)\omega^2 + \mathcal{O}(\omega^3) , \tag{3.24}$$

where we have used that the conductivities must be finite at vanishing ω and we have assumed that $\mathcal{N}$, $\mathcal{E}$ and $\mathcal{P}$ are independent of frequency up to and including $\mathcal{O}(\omega^2)$. In particular, requiring finite behavior as $\omega \to 0$ in the Ward identities[1] constrains

$$\sigma_{\rm L}(0) = \alpha_{\rm L}(0) = 0 , \qquad \sigma_{\rm H}(0) = \mathcal{N} , \qquad \alpha_{\rm H}(0) = \mathcal{E}+\mathcal{P}-\mu\mathcal{N} , \tag{3.25}$$

but leaves $\kappa_{\rm L}(0)$ and $\kappa_{\rm H}(0)$ unconstrained and system dependent. In section 3.3 we will set them to be the values befitting the dyonic black hole.

We emphasise that we have not made any magnetization subtractions in our definition of the spatially projected currents and therefore the transport coefficients refer to the total current and not the "free current". Moreover we have ignored any of the normalizations by temperature often made to the thermal conductivity so as to not clutter notation.

[1]The magnetic field gaps excitations of the system to be at or above the cyclotron frequency in energy. Consequently one expects a smooth limit at low frequencies. This should be compared to relativistic charged hydrodynamics without a background field strength where there is a known δ-function singularity at low frequencies.

3.2.2 Equilibrium magnetohydrodynamics

A comprehensive derivation of the equilibrium configurations of polarizable matter is given in [62]; however we shall only need the results to lowest order in derivatives. The equilibrium charge current in a theory with only a non-vanishing magnetic field in the background (and no electric field) has the form

$$\langle J^\mu \rangle = \rho u^\mu - \nabla_\nu M^{\nu\mu} \,, \tag{3.26}$$

$$M^{\mu\nu} = -m\epsilon^{\mu\nu\rho}u_\rho \,, \tag{3.27}$$

to all orders in derivatives where $\rho = \frac{\partial \mathcal{F}}{\partial \mu}$ is the charge density, $m = -\frac{\partial \mathcal{F}}{\partial B}$ is the magnetization and $\mathcal{F}$ is the free energy. For our purposes the equilibrium configuration of the charge current decomposed with respect to the time-like vector at zeroth order in derivatives is

$$\mathcal{N} = \rho \,, \qquad \mathcal{J}^\mu = 0 \,, \tag{3.28}$$

where we have taken a ground state with no vorticity.

Turning now to the SEM tensor, we identify the following expressions at order zero in derivatives,

$$\mathcal{E} = -P + Ts + \mu\rho \,, \qquad \mathcal{P} = P - mB \,, \qquad \mathcal{P}^\mu = 0 \,, \qquad \mathcal{T}^{\mu\nu} = 0 \,. \tag{3.29}$$

In the above P is the pressure, T the temperature and s the entropy density. Again we have assumed the electric field vanishes in the background. Our microscopic theory will be conformal such that the trace of the SEM tensor gives

$$\mathcal{E} - 2\mathcal{P} = (\varepsilon - 2P + 2mB) = 0 \,, \tag{3.30}$$

where ε is the energy density. We note that the equilibrium configuration of the system depends on the external magnetic field B; as will the leading terms in the derivative expansion of the transport coefficients. In systems where the magnetic field is extremely weak - such that it can be treated as $\mathcal{O}(\partial)$ in derivatives - the thermodynamic quantities and transport coefficients can still depend on B but this dependence appears as higher order terms in the derivative expansion i.e. the leading terms in this latter case are B independent.

3.2.3 AC diffusivities in magnetohydrodynamics

We wish to work to order one in fluctuations about a flat background at constant temperature T_b, chemical potential μ_b and magnetic field B. Let $u^\mu = u^\mu_b + \delta u^\mu$, with $u^\mu_b = (1, \vec{0})$, be the time-like Killing vector field of the system to order one in fluctuations. We require our fluctuation to maintain $u_\mu u^\mu = -1$; whence it is the case that δu^μ needs to be entirely transverse. At this order in fluctuations the conservation

equations have the form

$$\partial_\mu \delta\langle T^{\mu\nu}\rangle = F_b^{\nu\mu}\delta\langle J_\mu\rangle + \delta F^{\mu\nu}\langle J^b_\mu\rangle \,, \tag{3.31}$$

$$\partial_\mu \delta\langle J^{\mu}\rangle = 0 \,. \tag{3.32}$$

Just as for the full currents, the fluctuations can be decomposed with respect to a time-like vector field. In this case it is useful to use u_b^μ. Consequently, we can identify

$$\delta\langle T^{\mu\nu}\rangle = \delta\mathcal{E}u_b^\mu u_b^\nu + \left(\delta\mathcal{P}^\mu u_b^\nu + \delta\mathcal{P}^\nu u_b^\mu\right) + \delta\mathcal{P}\Pi_b^{\mu\nu} + \delta\mathcal{T}^{\mu\nu} \,, \tag{3.33}$$

$$\delta\langle J^{\mu}\rangle = \delta\mathcal{N}u_b^\mu + \delta\mathcal{J}^\mu \,, \tag{3.34}$$

$$\delta F^{\mu\nu} = u_b^\mu \delta E^\nu - u_b^\nu \delta E^\mu \,. \tag{3.35}$$

With these expressions we can decompose the spatial part of the SEM tensor (non-) conservation equation into the following form

$$u_b^\mu \partial_\mu \delta\mathcal{P}^\nu = -\Pi_b^{\nu\mu}\left(\partial_\mu\delta\mathcal{P} + \partial_\mu\delta\mathcal{T}^{\mu\nu}\right) + \mathcal{N}_b\delta E^\nu + B\Sigma_b^{\nu\mu}\delta\mathcal{J}_\mu \,, \tag{3.36}$$

This will be the only relevant differential equation that we need to solve.

An unusual feature of any hydrodynamic theory with an explicitly sourced momentum term is the ability to work in the diffusive sector assuming vanishing wavevector $\vec{k}$ from the get-go. This is due to the fact that the diffusive pole does not move to the origin of the complex frequency plane as $\vec{k}\to 0$. To compare this with ungapped hydrodynamics, the diffusive pole has the form $\omega = -iD\vec{k}^2$ and taking $\vec{k}^2 \to 0$ in the conservation equations (if one is not careful) gives a trivial result. This inspires us to ignore spatial derivatives in our conservation equations such that the relevant momentum flow equations become

$$u_b^\mu \partial_\mu \delta\mathcal{P}^\nu = \mathcal{N}_b\delta E^\nu + B\Sigma_b^{\nu\mu}\delta\mathcal{J}_\mu \,, \tag{3.37}$$

for arbitrary - slowly varying - time dependent profiles.

At the level of linear response we need only determine the fluctuating part of the constitutive relations that are non-zero for completely time dependent profiles. We remind the reader that the electric field is external and permitted to have any time dependence we choose on the condition that the time dependence is sufficiently slow. As such, we will choose it to be a plane wave at a single frequency. With this in mind the constitutive relation for the current takes the form,

$$\delta\mathcal{J}^\mu(\omega) = \hat{\sigma}_0^{\mu\nu}\delta E_\nu + \hat{\chi}^{\mu\nu}\delta\mathcal{P}_\nu(\omega) \,, \tag{3.38}$$

where the subscript $_0$ indicates the fundamental (incoherent) conductivity of the theory and the tensor transport coefficients are constant. We have chosen spatial momentum rather than spatial velocity to be one of our fluid variables as it is more

convenient for solving the resultant hydrodynamic equations of motion. Spatial rotational invariance allows us to break the transverse tensor structures of (3.38) into a piece proportional to $\Pi^{\mu\nu}$ and one proportional to $\Sigma^{\mu\nu}$.

We would like to highlight a point that will return later, the constitutive relation of (3.38) represents the complete response of the charge current in hydrodynamics. We are working at $\vec{k} = 0$ so there are no derivative corrections proportional to $\vec{k}$. Moreover one cannot add derivative corrections in ω without introducing additional modes and taking us outside the hydrodynamic regime. As we are working to order one in fluctuations and both the electric field and momentum vanish in the background there cannot be non-linear tensor structures that correct (3.38). Thus (3.38) contains everything consistent with hydrodynamics.

Applying the definitions of (3.38) to (3.37) we see that the spatial momentum (non-) conservation equation becomes

$$u_b^\mu \partial_\mu \delta\mathcal{P}^\nu(t) = -\Gamma^{\nu\mu}\delta\mathcal{P}_\mu(t) + \Theta^{\mu\nu}\delta E_\nu(t) \,, \tag{3.39}$$

where we have defined

$$\Gamma^{\mu\nu} = -B\Sigma_b{}^\mu{}_\rho \hat{\chi}^{\rho\nu} \,, \tag{3.40}$$

$$\Theta^{\mu\nu} = \mathcal{N}_b \Pi_b^{\mu\nu} + B\Sigma_b{}^\mu{}_\rho \hat{\sigma}_0^{\rho\nu} \,. \tag{3.41}$$

It is important to note that, unlike in the case of $B = 0$ or $B \sim O(\partial^1)$, the conservation equation (3.39) is a non-trivial and solvable linear differential equation for the spatial momentum because there is a gap in excitations of the system generated by the magnetic field. In the case of $B = 0$ or $B \sim O(\partial^1)$ the expression on the right hand side of (3.39) vanishes at lowest order in derivatives.

In the Martin-Kadanoff procedure [63] we assume that we turn on some source for our conserved quantities at $t = 0$ and allow them to evolve according to the conservation equations. Performing a Laplace transform in time (accounting for boundary conditions at $t = 0$) of (3.39) we arrive at

$$-i\omega\delta\mathcal{P}^i(\omega) - \delta\mathcal{P}_0^i = -\Gamma^i{}_j\delta\mathcal{P}^j(\omega) + \Theta^i{}_j\delta E^j \,, \tag{3.42}$$

where $\delta\mathcal{P}_0^i$ is the perturbed value of the spatial momentum at $t = 0$. Consequently the momentum evolves in frequency according to

$$\delta\mathcal{P}(\omega) = (\Gamma - i\omega\mathbb{1}_2)^{-1}\left(\Theta\delta E + \delta\mathcal{P}_0\right) \,, \tag{3.43}$$

where indices are implied.

The frequency evolution of the charge currents can now be determined by substituting (3.43) into the charge conservation equation employing the constitutive relations (3.38). The result for the charge current is

$$\delta\mathcal{J} = \left(\hat{\sigma}_0 + \hat{\chi}\left(\Gamma - i\omega\mathbb{1}_2\right)^{-1}\Theta\right)\delta E + \hat{\chi}\left(\Gamma - i\omega\mathbb{1}_2\right)^{-1}\delta\mathcal{P}_0 \,. \tag{3.44}$$

From these expressions the frequency evolution of the electric conductivity can be readily determined to be

$$\sigma(\omega) = \hat{\sigma}_0 + \hat{\chi}\left(\Gamma - i\omega\mathbb{1}_2\right)^{-1}\Theta \,. \tag{3.45}$$

To determine the thermal conductivity from the constitutive relations we would in principle need a non-zero spatial momentum. However, we are saved from having to do this by making use of the Ward identities of (3.15) and (3.16).

There are some important observations to make about our expressions for the AC diffusivities. Firstly, all poles in these correlation functions must originate in the inverse matrix $\left(\Gamma - i\omega\mathbb{1}_2\right)^{-1}$. The zeroes of the determinant of this matrix will correspond to the quasinormal modes of our dyonic black hole model. Secondly, if we determine the AC response of the charge conductivity, the fundamental conductivities are given entirely in terms of other quantities,

$$\mathrm{Tr}\left[\sigma(\omega)\right] = \mathrm{Tr}\left[\hat{\sigma}_0\right] - \mathrm{Tr}\left[\hat{\chi}\left(\Gamma - i\omega\mathbb{1}_2\right)^{-1}\Theta\right] \,, \tag{3.46}$$

$$\mathrm{Tr}\left[\sigma(\omega)\epsilon\right] = \mathrm{Tr}\left[\hat{\sigma}_0\epsilon\right] - \mathrm{Tr}\left[\hat{\chi}\left(\Gamma - i\omega\mathbb{1}_2\right)^{-1}\Theta\epsilon\right] \,, \tag{3.47}$$

with

$$\epsilon = \begin{pmatrix} 0 & 1 \\ -1 & 0 \end{pmatrix} \,, \tag{3.48}$$

where we assume we are away from any singularities associated with the inverse operation. In what follows we will decompose our fundamental conductivities as

$$\hat{\sigma}_0^{ij} = \sigma_0\delta^{ij} + \tilde{\sigma}_{\mathrm{H}}F^{ij} \,, \tag{3.49}$$

$$\hat{\chi}^{ij} = \chi_0\delta^{ij} + \chi_{\mathrm{H}}F^{ij} \,, \tag{3.50}$$

where we have used spatial parity invariance to argue that the scalar Hall conductivities $\tilde{\sigma}_{\mathrm{H}}$, χ_{H} must be even in B when they multiply the tensor structure F^{ij}. We note that unlike some previous formulations [41, 48, 64] we have allowed for an incoherent Hall conductivity in (3.49). Such a term is not forbidden (in particular by transformations under spatial parity as it multiplies F^{ij}) and should therefore be included. In fact it turns out to be necessary. It is consistent with the previous results [53] where the magnetic field is treated as $\mathcal{O}(\partial)$ because it would only appear at $\mathcal{O}(\partial^2)$.

3.2.4 Constraining hydrodynamic correlators with the Ward identities

We are now ready to compare the electric conductivities derived in (3.46) and (3.47) to the Ward identities (3.23) and (3.24), expanding them order by order in the frequency ω. Eventually we constrain the unknown transport coefficients σ_0, $\tilde{\sigma}_{\rm H}$, χ_0 and $\chi_{\rm H}$ of (3.49) and (3.50).

The order $\mathcal{O}(\omega^0)$ equations are trivial so we immediately turn to $\mathcal{O}(\omega^1)$. In the small frequency expansion of the AC correlators, the trace relations (3.46) and (3.47) become

$$\frac{i}{2}\mathrm{Tr}[\sigma'(0)] = \frac{\rho\chi_0 + (\sigma_0\chi_{\rm H} + \chi_0\tilde{\sigma}_{\rm H})\,B^2}{B^2\left(\chi_0^2 + B^2\chi_{\rm H}^2\right)}\,, \tag{3.51}$$

$$-\frac{i}{2}\mathrm{Tr}[\sigma'(0)F] = \frac{\sigma_0\chi_0 - \rho\chi_{\rm H} + \chi_{\rm H}\tilde{\sigma}_{\rm H}B^2}{B^2\left(\chi_0^2 + B^2\chi_{\rm H}^2\right)}\,. \tag{3.52}$$

Comparing the previous expressions with (3.23) and (3.24), at $\mathcal{O}(\omega^1)$ we can constrain

$$\chi_0 = \frac{\rho - B^2\tilde{\sigma}_{\rm H}}{sT + \mu\rho - mB}\,, \qquad \chi_{\rm H} = \frac{\sigma_0}{sT + \mu\rho - mB}\,, \tag{3.53}$$

which agree with the standard result of (B.5) up to the introduction of the magnetization (a known result) and a fundamental Hall conductivity.

At $\mathcal{O}(\omega^2)$ we can apply the same process, which will yield expressions for σ_0 and $\tilde{\sigma}_{\rm H}$ in terms of the DC thermal conductivities $\kappa_{\rm L}(0)$ and $\kappa_{\rm H}(0)$ and the thermodynamic variables. The resultant expressions are

$$\Xi\sigma_0(0) = (sT + \mu\rho - mB)^2\kappa_{\rm L}(0)\,, \tag{3.54}$$

$$\begin{aligned}\Xi\tilde{\sigma}_{\rm H}(0) = &-\left(m^2\left(\kappa_{\rm H}(0) + \mu^2\rho + 6\mu sT\right) - \rho\kappa_{\rm L}(0)^2\right)\\ &+\frac{2m}{B}\left(\kappa_{\rm H}(0)(sT - \mu\rho) + \mu sT(\mu\rho + 3sT)\right)\\ &-\frac{1}{B^2}\left(s^2T^2 - \rho\kappa_{\rm H}(0)\right)\left(\kappa_{\rm H}(0) + \mu^2\rho + 2\mu sT\right) + 2B\mu m^3\,,\end{aligned} \tag{3.55}$$

$$\begin{aligned}\Xi = &\,B^2\left(\kappa_{\rm L}(0)^2 + 4\mu^2m^2\right) - 4B\mu m\left(\kappa_{\rm H}(0) + \mu^2\rho + 2\mu sT\right)\\ &+\left(\kappa_{\rm H}(0) + \mu^2\rho + 2\mu sT\right)^2\,.\end{aligned} \tag{3.56}$$

These expressions are valid to all orders in B and we remind the reader that $\kappa_{\rm L}(0)$ and $\kappa_{\rm H}(0)$ are the DC thermal conductivities of the total currents - not the free current. Parenthetically, we note that on the condition $\kappa_{\rm L}(0) \neq 0$ there is a non-zero σ_0. Moreover, the incoherent Hall conductivity $\tilde{\sigma}_{\rm H}$ can only be zero if the thermal conductivities are related by the constraint (3.55) (with $\tilde{\sigma}_{\rm H} = 0$). As we will see in section 3.3 this is not true in general and as such we generically expect $\tilde{\sigma}_{\rm H}$ to be non-zero in all but a very special subset of systems.

Our AC charge conductivity correlator at order one in hydrodynamic derivatives takes the form

$$\sigma_{\rm L}(\omega) = \frac{i\omega\left(\gamma_*^2+i\gamma_*\omega+\omega_*^2\right)(sT+\mu\rho-mB)}{B^2\left((\omega-i\gamma_*)^2-\omega_*^2\right)}\,, \tag{3.57}$$

$$\frac{\sigma_{\rm H}(\omega)}{B} = \frac{\rho}{B}+\frac{\omega^2\omega_*(sT+\mu\rho-mB)}{B^2\left((\omega-i\gamma_*)^2-\omega_*^2\right)}\,, \tag{3.58}$$

where

$$\omega_* = \frac{B(sT+\mu\rho-mB)\left(-\kappa_{\rm H}(0)+2B\mu m-\mu(\mu\rho+2sT)\right)}{\Xi}\,, \tag{3.59}$$

$$\gamma_* = \frac{B^2\kappa_{\rm L}(0)(sT+\mu\rho-mB)}{\Xi}\,, \tag{3.60}$$

and Ξ has been defined in (3.56). We include in appendix B.2 the AC thermo-electric and thermal conductivities. This is one of our key results as it represents an excellent approximation to the charge correlators that yields the correct values for the DC electric, thermo-electric and thermal conductivities. Moreover, it demonstrates that obtaining the correct DC value of the thermal correlator has nothing to do with including higher order derivative terms nor a frame transformation [64] - everything is fixed at $\mathcal{O}(\partial)$ in the constitutive relations, once one takes into account the constraints between the incoherent and the thermal DC conductivities (3.55)-(3.56), which are dictated by the Ward identities.

Since it will be useful in what follows, we also introduce the complexified conductivity,

$$\begin{aligned}\sigma_+(\omega) &\equiv \frac{\sigma_H(\omega)}{B}+i\sigma_L(\omega)\\ &= B\tilde{\sigma}_{\rm H}+i\sigma_0-\frac{(sT+\mu\rho-mB)(\omega_*-i\gamma_*)^2}{B^2(\omega-(\omega_*-i\gamma_*))}\,.\end{aligned} \tag{3.61}$$

The advantage of this complexified representation is that σ_+ depends in a straightforward way only on a single hydrodynamic pole located at $\omega_*-i\gamma_*$, as is evident in (3.61).

Some notes about (3.61) are rather important. Relativistic hydrodynamics is a derivative expansion in time and space describing the lowest lying quasinormal modes (typically one or two such modes with similar imaginary part). In [45] for example there are two constant terms sourcing the momentum and one finds two quasinormal modes are necessary to specify the hydrodynamic limit of the AC conductivity. As hydrodynamics does not incorporate other quasinormal modes, in our case, one expects it to at most get the AC correlator correct to $\mathcal{O}(\omega^2)$. One can motivate this from arguing for the general form of $\sigma_+(\omega)$, which is

$$\sigma_+(\omega) = \frac{\alpha_1+\alpha_2\omega}{\omega+\alpha_3}\,, \tag{3.62}$$

where α_1, α_2 and α_3 are complex numbers. We can use the Ward identities to fix α_1, α_2 and α_3 in terms of the three complex DC conductivities - determining (3.62) uniquely.

There can be no further corrections in hydrodynamics to (3.61). Any ω dependent corrections to (3.61) necessarily introduce additional modes and take us outside the regime of hydrodynamics. Similarly, attempting to improve the position of the quasi-normal mode necessarily requires that we modify the α_3 of (3.62) and subsequently no longer match the DC conductivities[2]. There is in fact a good motivation for fixing the DC conductivities in preference to the quasi-normal mode as one can see that errors in the position of the latter are suppressed by the distance of the complex pole from the real frequency axis. Hence (3.61) is the complete hydrodynamic correlator. Any errors between it and the observed AC conductivity cannot be removed within the hydrodynamic regime.

3.3 Revisiting the dyonic black hole

We will check the results of the previous section using the holographic dyonic black hole. Eventually, we consider the following action

$$S = \int d^{3+1}x \sqrt{-g}\left(R - 6 - \frac{1}{4}F^2\right) , \tag{3.63}$$

where F is a $U(1)$ gauge field strength. The bulk spacetime corresponding to a $(2+1)$-dimensional conformal field theory at strong coupling with a non-zero charge density and magnetic field is the asymptotically AdS_4 dyonic black hole solution to the equations of motion coming from (3.63). This black hole has the metric

$$ds^2 = \frac{dz^2}{f(z)} + \frac{\alpha^2}{z^2}\left(-f(z)dt^2 + dx^2 + dy^2\right) , \tag{3.64a}$$

$$f(z) = 1 + \left(\rho^2 + B^2\right)\left(\frac{z}{\alpha}\right)^4 - \frac{1}{\alpha}\left(\alpha^4 + \rho^2 + B^2\right)\left(\frac{z}{\alpha}\right)^3 , \tag{3.64b}$$

with the horizon at $z = 1$, the boundary at $z = 0$ and bulk gauge field strength

$$F = -\mu \mathrm{d}z \wedge \mathrm{d}t + B\mathrm{d}x \wedge \mathrm{d}y . \tag{3.65}$$

The thermodynamics of this black brane is well known, and here we only list the results. The temperature T, the entropy density s, the charge density ρ and the magnetization density m are expressed in terms of the bulk data μ, α and B as follows:

$$T = \frac{(3\alpha^4 - \mu^2 - B^2)}{4\pi\alpha^3} , \qquad \rho = \alpha\mu , \qquad m = -\frac{B}{\alpha} , \qquad s = \pi\alpha^2 . \tag{3.66}$$

[2] A discussion of how well our hydrodynamic expression matches the lowest quasinormal mode of the dyonic black hole is relegated to appendix B.2.

As the system is conformally invariant it satisfies a scaling Ward identity which relates the pressure P and the energy density ε:

$$\varepsilon = 2\left(P - mB\right) \ , \qquad \varepsilon = \frac{1}{2\alpha}\left(\alpha^4 + \rho^2 + B^2\right) \ . \tag{3.67}$$

Additionally the system is extensive and therefore satisfies a first law with $\varepsilon + P = \mu\rho + sT$.

We will be interested in finite frequency fluctuations about the background (3.64) and (3.65) corresponding to fluctuations of the boundary electric field. This requires that we consider fluctuations of the tx and ty components, δg_{tx} and δg_{ty}, of the metric and x and y components of the gauge field, δa_x and δa_y. The analysis of these perturbations at first order in small frequency was completed in [47]. We record them here

$$\langle \mathcal{J}^\mu \mathcal{J}^\nu \rangle = -i\omega \frac{\rho}{B} \Sigma^{\mu\nu} + \mathcal{O}(\omega^2) \ , \tag{3.68}$$

$$\langle \mathcal{J}^\mu \mathcal{Q}^\nu \rangle = -\frac{i\omega}{B}\left(\frac{3}{2}\varepsilon - \mu\rho\right) \Sigma^{\mu\nu} + \mathcal{O}(\omega^2) \ , \tag{3.69}$$

$$\begin{aligned} \langle \mathcal{Q}^\mu \mathcal{Q}^\nu \rangle = \ & i\omega \left(\frac{(sT)^2}{\rho^2 + B^2}\right) \Pi^{\mu\nu} \\ & -i\omega \left(\frac{\rho}{B(\rho^2 + B^2)}\left((sT)^2 - (m^2 + \mu^2)B^2\right)\right) \Sigma^{\mu\nu} + \mathcal{O}(\omega^2) \ . \end{aligned} \tag{3.70}$$

These were determined analytically and hold for all values of the magnetic field and charge. Comparing with (3.25) we see that we can identify

$$\mathcal{N} = \rho \ , \qquad \mathcal{E} + \mathcal{P} = \frac{3\varepsilon}{2} \ , \tag{3.71}$$

and additionally we have

$$\kappa_{\rm L}(0) = \frac{(sT)^2}{\rho^2 + B^2} \ , \qquad \kappa_{\rm H}(0) = \frac{\rho}{\rho^2 + B^2}\left((sT)^2 - (m^2 + \mu^2)B^2\right) \ . \tag{3.72}$$

The AdS-CFT correspondence gives the total current as a variation of the on-shell action. Consequently our DC conductivities are with reference to the total current, and not the magnetization subtracted versions that sometimes appear in the literature [41, 48–51] .

The Ward identities were demonstrated to hold in the holographic case of the dyonic black hole in [48]. Through them, should we evaluate the charge conductivity at arbitrary frequency, we will be able to determine the thermo-electric and thermal conductivities. This analysis has been done previously and we refer the reader to [48]. The result is that the independent response of our theory is described by the

coupled bulk equations

$$f(z)\left(-\rho\mathcal{E}'_+(z)+B\mathcal{B}'_+(z)\right)+\omega\left(B\mathcal{E}'_+(z)+\rho\mathcal{B}'_+(z)\right) = 0\,, \tag{3.73}$$

$$\frac{\omega}{4z^2}\left(\mathcal{E}'_+(z)-\frac{\omega}{f(z)}\mathcal{B}_+(z)\right)+B^2\mathcal{B}_+(z)-\rho B\mathcal{E}_+(z) = 0\,, \tag{3.74}$$

where

$$\mathcal{E}_+(z) = i\omega\left(\delta a_x(z)+i\delta a_y(z)\right)+\frac{iB}{z^2}\left(\delta g_{tx}(z)+i\delta g_{ty}(z)\right)\,, \tag{3.75}$$

$$\mathcal{B}_+(z) = -Bf(z)\left(\delta a'_x(z)-i\delta a'_y(x)\right)\,. \tag{3.76}$$

The asymptotic expansion of the fields $\mathcal{E}_+(z)$ and $\mathcal{B}_+(z)$ yield the boundary electric field and charge currents respectively,

$$\lim_{z\to 0}\mathcal{E}_+(z)=E_x+iE_y\,,\qquad -i\lim_{z\to 0}\mathcal{B}_+(z)=J_x+iJ_y\,. \tag{3.77}$$

This provides another motivation for us to consider the complex charge conductivity

$$\lim_{z\to 0}\frac{\mathcal{B}_+(z)}{\mathcal{E}_+(z)}=\sigma_+(\omega)=\sigma_{xy}(\omega)+i\sigma_{xx}(\omega)\,. \tag{3.78}$$

Expressed in terms of this complexified conductivity, and having substituted the dyonic black hole results (3.71) for $\mathcal{N}$, $\mathcal{E}$ and $\mathcal{P}$, the Ward identities (3.23) and (3.24) give:

$$\begin{aligned}\sigma_+(\omega) &= \frac{\rho}{B}+\frac{sT+\mu\rho-mB}{B^2}\omega \\ &\quad+\left[\frac{2\left(\kappa_{\rm H}(0)+\mu^2\rho+2\mu sT-2\mu mB\right)}{2B^3}+i\frac{\kappa_{\rm L}(0)}{B^2}\right]\omega^2+O\left(\omega^3\right)\,.\end{aligned} \tag{3.79}$$

3.3.1 An incoherent conductivity

We now prove that the formulae for the incoherent conductivities given in (3.54) and (3.55) are actually valid in the dyonic black hole. The usual definition of such a quantity in terms of the charge current orthogonal to momentum [65] will no longer suffice as the magnetic field B mixes the two spatial components of the momentum. Consequently there is no part of the charge current which is orthogonal to the momentum at all points in space. Instead, we return to the original motivation for defining the incoherent conductivity - it is the contribution to the correlator that is independent of coherent dissipative mechanisms. Such mechanisms when relevant to hydrodynamics can be introduced into the formalism by modifying the source term of the momentum equation by shifting Γ^{ij} to $\Gamma^{ij}+\Gamma^{ij}_{\rm coherent}$.

With this remark in mind we define the incoherent conductivity to be the constant term in the Laurent expansion of the complexified conductivity σ_+ as defined in (3.61) about the hydrodynamic pole located at $\omega_*-i\gamma_*$. This is invariant under the

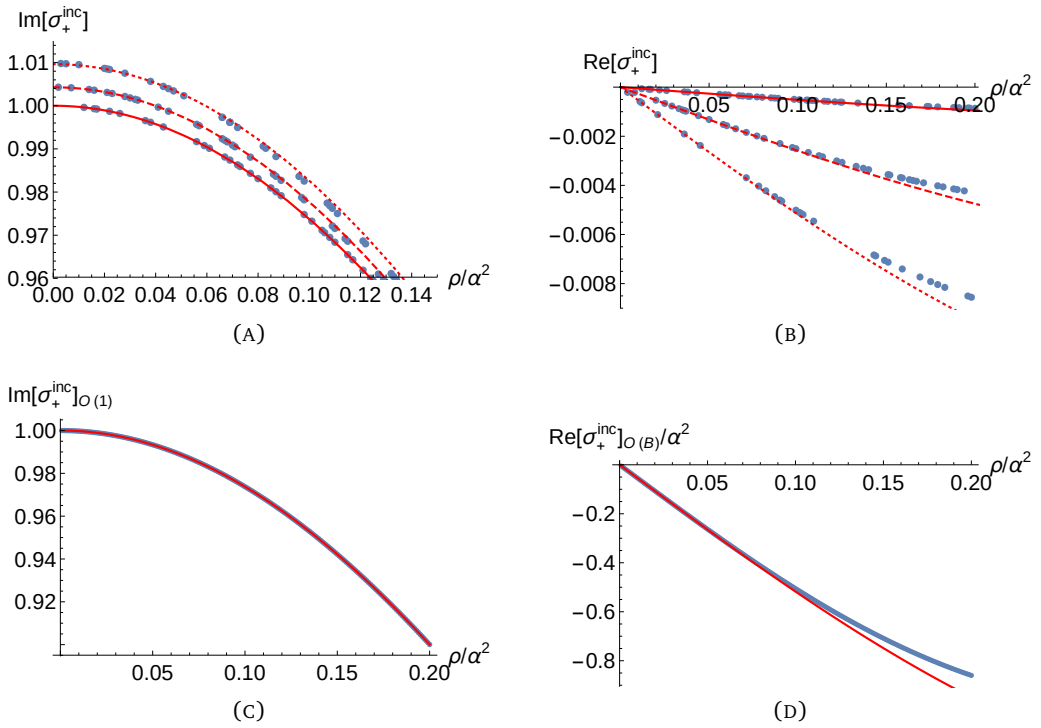

FIGURE 3.1: Plots of the constant term in the Laurent expansion of the charge correlator about the hydrodynamic pole against the charge density. The blue dots are data. **Upper left:** The imaginary part of $\sigma_+^{\text{inc.}}$ against our analytic expression for σ_0. The three red lines represent $B/\alpha^2 = 1/1000$ (solid), $1/25$ (dashed) and $3/50$ (dotted). Notice that $\sigma_0 > 1$ which stands in contradiction to the standard prescription where $\sigma_0 = (sT/(\varepsilon + P))^2 \leq 1$. **Upper right:** The real part of $\sigma_+^{\text{inc.}}$ against our analytic expression for $\tilde{\sigma}_{\text{H}}$. The three red lines represent $B/\alpha^2 = 1/1000$ (solid), $5/1000$ (dashed) and $10/1000$ (dotted). **Lower left:** The leading contribution at small B to the imaginary part of the constant term. The solid red line is the analytic expression for $[\sigma_0]_{B=0}$. **Lower right:** The $\mathcal{O}(B^1)$ contribution to the constant part of the Laurent expansion. The red line is our analytic result for $[\tilde{\sigma}_{\text{H}}]_{B=0}$.

translation $\omega \to \omega - i\Gamma_{\text{coherent}}$ and equal to the first term of (3.61) i.e.

$$\sigma_+^{\text{inc.}} \equiv B\tilde{\sigma}_{\text{H}} + i\sigma_0 \ . \tag{3.80}$$

At lowest order in B these terms are

$$[\sigma_0]_{B=0} = \left(\frac{3\alpha^4 - \rho^2}{3(\rho^2+\alpha^4)^2}\right)^2 \ , \quad [\tilde{\sigma}_{\text{H}}]_{B=0} = -\frac{16\rho\left(\rho^2+3\alpha^4\right)\left(5\rho^4+6\alpha^4\rho^2+9\alpha^8\right)}{81\left(\rho^2+\alpha^4\right)^4} \ , \tag{3.81}$$

when expressed in dyonic black hole data. In fact, it should be noted that $\tilde{\sigma}_{\text{H}}$ vanishes as $\mathcal{O}(\rho)$ independent of the value of B for the dyonic black hole.

We have checked the validity of the relation (3.80) against the numerics. Displayed in the upper plots of fig. 3.1 are our analytic expressions for the incoherent conductivities against charge density at various values of the magnetic field. For low magnetic fields the match is excellent as expected, becoming progressively worse as

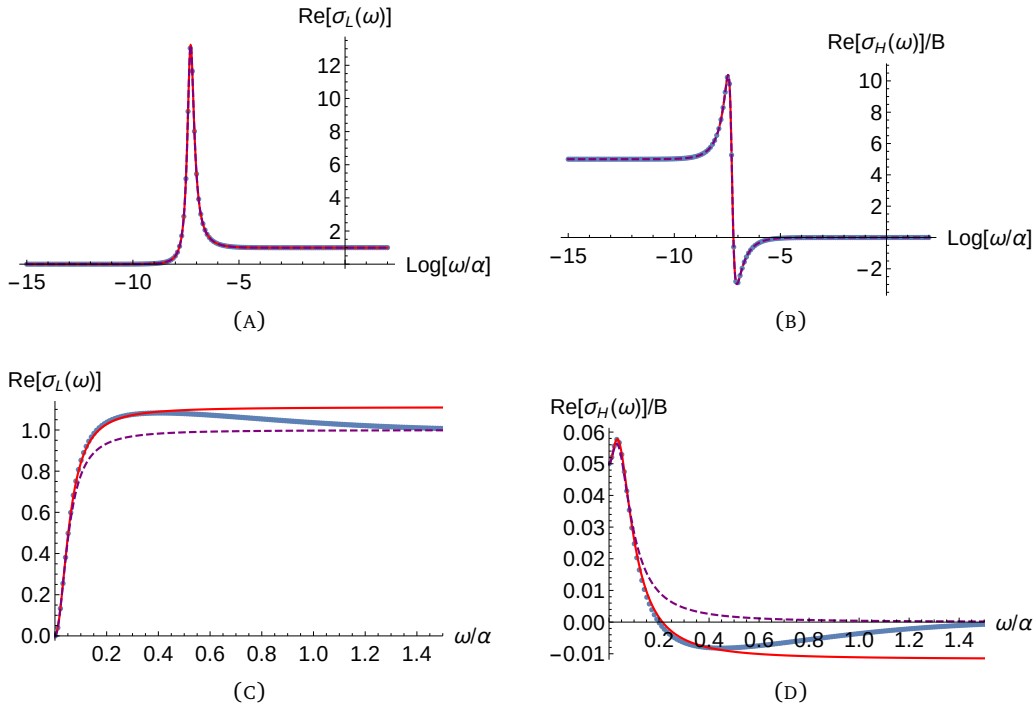

FIGURE 3.2: The real parts of the AC charge conductivity as a function of frequency for two choices of charge density and magnetic field. Blue dots are data, the solid red line is our analytic result and the purple dashed line is the result of standard magnetohydrodynamics (see appendix B.1). **Upper:** The longitudinal (left) and Hall (right) AC conductivities with $B/\alpha^2 = 1/100$ and $\rho/\alpha^2 = 1/20$. **Lower:** The longitudinal (left) and Hall (right) AC conductivities with $B/\alpha^2 = 1/20$ and $\rho/\alpha^2 = 1/100$ i.e. $B > \rho$.

we increase the magnetic field and charge density (and therefore effectively lower the temperature). Moreover, our result for σ_0 becomes greater than one for $B > \rho$, in agreement with the data. The result from the standard magentohydrodynamic approach to the dyonic black hole leads to an incoherent conductivity σ_0 bounded above by one.

Additionally, in fig. 3.1 we display $[\sigma_0]_{B=0}$ against the numerically extracted constant Laurent coefficient at low B in the lower left hand plot of fig. 3.1 and the matching is excellent. In the lower right plot we also show $[\tilde{\sigma}_{\rm H}]_{B=0}$. The match is a little less accurate as ρ increases, or equivalently T decreases. This is most likely due to higher order pole corrections which become relevant at low T and one expects hydrodynamics to be less accurate. These comparisons at least prove that $\tilde{\sigma}_{\rm H}$ is nonzero in the dyonic black hole and that (3.54) and (3.55) are accurate expressions for σ_0 and $\tilde{\sigma}_{\rm H}$.

3.3.2 Matching the correlators

We can now proceed to match the full correlators (3.57) and (3.58) (considering the pole position (3.59)) against the numerical results for the dyonic black hole. The outcome is shown in figure 3.2. We distinguish two different regimes. When $\rho > B$

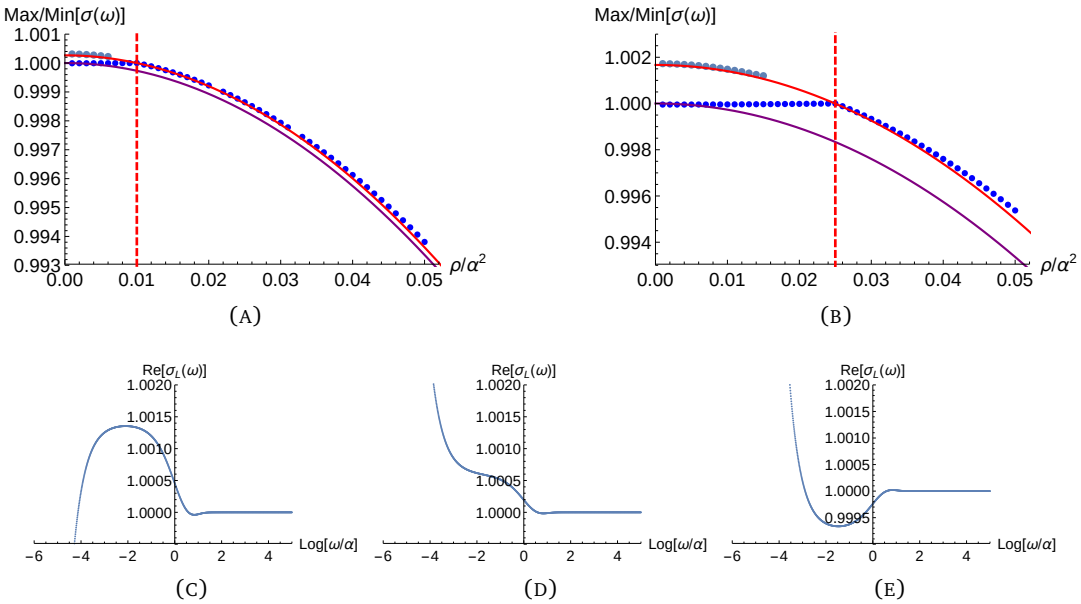

FIGURE 3.3: Turning points of the AC charge conductivity as a function of charge density for two values of the magnetic field: $B/\alpha^2 = 0.01$ (top left) and $B/\alpha^2 = 0.025$ (top right). The blue dots are data while the solid red line is our analytic result for the incoherent conductivity σ_0. The dashed red line indicates the point where $\rho = B$ while the purple line indicates the $B = 0$ limit of our analytic result, coinciding with the conductivity given by [48]. In particular, the light blue uppermost dots of both figures which occur in the region $B > \rho$ are maxima, while the dark blue dots in the region $\rho > B$ are minima. In the bottom row we display a zoomed in plot of real part of the longitudinal charge conductivity against the logarithm of frequency at $B/\alpha^2 = 0.025$. The leftmost plot with $\rho/\alpha^2 = 1/100$ such that $B \gg \rho$ shows the local maximum at $\log\omega/\alpha \approx -2$ which corresponds to the light blue dots in the upper right figure. The rightmost plot is taken at $\rho/\alpha^2 = 3/100$ so that $\rho > B$ and we have a minimum at $\log\omega/\alpha \approx -1.5$. The middle plot on the bottom row indicates what happens in the intermediate region $\rho \lesssim B$.

(figures 3.2 (a) and (b)), the agreement between (3.57) and (3.58) and the numerics is excellent in a wide range of temperature. In this case, at large ω the conductivity $\sigma_{\rm L}$ reaches a minimum before approaching the conformal value ($\sigma_{\rm L} = 1$) as shown in figure 3.3. The same figure shows that the value of this minimum is very well approximated by the incoherent conductivity σ_0 defined in (3.54), which is less than 1 in this regime. The frequency at which the conductivity shows this minimum can be considered as a high frequency cut-off for the validity of the hydrodynamic regime. It is worth mentioning that, as it is evident from the purple line in figure 3.3, the $B = 0$ limit of σ_0, namely the well known result $[\sigma_0]_{B=0} = \left[(sT/(\varepsilon + P))^2\right]_{B=0}$ of standard magnetohydrodynamics (see appendix B.1), approximates the minimum in a significantly worse way than the full σ_0 in (3.81).

In the opposite regime, $\rho < B$, the matching is good in a shorter range of frequencies as shown in figures 3.2 (c) and (d). This is reasonable since B is becoming

large and hydrodynamics is expected to be a worse approximation in this regime. In any case the correlators (3.57) and (3.58) approximate the numerics consistently better than the standard magnetohydrodynamics (see appendix B.1), which does not take into account the existence of a non-trivial $\tilde{\sigma}_{\mathrm{H}}$ (see the purple dashed line in figure 3.2 (c) and (d)). In this regime $\sigma_0 > 1$ as one can see in figure 3.3, and the conductivity does not show anymore a minimum at high frequency, approaching the conformal value from above. However, when $B \gg \rho$, σ_0 approximates the maximum of the conductivity, as shown in figure 3.3. Eventually, in this case the frequency at which the conductivity reaches its maximum can be defined as the UV cut-off for hydrodynamics.

We reiterate an important point in our discussion here. Hydrodynamics, like any theory, depends on a set of a priori unknown variables - the transport coefficients which must be fixed by reference to data; in our case the DC conductivities. We can of course choose different data such as the quasinormal modes to match against. However, while hydrodynamics remains a theory of a single quasinormal mode there are at most three complex constants one can fix (3.62). Any improvement in matching against other quantities, for example the AC correlator at larger B or the quasinormal mode, comes at the cost of losing an exact match with the DC conductivity.

In any case, we have proved that including a non-zero incoherent Hall conductivity $\tilde{\sigma}_{\mathrm{H}}$, in addition to the previously considered longitudinal incoherent charge conductivity σ_0, it is possible to match hydrodynamics to the value of the DC thermal current beyond order zero in the magnetic field expansion. These incoherent conductivities - and subsequently thermo-electric correlation functions - can be expressed in terms of the DC thermal conductivities κ_{L} and κ_{H} and the thermodynamics once one appreciates that these thermal DC transport coefficients fix the $\mathcal{O}(\omega^2)$ piece of the charge current correlator. This is a consequence of the structure of the diffeomorphism and $U(1)$ gauge Ward identities [48, 52]. Subsequently, we have shown that this modified hydrodynamics leads to the correct effective field theory necessary to describe the hydrodynamic regime of the holographic dyonic black hole.

Chapter 4

Final discussion

In this thesis, we have faced several problems that at a first sight might seem a little unrelated. However, analyzing more carefully the systems we have presented here, it is possible to observe that they all share a common thread, since they are somehow related to different aspects of Conformal Field Theories.

Here we have discussed some general but very important features of Conformal Field Theories, which allowed us to understand better the power of the conformal invariance. The presence of the strong constraints imposed by conformal invariance indeed, makes the system easier to solve (e.g. the shape of the 2- and 3-point functions is determined by symmetry constraints). Nevertheless, despite the great success and diffusion of CFTs in very different fields of physics (from string theory to condensed matter physics), in many cases they are not sufficient to explain some interesting phenomena. We have proposed two approaches that can be useful when a CFT is perturbed by different kinds of operators and the tools of standard approaches to conformal field theories become ineffective.

The approach based on conformal perturbation theory has demonstrated to be very adaptable to achieve different goals in many contexts. In fact, not only we have shown that it can be applied to various systems (whether classical or quantum systems, and in any dimensions), but also we have applied it for different purposes. In the first example, we were able to study the inter-quark potential using a new approach, and the numerical results from Monte Carlo simulations confirmed the reliability of our method in a quite large range of temperatures. In the second example instead, we used the results for the perturbed two-point functions to extract a numerical estimates of OPE coefficients. Our findings are in good agreement with the known results in literature, for instance using the conformal bootstrap approach, even if we are far from its precision. In any case, the method presented here is a reliable alternative and the precision of our results could be further improved by performing high precision Monte Carlo simulations.

The successful tests of conformal perturbation theory open up the possibility of interesting generalizations. Of particular relevance could be the one for the critical end-point in the phase diagram of QCD, which, if it exists, is expected to be in the universality class of the Ising model in three dimensions. It should be emphasized that the origin of the critical point in the QCD phase diagram is totally different from

the one in the purely gluonic $SU(2)$ Yang-Mills theory, with $N = 2$ color charges, that we have considered before. In QCD, even though the quark condensate vanishes at a finite temperature and for $\mu = 0$, this change of state from the hadronic phase to a deconfined, chirally symmetric phase is not a transition, but rather a crossover. At finite μ the transition between the two phases should be given by a line of first-order transitions. If that line exists, then it should turn into the crossover band at a critical end-point which is expected to be described in terms of a conformal field theory in the universality class of the three-dimensional Ising model [66].

The discussion above clarifies that, although the symmetries of $SU(2)$ Yang-Mills theory at finite temperature (and vanishing chemical potential) and those of QCD with dynamical quarks of physical masses at finite temperature and finite chemical potential are remarkably different, their critical behavior at the deconfinement phase transition and at the QCD critical end point are remarkably described by the same universality class, i.e. their static, long-range properties are expected to be those characteristic of the Ising model in three dimensions. With the previous discussion, we have shown that it would be possible to formulate theoretical predictions in its neighborhood using conformal perturbation theory.

Another fascinating possible generalization could be the application of conformal perturbation theory to systems where the critical point is broken by a lattice operator. The results could be also compared with what has been done in [67] by means of AdS/CFT techniques. In this sense it becomes clearer how the two approaches presented in this thesis, despite being so different, are actually strictly connected and somehow complementary. Indeed, one of the major problems concerning perturbative approaches is the strong coupling limit, where perturbative methods usually fail. On the other hand, the Gauge/Gravity duality offers a solution, mapping the strong coupled problem to a weakly coupled, classical theory of gravity in one dimension more, which is usually easier to treat. In Chapter 3 we have seen an application to a relatively simple model and the results perfectly matched the hydrodynamic ones. It would be also interesting to understand if the present discussion can be generalized to systems with Goldstone bosons in the presence of the magnetic field, like the charge density wave models described in [68–72].

As we have seen, the Physics of critical phenomena and of systems near a critical point is extremely rich and one of the most studied topics in the last decades, both theoretically and experimentally. We have described some tools to study these fascinating systems and provided some relatively simple example to show the reliability of the methods. Of course, much can still be done for a more complete and deeper knowledge about critical phenomena.

Appendix A

Mellin transform technique

Integrals such as 2.96 and 2.129 can not be directly computed because one needs to carefully treat their behavior in the IR regime. Thus it is useful to write a general integral of this kind as:

$$I(m) = \int d^3z \Theta(m|z|)g(z) \ , \tag{A.1}$$

where $\Theta(|m|z) = e^{-m|z|}$ is an IR-regulator needed to guarantee the convergence of the integral. We are interested in the $m \sim 0$ expansion of $I(m)$, that can be recovered by considering its Mellin transform. Assuming that the leading behavior of $I(m)$ as $m \to 0$ is m^a, while it approaches m^{-b} when $m \to \infty$, the Mellin transform $\tilde{I}(s)$ is defined on the strip $-a < Re(s) < b$ in the complex s plane as:

$$\tilde{I}(s) = \int_0^\infty \frac{dm}{m} m^s I(m) \ . \tag{A.2}$$

Even though the integrals we are interested in consist of two pieces, it can be proven that only the first term of the integrals contributes, while the second one leads to a null strip so that the transform is not well defined. This is due to the fact that the true information of the Wilson coefficient is contained in the first term, while the second one acts as an IR regulator.

However, it is known that the asymptotic expansion of the original function $I(m)$ at $m = 0$ is in a one to one correspondence with the poles of the Mellin transform, namely:

$$I(m) = \sum_i Res(\tilde{I}(s))_{s=-a_i} m^{-s} \ , \tag{A.3}$$

where $a_1 \equiv a < a_2 < ...$ are the powers of m in the asymptotic expansion of $I(m)$ at $m \sim 0$. (A.3) tells us that we can get the corrections to the Wilson coefficients by taking the residue of the perturbative expansions at $s = 0$ if the infrared counter-terms do not give any finite contribution.

With our choice of the regulator, the Mellin transform of $I(m)$ can be easily obtained by using the convolution theorem, finding:

$$\tilde{I}(s) = \Gamma(s)\tilde{g}(1-s) \ , \tag{A.4}$$

where

$$\tilde{g}(1-s) = \int d^3z|z|^{-s}g(z)\ , \tag{A.5}$$

is essentially the Mellin transform of g up to angular coefficients. This means that in order to find an expression for the derivatives of the Wilson coefficients, one just needs to evaluate the Mellin transform of the function $g(z)$.

In our case, the function $g(z)$ can be written as:

$$g(z) = \frac{z^{p-\Delta_\epsilon}}{(1+z^2-2z\cos\theta)^{\frac{\Delta_\epsilon}{2}}}\ . \tag{A.6}$$

where depending on the value of p we recover one of the two integrals: if $p=0$ we get 2.96 while for $p=2$ we find 2.129.

The Mellin transform of $g(z)$ can be evaluated by performing the angular integral and rewriting the result in terms of beta-functions as follows:

$$\begin{aligned}\tilde{I}(s) = \Gamma(s)\frac{2\pi}{2-\Delta_\epsilon}\Big[&B(p+2-\Delta_\epsilon-s, 2\Delta_\epsilon-4-p+s)+\\ &-B(p+2-\Delta_\epsilon-s, 3-\Delta_\epsilon)-B(3-\Delta_\epsilon, 2\Delta_\epsilon-4-p+s)\Big]\end{aligned} \tag{A.7}$$

Then, we are ready to extract the $m\sim 0$ behavior from A.3. The only contribution comes from the residue at $s=0$, so that

$$\begin{aligned}I(p) = \frac{2\pi}{2-\Delta_\epsilon}\Big[&B(p+2-\Delta_\epsilon, 2\Delta_\epsilon-4-p)+\\ &-B(p+2-\Delta_\epsilon, 3-\Delta_\epsilon)-B(3-\Delta_\epsilon, 2\Delta_\epsilon-4-p)\Big],\end{aligned} \tag{A.8}$$

which gives $I(0) = -62.5336$ for $p=0$ and $I(2)\simeq -8.4448$ for $p=2$.

Appendix B

Additional details on magnetohydrodynamics

B.1 Standard formulation of relativistic magnetohydrodynamics

We take a moment here to compare our expressions with the standard versions in magneto-hydrodynamics in the Landau frame. We set $\delta u^\mu = (0, \vec{v})$ and note the constitutive relation for the current

$$\langle J^\mu \rangle = q u^\mu + \sigma_{\rm Q} \left(F^{\mu\nu} u_\nu - T \Pi^{\mu\nu} \nabla_\nu \left(\frac{\mu}{T} \right) \right) . \tag{B.1}$$

The fluctuation of this expression around a flat background of constant μ, T and B gives

$$\delta \langle J^\mu \rangle = \delta q u_b^\mu + \Pi_b^{\mu\nu} \left(\left(\rho \Pi^b_{\nu\rho} + B \sigma_{\rm Q} \Sigma^b_{\nu\rho} \right) \delta u^\rho + \delta E_\nu - \sigma_{\rm Q} \partial_\nu \delta\mu + \sigma_{\rm Q} \frac{\mu_b}{T_b} \partial_\nu \delta T \right) . \tag{B.2}$$

Examining only time dependent profiles we identify the spatial part of the current

$$\delta \vec{\mathcal{J}} = (\rho \mathbb{1}_2 + \sigma_{\rm Q} B \epsilon)\, \delta \vec{v} + \sigma_{\rm Q} \delta \vec{E} , \qquad \epsilon^2 = -\mathbb{1}_2 . \tag{B.3}$$

From the constitutive relation of the stress-energy-momentum tensor we have

$$\delta \vec{\mathcal{P}}(\omega) = (\varepsilon + P) \delta \vec{v}(\omega) , \tag{B.4}$$

to order one in fluctuations which we can back substitute into (B.3). Employing this relationship we determine

$$\chi = \frac{1}{B} \left(\omega_c \mathbb{1}_2 + \gamma_c \epsilon \right) , \qquad \sigma_0 = \sigma_{\rm Q} \mathbb{1} , \qquad \omega_c = \frac{\rho B}{(\varepsilon + P)} , \qquad \gamma_c = \frac{\sigma_0 B^2}{(\varepsilon + P)} , \tag{B.5}$$

where ω_c is the cyclotron frequency and γ_c is the cyclotron decay rate and $\sigma_{\rm Q} = (sT/(\varepsilon + P))^2$. From these expressions it follows that

$$\Gamma = \gamma_c \mathbb{1}_2 - \omega_c \epsilon , \qquad \Theta = \rho \mathbb{1}_2 + \sigma_0 B \epsilon . \tag{B.6}$$

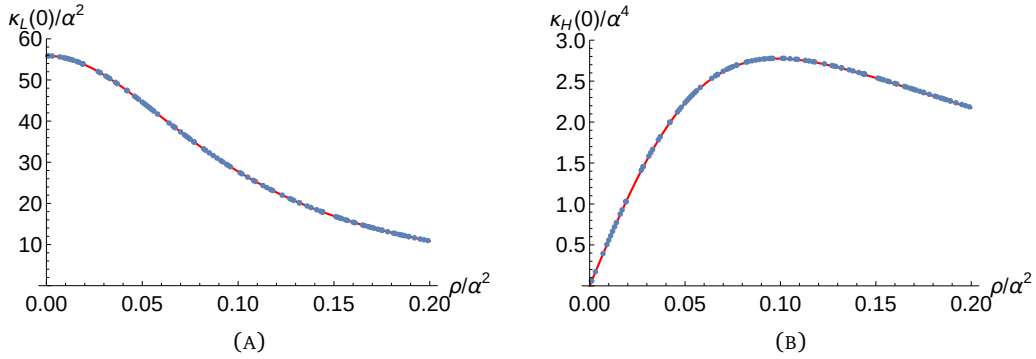

(A) (B)

FIGURE B.1: Plots of the longitudinal and Hall thermal conductivites at $B/\alpha^2 = 1/100$ against ρ/α^2. The blue dots represent data while the red lines are analytic expressions. The matching is generally on the order of $\sim 10^{-15}$.

In the standard formulation of magnetohydrodynamics it follows from our expressions that

$$(\Gamma - i\omega\mathbb{1}_2)^{-1} = \frac{1}{(\omega+i\gamma_c)^2-\omega_c^2}\left(-\omega_c\epsilon\,(i\omega-\gamma_c)\,\mathbb{1}_2\right) . \tag{B.7}$$

From this we determine that the charge conductivity is

$$\sigma(\omega) = \sigma_{\mathrm{Q}}\frac{\omega\left(\omega+i\gamma_c+i\frac{\omega_c^2}{\gamma_c}\right)}{(\omega+i\gamma_c)^2-\omega_c^2}\mathbb{1}_2 - \frac{\rho}{B}\frac{\omega_c^2-2i\gamma_c\omega+\gamma_c^2}{(\omega+i\gamma_c)^2-\omega_c^2}\epsilon\,, \tag{B.8}$$

which agrees with [48] and [41]. We know that this expression fails to correctly evaluate the thermal conductivities except at extremely small magnetic fields.

B.2 Miscellaneous additional results

As a check on the strength of our numerics, we have extracted numerically κ_{L} and κ_{H} using the c_2 coefficient of the Laurent expansion around $\omega = 0$,

$$c_2 = \frac{1}{2\pi}\oint_\Gamma d\omega\,\frac{\sigma_+(\omega)}{\omega^3} \tag{B.9}$$

and compared to the analytical expressions (3.72). The results for $B/\alpha^2 = 1/100$ as a function of ρ/α^2 are displayed in fig. B.1, showing that the analytical and numerical results match with a very high degree of accuracy. We have confirmed this for general B.

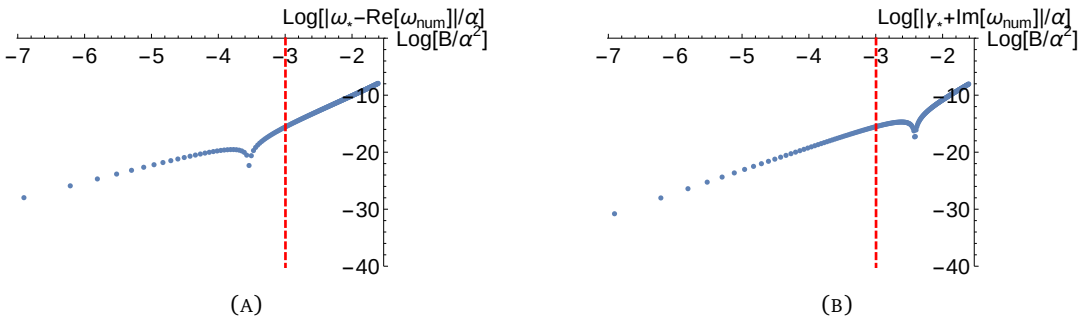

(A) (B)

FIGURE B.2: Plots of the logarithm of the absolute difference between our analytic expression for the position of the hydrodynamic mode and the numerical position for the dyonic black hole against the magnetic field at $\rho/\alpha^2 = 1/20$. The red dashed line indicates the point where $B = \rho$. **Left:** The difference in the real part. The trough in the data indicates the point where our analytic result almost coincides with the numerical result. On the left of this trough the difference grows as B^3 while on the right it behaves as B^5. **Right:** The difference in the imaginary part. Again, the trough in the data indicates the point where our analytic result almost coincides with the numerical result. On the left of this trough the difference grows as B^4 while on the right it behaves as B^6.

For completeness we record here the longitudinal and Hall thermo-electric and thermal AC conductivities. These are given by the expressions

$$\alpha_{\rm L}(\omega) = \frac{i\omega(sT+\mu\rho-mB)\left(B\omega_*-\mu\left(\gamma_*^2-i\gamma_*\omega+\omega_*^2\right)\right)}{B^2\left((\omega-i\gamma_*)^2-\omega_*^2\right)}\,, \tag{B.10}$$

$$\begin{aligned}\alpha_{\rm H}(\omega) &= -\frac{B(\omega+i\gamma_*)(\mu\rho\omega-i(sT-mB)\gamma_*)+B\omega_*^2(sT-mB)}{B^2\left((\omega-i\gamma_*)^2-\omega_*^2\right)}\\ &\quad -\frac{\mu\omega_*(sT+\mu\rho-mB)}{B^2\left((\omega-i\gamma_*)^2-\omega_*^2\right)}\omega^2\,,\end{aligned} \tag{B.11}$$

and

$$\kappa_{\rm L}(\omega) = \frac{(sT+\mu\rho-mB)\left(B^2(\omega+i\gamma_*)-2B\mu\omega\omega_*+\mu^2\omega\left(\gamma_*^2-i\gamma_*\omega+\omega_*^2\right)\right)}{B^2\left((\omega-i\gamma_*)^2-\omega_*^2\right)} \tag{B.12}$$

$$\begin{aligned}\kappa_{\rm H}(\omega) &= \frac{B\mu\omega_*^2(2sT+\mu\rho-2Bm)-\omega_*\left(B^2+\mu^2\omega^2\right)(sT+\mu\rho-mB)}{B^2\left((\omega-i\gamma_*)^2-\omega_*^2\right)}\\ &\quad +\frac{i\mu(\omega+i\gamma_*)(2B\gamma_*m-i\mu\rho(\omega-i\gamma_*)-2\gamma_*sT)}{B\left((\omega-i\gamma_*)^2-\omega_*^2\right)}\,,\end{aligned} \tag{B.13}$$

respectively. Defining complex correlators and expanding about the pole at $\omega = \omega_* - i\gamma_*$ we find that the incoherent conductivities satisfy the relationship

$$\alpha^{\rm inc.} = -\mu\sigma^{\rm inc.}\,, \qquad \kappa^{\rm inc.} = \mu^2\sigma^{\rm inc.}\,, \tag{B.14}$$

which, up to the usual normalization of $\alpha^{\rm inc.}$ and $\kappa^{\rm inc.}$ by temperature (which we chose not to include in our work) is a known result. In terms of real and imaginary

parts this relationship becomes

$$\alpha_0 = -\mu\sigma_0 \,, \qquad \kappa_0 = \mu^2\sigma_0 \,, \tag{B.15}$$

$$\alpha_{\mathrm{H}} = -\mu\tilde{\sigma}_{\mathrm{H}} \,, \qquad \kappa_{\mathrm{H}} = \mu^2\tilde{\sigma}_{\mathrm{H}} \,. \tag{B.16}$$

To get an idea of the error in our hydrodynamic charge correlator compared to the numerical charge correlator one can compare the quasi-normal mode defined by the pole in our correlator - see (3.59) and (3.60) - to the numerics. We do this in fig. B.2. We can see that the accuracy and precision are quite good, although there is a systematic difference. The trough in the plots corresponds to a point where our analytic result almost matches the numerical one. To the left of this trough the analytic result overestimates the position, while to the right it underestimates.

Bibliography

1. Pelissetto, A. & Vicari, E. Critical phenomena and renormalization group theory. *Phys. Rept.* **368,** 549–727. arXiv: cond-mat/0012164 (2002).
2. Cardy, J. L. *Scaling and renormalization in statistical physics* (1996).
3. Belavin, A., Polyakov, A. M. & Zamolodchikov, A. Infinite Conformal Symmetry in Two-Dimensional Quantum Field Theory. *Nucl. Phys. B* **241** (eds Khalatnikov, I. & Mineev, V.) 333–380 (1984).
4. Di Francesco, P., Mathieu, P. & Senechal, D. *Conformal Field Theory* ISBN: 9780387947853, 9781461274759 (Springer-Verlag, New York, 1997).
5. Rychkov, S. *EPFL Lectures on Conformal Field Theory in D>= 3 Dimensions* ISBN: 978-3-319-43625-8, 978-3-319-43626-5. arXiv: 1601.05000 [hep-th] (Jan. 2016).
6. Wilson, K. G. Nonlagrangian models of current algebra. *Phys. Rev.* **179,** 1499–1512 (1969).
7. Guida, R. & Magnoli, N. All order IR finite expansion for short distance behavior of massless theories perturbed by a relevant operator. *Nucl. Phys. B* **471,** 361–388. arXiv: hep-th/9511209 (1996).
8. Svetitsky, B. & Yaffe, L. G. Critical Behavior at Finite Temperature Confinement Transitions. *Nucl. Phys. B* **210,** 423–447 (1982).
9. Kos, F., Poland, D., Simmons-Duffin, D. & Vichi, A. Precision islands in the Ising and O(N) models. *Journal of High Energy Physics* **2016.** ISSN: 1029-8479. http://dx.doi.org/10.1007/JHEP08(2016)036 (2016).
10. Wilson, K. G. Confinement of quarks. *Phys. Rev. D* **10,** 2445–2459. https://link.aps.org/doi/10.1103/PhysRevD.10.2445 (8 1974).
11. Caselle, M., Nada, A. & Panero, M. Hagedorn spectrum and thermodynamics of SU(2) and SU(3) Yang-Mills theories. *Journal of High Energy Physics* **2015.** ISSN: 1029-8479. http://dx.doi.org/10.1007/JHEP07(2015)143 (2015).
12. Lucini, B., Teper, M. & Wenger, U. The high temperature phase transition in SU(N) gauge theories. *Journal of High Energy Physics* **2004,** 061–061. ISSN: 1029-8479. http://dx.doi.org/10.1088/1126-6708/2004/01/061 (2004).
13. Caselle, M & Hasenbusch, M. Universal amplitude ratios in the three-dimensional Ising model. *Journal of Physics A: Mathematical and General* **30,** 4963–4982. ISSN: 1361-6447. http://dx.doi.org/10.1088/0305-4470/30/14/010 (1997).

14. Caselle, M., Costagliola, G. & Magnoli, N. Conformal perturbation of off-critical correlators in the 3D Ising universality class. *Physical Review D* **94.** ISSN: 2470-0029. http://dx.doi.org/10.1103/PhysRevD.94.026005 (2016).

15. Hasenbusch, M. Finite size scaling study of lattice models in the three-dimensional Ising universality class. *Phys. Rev. B* **82,** 174433. https://link.aps.org/doi/10.1103/PhysRevB.82.174433 (17 2010).

16. Caselle, M., Costagliola, G. & Magnoli, N. Numerical determination of the operator-product-expansion coefficients in the 3D Ising model from off-critical correlators. *Physical Review D* **91.** ISSN: 1550-2368. http://dx.doi.org/10.1103/PhysRevD.91.061901 (2015).

17. Costagliola, G. Operator product expansion coefficients of the 3D Ising model with a trapping potential. *Physical Review D* **93.** ISSN: 2470-0029. http://dx.doi.org/10.1103/PhysRevD.93.066008 (2016).

18. Campostrini, M. & Vicari, E. Critical behavior and scaling in trapped systems. *Phys. Rev. Lett.* **102,** 240601. arXiv: 0903.5153 [cond-mat.stat-mech] (2009).

19. Campostrini, M. & Vicari, E. Trap-size scaling in confined particle systems at quantum transitions. *Physical Review A* **81** (June 2009).

20. Ceccarelli, G., Torrero, C. & Vicari, E. Critical parameters from trap-size scaling in systems of trapped particles. *Physical Review B* **87.** ISSN: 1550-235X. http://dx.doi.org/10.1103/PhysRevB.87.024513 (2013).

21. Cornell, E. A. & Wieman, C. E. Nobel Lecture: Bose-Einstein condensation in a dilute gas, the first 70 years and some recent experiments. *Rev. Mod. Phys.* **74,** 875–893. https://link.aps.org/doi/10.1103/RevModPhys.74.875 (3 2002).

22. Ketterle, W. Nobel lecture: When atoms behave as waves: Bose-Einstein condensation and the atom laser. *Rev. Mod. Phys.* **74,** 1131–1151. https://link.aps.org/doi/10.1103/RevModPhys.74.1131 (4 2002).

23. Hasenbusch, M. Thermodynamic Casimir effect: Universality and corrections to scaling. *Physical Review B* **85.** ISSN: 1550-235X. http://dx.doi.org/10.1103/PhysRevB.85.174421 (2012).

24. El-Showk, S. *et al.* Solving the 3D Ising model with the conformal bootstrap. *Physical Review D* **86.** ISSN: 1550-2368. http://dx.doi.org/10.1103/PhysRevD.86.025022 (2012).

25. Caselle, M., Hasenbusch, M. & Panero, M. String effects in the 3d gauge Ising model. *Journal of High Energy Physics* **2003,** 057–057. ISSN: 1029-8479. http://dx.doi.org/10.1088/1126-6708/2003/01/057 (2003).

26. Herdeiro, V. Numerical estimation of structure constants in the three-dimensional Ising conformal field theory through Markov chain uv sampler. *Phys. Rev. E* **96,** 033301. https://link.aps.org/doi/10.1103/PhysRevE.96.033301 (3 2017).

27. Guida, R. & Magnoli, N. On the short distance behavior of the critical Ising model perturbed by a magnetic field. *Nuclear Physics B* **483,** 563–579. ISSN: 0550-3213. http://dx.doi.org/10.1016/S0550-3213(96)00585-8 (1997).

28. Amoretti, A. & Magnoli, N. Conformal perturbation theory. *Phys. Rev. D* **96,** 045016. arXiv: 1705.03502 [hep-th] (2017).

29. Simmons-Duffin, D. The lightcone bootstrap and the spectrum of the 3d Ising CFT. *Journal of High Energy Physics* **2017.** ISSN: 1029-8479. http://dx.doi.org/10.1007/JHEP03(2017)086 (2017).

30. Rychkov, S., Simmons-Duffin, D. & Zan, B. Non-gaussianity of the critical 3d Ising model. *SciPost Physics* **2.** ISSN: 2542-4653. http://dx.doi.org/10.21468/SciPostPhys.2.1.001 (2017).

31. Komargodski, Z. & Simmons-Duffin, D. The random-bond Ising model in 2.01 and 3 dimensions. *Journal of Physics A: Mathematical and Theoretical* **50,** 154001. ISSN: 1751-8121. http://dx.doi.org/10.1088/1751-8121/aa6087 (2017).

32. Behan, C., Rastelli, L., Rychkov, S. & Zan, B. A scaling theory for the long-range to short-range crossover and an infrared duality. *Journal of Physics A: Mathematical and Theoretical* **50,** 354002. ISSN: 1751-8121. http://dx.doi.org/10.1088/1751-8121/aa8099 (2017).

33. Maldacena, J. *International Journal of Theoretical Physics* **38,** 1113–1133. ISSN: 0020-7748. http://dx.doi.org/10.1023/A:1026654312961 (1999).

34. Haehl, F. M., Loganayagam, R. & Rangamani, M. The eightfold way to dissipation. *Phys. Rev. Lett.* **114,** 201601. arXiv: 1412.1090 [hep-th] (2015).

35. Hernandez, J. & Kovtun, P. Relativistic magnetohydrodynamics. *JHEP* **05,** 001. arXiv: 1703.08757 [hep-th] (2017).

36. Grozdanov, S. s., Hofman, D. M. & Iqbal, N. Generalized global symmetries and dissipative magnetohydrodynamics. *Phys. Rev. D* **95,** 096003. arXiv: 1610.07392 [hep-th] (2017).

37. Armas, J. & Jain, A. One-form superfluids & magnetohydrodynamics. *JHEP* **01,** 041. arXiv: 1811.04913 [hep-th] (2020).

38. Armas, J. & Jain, A. Magnetohydrodynamics as superfluidity. *Phys. Rev. Lett.* **122,** 141603. arXiv: 1808.01939 [hep-th] (2019).

39. Benenowski, B. & Poovuttikul, N. Classification of magnetohydrodynamic transport at strong magnetic field. arXiv: 1911.05554 [hep-th] (Nov. 2019).

40. Goedbloed, J. P. H. & Poedts, S. *Principles of Magnetohydrodynamics: With Applications to Laboratory and Astrophysical Plasmas* (Cambridge University Press, 2004).

41. Hartnoll, S. A., Kovtun, P. K., Muller, M. & Sachdev, S. Theory of the Nernst effect near quantum phase transitions in condensed matter, and in dyonic black holes. *Phys. Rev. B* **76,** 144502. arXiv: 0706.3215 [cond-mat.str-el] (2007).

42. Blake, M. & Donos, A. Quantum Critical Transport and the Hall Angle. *Phys. Rev. Lett.* **114,** 021601. arXiv: 1406.1659 [hep-th] (2015).

43. Lucas, A. & Sachdev, S. Memory matrix theory of magnetotransport in strange metals. *Phys. Rev. B* **91,** 195122. arXiv: 1502.04704 [cond-mat.str-el] (2015).

44. Patel, A. A., McGreevy, J., Arovas, D. P. & Sachdev, S. Magnetotransport in a model of a disordered strange metal. *Phys. Rev. X* **8,** 021049. arXiv: 1712.05026 [cond-mat.str-el] (2018).

45. Delacrétaz, L. V., Goutéraux, B., Hartnoll, S. A. & Karlsson, A. Theory of collective magnetophonon resonance and melting of a field-induced Wigner solid. *Phys. Rev. B* **100,** 085140. arXiv: 1904.04872 [cond-mat.mes-hall] (2019).

46. Amoretti, A. *et al.* A hydrodynamical description for magneto-transport in the strange metal phase of Bi-2201. *Phys. Rev. Res.* **2,** 023387. arXiv: 1909.07991 [cond-mat.str-el] (2020).

47. Hartnoll, S. A. & Kovtun, P. Hall conductivity from dyonic black holes. *Phys. Rev. D* **76,** 066001. arXiv: 0704.1160 [hep-th] (2007).

48. Hartnoll, S. A. & Herzog, C. P. Ohm's Law at strong coupling: S duality and the cyclotron resonance. *Phys. Rev. D* **76,** 106012. arXiv: 0706.3228 [hep-th] (2007).

49. Amoretti, A. & Musso, D. Magneto-transport from momentum dissipating holography. *JHEP* **09,** 094. arXiv: 1502.02631 [hep-th] (2015).

50. Blake, M., Donos, A. & Lohitsiri, N. Magnetothermoelectric Response from Holography. *JHEP* **08,** 124. arXiv: 1502.03789 [hep-th] (2015).

51. Blake, M. Momentum relaxation from the fluid/gravity correspondence. *JHEP* **09,** 010. arXiv: 1505.06992 [hep-th] (2015).

52. Herzog, C. P. Lectures on Holographic Superfluidity and Superconductivity. *J. Phys. A* **42,** 343001. arXiv: 0904.1975 [hep-th] (2009).

53. Jensen, K. *et al.* Parity-Violating Hydrodynamics in 2+1 Dimensions. *JHEP* **05,** 102. arXiv: 1112.4498 [hep-th] (2012).

54. Amoretti, A., Blasi, A., Caruso, G., Maggiore, N. & Magnoli, N. Duality and Dimensional Reduction of 5D BF Theory. *Eur. Phys. J. C* **73,** 2461. arXiv: 1301.3688 [hep-th] (2013).

55. Donos, A. & Gauntlett, J. P. Thermoelectric DC conductivities from black hole horizons. *JHEP* **11,** 081. arXiv: 1406.4742 [hep-th] (2014).

56. Amoretti, A., Braggio, A., Maggiore, N., Magnoli, N. & Musso, D. Analytic dc thermoelectric conductivities in holography with massive gravitons. *Phys. Rev. D* **91,** 025002. arXiv: 1407.0306 [hep-th] (2015).

57. Amoretti, A., Braggio, A., Maggiore, N., Magnoli, N. & Musso, D. Thermo-electric transport in gauge/gravity models with momentum dissipation. *JHEP* **09,** 160. arXiv: 1406.4134 [hep-th] (2014).

58. Amoretti, A., Braggio, A., Caruso, G., Maggiore, N. & Magnoli, N. Holography in flat spacetime: 4D theories and electromagnetic duality on the border. *JHEP* **04,** 142. arXiv: 1401.7101 [hep-th] (2014).

59. Donos, A., Gauntlett, J. P., Griffin, T. & Melgar, L. DC Conductivity of Magnetised Holographic Matter. *JHEP* **01,** 113. arXiv: 1511.00713 [hep-th] (2016).

60. Amoretti, A., Braggio, A., Maggiore, N. & Magnoli, N. Thermo-electric transport in gauge/gravity models. *Advances in Physics: X* **2,** 409–427. eprint: https://doi.org/10.1080/23746149.2017.1300509. https://doi.org/10.1080/23746149.2017.1300509 (2017).

61. Amoretti, A. *Condensed Matter Applications of AdS/CFT: Focusing on strange metals* PhD thesis (Genoa U., 2016).

62. Kovtun, P. Thermodynamics of polarized relativistic matter. *JHEP* **07,** 028. arXiv: 1606.01226 [hep-th] (2016).

63. Kadanoff, L. P. & Martin, P. C. Hydrodynamic equations and correlation functions. *Annals of Physics* **24,** 419–469 (Oct. 1963).

64. Blake, M. Magnetotransport from the fluid/gravity correspondence. *JHEP* **10,** 078. arXiv: 1507.04870 [hep-th] (2015).

65. Davison, R. A., Goutéraux, B. & Hartnoll, S. A. Incoherent transport in clean quantum critical metals. *JHEP* **10,** 112. arXiv: 1507.07137 [hep-th] (2015).

66. Hatta, Y. & Ikeda, T. Universality, the QCD critical / tricritical point and the quark number susceptibility. *Phys. Rev. D* **67,** 014028. arXiv: hep-ph/0210284 (2003).

67. Amoretti, A., Aréan, D., Goutéraux, B. & Musso, D. Diffusion and universal relaxation of holographic phonons. *Journal of High Energy Physics* **2019.** ISSN: 1029-8479. http://dx.doi.org/10.1007/JHEP10(2019)068 (2019).

68. Amoretti, A., Areán, D., Goutéraux, B. & Musso, D. DC resistivity of quantum critical, charge density wave states from gauge-gravity duality. *Phys. Rev. Lett.* **120,** 171603. arXiv: 1712.07994 [hep-th] (2018).

69. Amoretti, A., Areán, D., Goutéraux, B. & Musso, D. Universal relaxation in a holographic metallic density wave phase. *Phys. Rev. Lett.* **123,** 211602. arXiv: 1812.08118 [hep-th] (2019).

70. Amoretti, A., Areán, D., Goutéraux, B. & Musso, D. Diffusion and universal relaxation of holographic phonons. *JHEP* **10,** 068. arXiv: 1904.11445 [hep-th] (2019).

71. Amoretti, A., Areán, D., Goutéraux, B. & Musso, D. Gapless and gapped holographic phonons. *JHEP* **01,** 058. arXiv: 1910.11330 [hep-th] (2020).

72. Baggioli, M., Grieninger, S. & Li, L. Magnetophonons & type-B Goldstones from Hydrodynamics to Holography. arXiv: 2005.01725 [hep-th] (May 2020).